THE PERCEPTION OF GLOBAL MOTION IN TYPICAL AND ATYPICAL VISUAL DEVELOPMENT

by

Kimberly Meier

B.A., Simon Fraser University, 2010
M.A., The University of British Columbia, 2013

A THESIS SUBMITTED IN PARTIAL FULFILLMENT OF
THE REQUIREMENTS FOR THE DEGREE OF

DOCTOR OF PHILOSOPHY
in
THE FACULTY OF GRADUATE AND POSTDOCTORAL STUDIES
(Psychology)

THE UNIVERSITY OF BRITISH COLUMBIA
(Vancouver)

July 2018

The following individuals certify that they have read, and recommend to the Faculty of Graduate and Postdoctoral Studies for acceptance, the dissertation entitled:

The perception of global motion in typical and atypical visual development

submitted by Kimberly Meier in partial fulfillment of the requirements for

the degree of Doctor of Philosophy

in Psychology

Examining Committee:

Deborah Giaschi
Supervisor

Todd C Handy
Supervisory Committee Member

Darko Odic
Supervisory Committee Member

James T Enns
University Examiner

Romeo Chua
University Examiner

Abstract

Sensitivity to motion information emerges early in life, but full maturation of motion perception can take many years. Reports on the age at which typically-developing children reach adult-like global motion perception have ranged from 3-14 years. There are also conflicting reports on whether people with amblyopia (a visual disorder that occurs when a young child experiences abnormal visual input to one eye for a prolonged period) show deficits on these tasks. This dissertation examines the spatio-temporal factors underlying immaturities and deficits in motion perception. I tested the hypothesis that perception of motion stimuli created with small spatial displacements would mature later than those created with large displacements; and as a consequence, children with amblyopia would show selective deficits for these small spatial displacements. First, I investigated typical maturation of motion perception across a range of stimulus parameters in people aged 7-30 years (Chapter 3). The youngest children performed similar to adults for large displacements, but mature performance was not reached until middle teenage years for small displacements. Second, I investigated performance for the same stimulus parameters in children with amblyopia (Chapter 4). Deficits were only present for parameters where healthy control children showed late maturation. Finally, I examined two factors that might account for the immaturities and deficits I found: spatial integration and eye stability. I determined that increasing the stimulus area had the same impact on coherence thresholds in 4-6 year-olds and adults (Chapter 5), suggesting children's immature performance for small displacements was not restricted by spatial integration limitations at stages prior to motion processing. I also determined that eye stability had no relationship with performance in healthy adults (Chapter 6), indicating that poor fixational stability alone could not account for poor performance on a global motion task. This work contributes to a better understanding of how the developing brain is impacted by amblyopia, in turn providing insight into sensitive periods for typical visual development.

Lay Summary

Human vision undergoes much development from birth through childhood. A visual disorder called amblyopia, or “lazy eye”, can impact healthy development of vision. I studied the development of motion perception and how it can be impacted by amblyopia using a task in which participants saw moving dots and had to say if they saw motion to the left or the right. I measured performance at a range of speeds, so that I could evaluate the pattern of development as a function of speed. I found that young children do not show adult-like performance for slow speeds until the middle teenage years, and that children with amblyopia have poor performance on slow speeds. I also ruled out two non-motion factors that might account for poor performance. My work shows that different aspects of motion perception develop at different rates, and the aspects that take longest to mature are vulnerable to damage by amblyopia.

Preface

I was the lead on all projects presented herein, and except where noted below, I was responsible for all aspects of conception, design, stimulus programming, analysis, interpretation, and manuscript composition. Data collection was carried out by myself and undergraduate research assistants in my lab. Deborah Giaschi supervised all aspects of this dissertation and provided feedback and edits to the manuscripts that resulted from this work. The work described in this dissertation was approved by the Children's and Women's Research Ethics Board, certificates H12-03331 (Chapters 3, 4, and 5), and H16-01912 (Chapter 6).

Chapter 1. Portions of the review material from the introduction were taken from *Meier, K., & Giaschi, D. (2017). Unilateral amblyopia affects two eyes: Fellow eye deficits in amblyopia. Investigative Ophthalmology & Vision Science, 58, 1997-1800.* I am fully responsible for the composition of that manuscript and the text in this chapter.

Chapter 3. A version of this material has been published as *Meier, K. & Giaschi, D. (2017). Effect of spatial and temporal stimulus parameters on the maturation of global motion perception. Vision Research, 135, 1-9.* Two graduate students in the UBC Department of Statistics, Jasmine Ju and David Kleppinger, provided statistical advising for the non-parametric analysis technique used therein as part of their enrollment in STAT 551 (Statistical Consulting Practicum).

Chapter 4. A version of this material has been published as *Meier, K., Sum, B., & Giaschi, D. (2016). Global motion perception in children with amblyopia as a function of spatial and temporal stimulus parameters. Vision Research, 127, 18-27.* BS was an undergraduate student working under the supervision of myself and DG, and was responsible for gathering relevant clinical details of participants with amblyopia.

Chapter 5. A version of this material was presented at the Vision Sciences Society 2017 Annual Meeting.

Chapter 6. A version of this material was presented at the Vision Sciences Society 2018 Annual Meeting. Dr. Miriam Spering provided advice on experimental design and data analysis, as well as access to the necessary equipment to conduct eye-tracking.

Table of Contents

Abstract ..... **iii**
Lay Summary ..... **iv**
Preface ..... **v**
Table of Contents ..... **vii**
List of Tables ..... **x**
List of Figures ..... **xi**
Acknowledgements ..... **xiii**
Chapter 1: Introduction **1**
1.1 Typical and atypical visual development 1
1.2 Global motion tasks 4
1.3 Global motion perception in typical development 8
1.4 Motion perception during abnormal development 11
1.5 Non-motion factors limiting performance in global motion 14
1.5.1 Spatial factors 15
1.5.2 Eye movements 18
1.6 Dissertation overview 20
Chapter 2: General methodology used in this paper **21**
2.1 General methods 21
2.2 Participant recruitment 21
2.3 Visual acuity and stereoacuity 21
2.4 Apparatus 21
2.5 Stimuli 22
2.6 Procedure 22
2.7 Coherence threshold estimation 22
Chapter 3: Typical maturation of global motion perception as a function of spatio-temporal stimulus parameters **24**
3.1 Introduction 24
3.2 Methods 24
3.2.1 Participants 24

3.2.2 Stimuli and experimental conditions 25
3.2.3 Procedure 25
3.2.4 Data analysis 25
3.3 Results 27
3.4 Discussion 32
Chapter 4: The impact of amblyopia on global motion perception as a function of spatio-temporal stimulus parameters 35
4.1 Introduction 35
4.2 Methods 35
4.2.1 Participants 35
4.2.1.1 Patient group 35
4.2.1.2 Control group 39
4.2.2 Stimuli and experimental conditions 39
4.2.3 Procedure 39
4.2.4 Data analysis 40
4.3 Results 40
4.3.1 Participant characteristics 40
4.3.2 Global motion perception in children with amblyopia vs. controls 41
4.3.3 Clinical factors and deficits in global motion perception 45
4.4 Discussion 48
4.4.1 Global motion perception in children with amblyopia vs. controls 48
4.4.2 Clinical factors and deficits in global motion perception 51
Chapter 5: The effect of stimulus area on global motion thresholds in children and adults 53
5.1 Introduction 53
5.2 Methods 53
5.2.1 Participants 53
5.2.2 Stimuli and experimental conditions 54
5.2.3 Procedure 54
5.2.4 Data analysis 55
5.3 Results 56
5.4 Discussion 59

Chapter 6: The relationship between fixation stability and motion perception in healthy controls 61
6.1 Introduction 61
6.2 Methods 61
6.2.1 Participants 61
6.2.2 Apparatus 61
6.2.3 Stimuli and experimental conditions 62
6.2.4 Procedure 62
6.2.5 Data analysis 63
6.2.5.1 Eye movement measures 63
6.3 Results 64
6.3.1 Vision assessment 64
6.3.2 Behavioural performance 65
6.3.3 Stability measures 65
6.3.4 The relationship between stability and performance 67
6.4 Discussion 70
Chapter 7: General Discussion 74
7.1 Summary of findings 74
7.2 Discussion 76
References 80
Appendices 104
Appendix A Staircase threshold estimation 104
A.1 Inspection of staircase runs during data collection 104
A.2 Inspection of coherence thresholds during data analysis 106
A.3 Exclusion of participants and data 109
Appendix B Eyetracking in participants with amblyopia 110
B.1 Participants 110
B.2 Behavioural performance 111
B.3 Stability measures 112

List of Tables

Table 4.1 Patient characteristics for children with amblyopia included in data analysis. 37
Table B.1 Vision characteristics for participants with amblyopia included in data analysis.....110

List of Figures

Figure 1.1 Global motion stimuli. 5
Figure 1.2 Two-stage model of global motion perception. 7
Figure 1.3 Motion sensitivity as a function of spatial displacement, for children and adults. 10
Figure 1.4 Motion sensitivity as a function of spatial displacement, for children with typical and atypical visual development. 13
Figure 3.1 Mean coherence thresholds as a function of age. 30
Figure 3.2 LOESS fits for coherence thresholds as a function of age. 31
Figure 3.3 Estimated age of maturation for each of the six spatio-temporal stimulus parameter conditions. 32
Figure 4.1 Mean motion coherence thresholds for the amblyopic eye in children with amblyopia and controls. 42
Figure 4.2 Mean motion coherence thresholds for the fellow eye in children with amblyopia and controls. 43
Figure 4.3 Coherence thresholds as a function of speed. 45
Figure 4.4 Coherence thresholds by amblyopia subtype. 46
Figure 4.5 Deficits in children with amblyopia. 47
Figure 5.1 Area effect at each speed for one adult participant. 56
Figure 5.2 Coherence thresholds as a function of area for each speed. 58
Figure 5.3 Effect of area by speed for both age groups. 58
Figure 6.1 Mean coherence thresholds for the two motion conditions in the experiment, separated by eye with the best- and worst visual acuity. 65
Figure 6.2 Mean $\log_{10}$ BCEA for the stationary condition, and for the high and threshold coherence stimuli for each speed. 66
Figure 6.3 Correlations between visual acuity and stability. 69
Figure 6.4 Correlations between stability ($\log_{10}$ BCEA) and performance (coherence threshold) 70
Figure A.1 Example of a good staircase. 104
Figure A.2 Example of a staircase that never converges. 105
Figure A.3 Example of a staircase that does not advance. 106

Figure A.4 Example of a Weibull function fit. 108
Figure B.1 Mean coherence thresholds, including participants with amblyopia..... 110
Figure B.2 Mean $\log_{10}$ BCEA for controls and participants with amblyopia for all conditions. 112
Figure B.3 Scatterplots showing visual acuity (logMAR) and stability ($\log_{10}$ BCEA) for participants with amblyopia. 113
Figure B.4 Scatterplots showing the relationship between stability ($\log_{10}$ BCEA) and performance (coherence threshold) in participants with amblyopia..... 114

Acknowledgements

Foremost, I must acknowledge the support of my advisor, who has imparted an innumerable set of skills to prepare me for the next stage of my career. Debbie has been an essential role model in all aspects of my education, not only in conducting research, but in writing, presenting, teaching, and mentoring. Thank you, Debbie.

I must also acknowledge my committee members, Darko Odic and Todd Handy, for their insightful perspectives on the work presented here. Both of you have pushed me to think beyond the results and consider the big picture – a helpful reminder for those of us in the trenches. Thank you also to the mentors who did not directly contribute to this work, but who have shaped my approaches to problem-solving in research: Mark Blair, Steven Brown, Rowan Candy, and Laurie Wilcox. Thank you, Ralph Hakstian, for inspiring a love of statistics.

Data collection for Chapter 4 would not be possible without the help of the clinicians and staff at the BC Children's Ophthalmology Clinic, who assisted with recruiting patients – special thanks to Christy Giligson, Vaishali Mehta, Andrea Quan, and the whole orthoptist team for their support and interest in our work.

None of this work would be possible without the dedicated members of my lab. Thank you to Marita Partanen for helping me navigate through grad school (and through brains), and for happily nerding out over statistics with me. Thank you to Marcus Watson, from whom I have learned many lessons, the most salient being the importance of well-commented code. Most importantly, thank you to the tireless undergrads and research assistants who have helped with recruiting, scheduling, and running participants – I can't imagine what this would have been like without you.

The work in this dissertation was funded by a Natural Sciences and Engineering Research Council of Canada grant to my supervisor, Deborah Giaschi. I have been supported by a Doctoral Alexander Graham Bell Canada Graduate Scholarship, and a UBC Four-Year Fellowship.

When we try to pick out anything by itself, we find it hitched to everything else in the universe.

- John Muir, My First Summer in the Sierra, 1911.

Chapter 1: Introduction

Sensitivity to motion information emerges early in life, but full maturation of motion perception can take many years. Reports on the age at which typically-developing children reach adult-like global motion perception have ranged from 3-14 years. There are also conflicting reports on whether people with amblyopia (a visual disorder that occurs when a young child experiences abnormal visual input to one eye for a prolonged period) show deficits on these tasks. This dissertation examines the spatio-temporal factors underlying immaturities and deficits in motion perception. In this chapter, I provide an outline of the current research on the development of motion perception, first as it develops in children with typical visual experience, then how it develops in children with the abnormal visual experience caused by amblyopia. Next, I consider other visual functions that may be able to account for the pattern of results I describe in this dissertation – spatial integration, and unstable eye fixation.

1.1 Typical and atypical visual development

While much of the human visual system develops in utero, many components continue to mature into late childhood, indicating very long periods for typical development. For example, visual acuity of infants is poor at birth and improves rapidly in the first six months of life (Mayer et al., 1995) but does not improve to adult-like levels, depending on the aspect of acuity measured, until at least age 11 years (Fern & Manny, 1986; Kothe, 1990). Sensitivity for texture-defined borders emerges around 4-9 months of age (Atkinson & Braddick, 1992; Norcia et al., 2005; Sireteanu & Rieth, 1992), but the ability to identify texture-defined shapes is not mature until age 11 (Parrish, Giaschi, Boden, & Dougherty, 2005). Furthermore, the ability to integrate spatially-separated contours into a form is still developing at age 14 years (Hadad, Maurer, & Lewis, 2010; Kovács, Kozma, Feher, & Benedek, 1999). Stereopsis – that is, sensitivity to depth information from retinal disparity between the two eyes – emerges around 4 months after birth (Birch & Petrig, 1996; Fox, Aslin, Shea, & Dumais, 1980; Takai, Sato, Tan, & Hirai, 2005) but is not adult-like until at least age 6 years (Heron, Dholakia, Collins, & McLaughlan, 1985; Leat, Pierre, Hassan-Abadi, & Faubert, 2001) or age 14 years (Giaschi, Narasimhan, Solski, Harrison, & Wilcox, 2013), depending on the task.

Abnormal visual experiences during development can cause atypical visual function (Lewis & Maurer, 2005). One prevalent naturally-occurring form of abnormal visual experience in humans comes as a visual developmental disorder called unilateral amblyopia ("lazy eye"), which arises after input to one eye is selectively disrupted early in life. There are multiple etiologies for amblyopia. Anisometropia, which is an unequal refractive error between the two eyes, and/or strabismus, which is a misalignment in fixation of one eye, are the two most common causes of amblyopia (Attebo et al., 1998; Caca et al., 2013; Chia et al., 2010; Høeg et al., 2015; Multi-ethnic Pediatric Eye Disease Study Group, 2008; Robaei et al., 2006; Robaei, Kifley, Rose, & Mitchell, 2008). Amblyopia can also be caused by more extreme deprivation as in developmental cataracts (cloudy lens) or ptosis (a drooping eyelid), which may prevent pattern stimulation in one eye altogether. Clinically, amblyopia is identified by assessing visual acuity with an optotype (letter or symbol) chart. If a child has at least a two-line difference in visual acuity between the eyes, even when the amblyogenic factors have been removed (i.e., through the appropriate lens prescription for anisometropia, corrective surgery to align the eyes in strabismus, or cataract extraction), amblyopia is diagnosed (Holmes & Clarke, 2006).

An amblyopic eye is an otherwise healthy eye, and the effects of amblyopia are widely assumed to be neural in origin, arising from the imbalance of input to the developing visual system during a sensitive period of development. In kittens (Hubel & Wiesel, 1970) and macaques (Horton & Hocking, 1997; LeVay, Wiesel, & Hubel, 1980), complete monocular deprivation in the weeks after birth causes changes in the lateral geniculate nucleus and early visual cortex. However, monocular deprivation induced at 8 or 12 weeks of age for these species, respectively, has minimal neural effects, indicating the sensitive period for damage has ended. Similarly, amblyopia typically arises between the ages of six months to eight years in humans (Holmes & Clarke, 2006; von Noorden, 1990), but if anisometropia, strabismus, or unilateral cataract develops later in life, amblyopia does not occur. Thus, amblyopia is a consequence of the abnormal progression of visual development during sensitive periods and cannot impact a mature visual system.

While amblyopia is diagnosed based on visual acuity of the effected eye, it is not simply a disorder of reduced visual acuity. Children and adults with amblyopia can show deficits on a range of other spatial vision tasks, including those that rely on contrast sensitivity (Bradley & Freeman, 1981; Hess, Campbell, & Greenhalgh, 1978; Hess & Howell, 1977; Howell, Mitchell,

& Keith, 1983; Katz, Levi, & Bedell, 1984; Levi & Harwerth, 1977), Vernier acuity and other hyperacuities (Bedell & Flom, 1981; Bedell, Flom, & Barbeito, 1985; Birch & Swanson, 2000; Carkeet, Levi, & Manny, 1997; Freeman & Bradley, 1980; Fronius, Sireteanu, & Zubcov, 2004; Levi & Klein, 1982a; Levi & Klein, 1982b; Levi & Klein, 1985; Levi, Waugh, & Beard, 1994; Rentschler & Hilz, 1985), and tasks that rely on spatially integrating long-range information across the visual field (Bonneh, Sagi, & Polat, 2004; Hess & Demanins, 1998; Kovács, Polat, Pennefather, Chandna, & Norcia, 2000; Levi, Yu, Kuai, & Rislove, 2007; Mussap & Levi, 2000; Rislove, Hall, Stavros, & Kiorpes, 2010; Simmers & Bex, 2004). Notably, these are tasks that tend to show long periods of maturation. For example, while the contrast sensitivity function generally retains the same shape throughout development (Movshon & Kiorpes, 1988), it is reduced at all spatial frequencies in four-year-olds (Atkinson, French, & Braddick, 1981). Although differences after around age 8 years can be small (Derefeldt, Lennerstrand, & Lundh, 1979), contrast sensitivity may not reach adult-like levels until adolescence (Beazley, Illingworth, Jahn, & Greer, 1980). Hyperacuity alignment thresholds of typically-developing children are not adult-like until five years of age (Zanker, Mohn, Weber, Zeitler-Driess, & Fahle, 1992) or later (Carkeet et al., 1997; Kim et al., 2000), with some estimates as late as age 14 years (Skoczenski & Norcia, 2002). Other hyperacuity tasks, such as the ability to detect minor perturbations in a circle, may not reach maturity until 21 years (Wang, Morale, Cousins, & Birch, 2009). Finally, it can take until ages 6 to 9 years (Lewis et al., 2004) or even 14 years (Hadad et al., 2010; Kovács et al., 1999), depending on the task, for typically-developing children to achieve adult-like status in spatial integration tasks.

In addition to these spatial visual functions, amblyopia is also associated with deficits in motion perception, including motion aftereffects (Hess, Demanins, & Bex, 1997), oscillatory movement displacement (Buckingham, Watkins, Bansal, & Bamford, 1991; Kelly & Buckingham, 1998), motion-defined form (Giaschi, Regan, Kraft, & Hong, 1992; Hayward et al., 2011; Ho et al., 2005; Wang, Ho, & Giaschi, 2007), maximum motion displacement (Ho et al., 2005; Ho & Giaschi, 2006; Ho & Giaschi, 2007; Ho & Giaschi, 2009) and attentive motion tracking (Ho et al., 2006; Secen, Culham, Ho, & Giaschi, 2011). Some animal models of motion perception indicate that the sensitive period for motion perception is very brief (Mitchell, Kennie, & Kung, 2009), but these behavioural findings indicate this is unlikely to be the case for all aspects of motion perception. In this dissertation, I follow the "last-in-first-out" stack

principle of development (Levi & Carkeet, 1993; Lewis & Maurer, 2009) which proposes that aspects of visual function that mature later in development are the most vulnerable to disruption by disorders that emerge after birth, such as amblyopia. In other words, once an aspect of visual function has matured, the period during which it is susceptible to damage has passed; if this aspect is immature, however, the plasticity of the mechanisms subserving a visual function can lead to abnormal development in the face of abnormal experience. *The primary goal of this dissertation is to gain a better understanding of the development of motion perception using this framework to assess performance on motion tasks in children with typically-developed visual systems as a function of age (Chapter 3), and in children whose visual systems have been impacted by amblyopia (Chapter 4). I also assess potential spatial (Chapter 5) and oculomotor (Chapter 6) influences on performance to rule these out as mitigating factors.*

1.2 Global motion tasks

The motion perception task under study in this dissertation is global motion perception (

Figure 1.1). Global motion perception, put simply, is the ability to perceive a set of elements moving in a coherent direction. A common way to assess global motion is with a random dot animation that contains signal dots moving coherently in the same direction and noise dots moving in random directions. Sometimes, researchers use Gabor elements or spatially filtered dots to control the spatial frequency content of the stimulus. Typically, a translational (left vs. right or up vs. down) motion pattern is used, although radial (expanding vs. contracting) and rotational (clockwise vs. counter-clockwise) patterns may also be assessed. Using these stimuli, a coherence threshold is measured, which represents the minimum proportion of signal dots needed to perceive coherent motion.

Figure 1.1 Global motion stimuli.

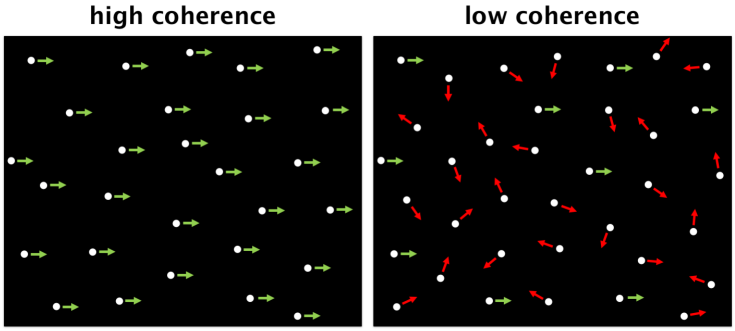

Note. Examples of global motion at high (100%; left column) and low (25%; right column) coherence levels. Green arrows indicate the direction of movement for signal dots; red arrows indicate noise dots moving in random directions. The participant is asked to indicate the overall direction in which the dots appeared to move.

While there are debates over the exact computational mechanisms by which the perception of global motion is accomplished (for review, see Braddick & Qian, 2001; Derrington, Allen, & Delicato, 2004; Snowden & Verstraten, 1999), it is generally considered to consist of two stages (See Figure 1.2): 1) a computation of motion vectors at local positions in direction-sensitive V1 cells with small receptive fields (Albright, 1984; Gattass & Gross, 1981), and 2) integration of these local vectors in MT cells with large receptive fields (Gattass & Gross, 1981; Mikami, Newsome, & Wurtz, 1986). Area MT (also called V5 or V5/MT+ in humans) is one of the most well-established motion processing regions (Tootell et al., 1995; Zeki et al., 1991), and is traditionally placed in the dorsal processing stream though may be better understood as an early visual area prior to the division of dorsal and ventral streams (Milner & Goodale, 2006; Schenk, Mai, Ditterich, & Zihl, 2000; Schenk & McIntosh, 2010) or even the primary input to a functionally distinct motion processing pathway (Gilaie-Dotan, 2016). However, motion processing recruits a network of cortical regions. Motion-sensitive areas in the dorsal stream areas include V3A (e.g., Braddick et al., 2001; Dumoulin, Baker, Hess, & Evans, 2003; Smith, Greenlee, Singh, Kraemer, & Hennig, 1998; Sunaert, van Hecke, Marchal, & Orban, 1999; Tootell et al., 1997), V6 in the dorsal parietal occipital sulcus (Cardin & Smith, 2010; Pitzalis et al., 2010), as well as anterior and inferior sections along the intraparietal sulcus (IPS; Bremmer et al., 2001; Helfrich, Becker, & Haarmeier, 2013; Holliday & Meese, 2008; Konen & Kastner, 2008; Orban et al., 2003, 2006; Sunaert et al., 1999; Wall & Smith, 2008). Global motion tasks also recruit ventral cortical areas (Braddick, O'Brien, Wattam-Bell,

Atkinson, & Turner, 2000; Braddick et al., 2001), including parts of the lingual and fusiform gyri (Orban et al., 2003; Sunaert et al., 1999).

Figure 1.2 Two-stage model of global motion perception.

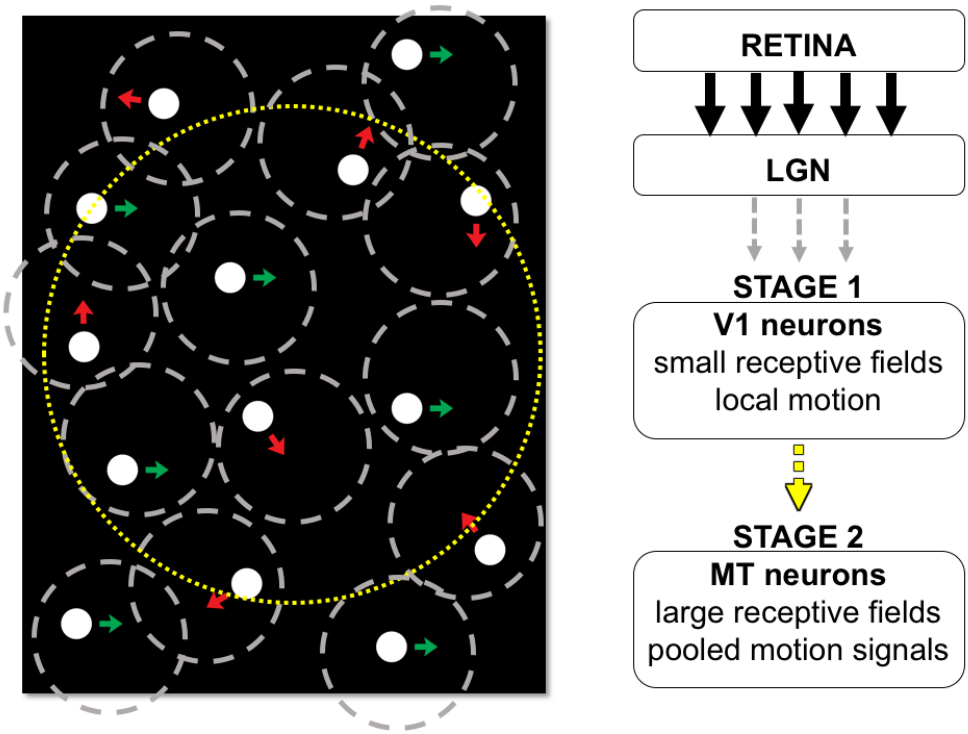

Note. According to the two-stage model of global motion perception, local motion vectors are computed in cortical area V1, and combined in cortical area MT for a global percept.

As will be discussed below, global motion tasks are widely used in studies of development and disorder. Rather than reflecting the sort of motion information we encounter in everyday life, these tasks use impoverished stimuli to probe the sensitivity of the cortical networks that underlie the ability to integrate local signals across time and space for a global percept. Performance is taken as an indicator of the maturity or resilience of these networks, which are involved in many visuospatial tasks. For example, motion coherence thresholds and stereoacuity are correlated in young children (Yu et al., 2013; Chakraborty et al., 2015), possibly reflecting parallel development of these functions as V5/MT+ matures: area MT in healthy macaques represents the binocular area of the visual field (Gattass et al., 2005), is sensitive to binocular disparity (Maunsell & van Essen, 1983), and are able to integrate motion and disparity signals (Bradley, Qian, & Andersen, 1995; Krug & Parker, 2011). Coherence thresholds are also

correlated with some measures of reading (Boets, Vandermosten, Cornelissen, Wouters, & Ghesquere, 2011; Talcott, Witton, McLean, Hansen, Rees, Green, & Stien, 2000) and math skills (Boets, De Smedt, & Ghesquiere, 2011) in typically-developing children. In addition to the amblyopic deficits described in this dissertation, there are a broad range of disorders that are associated with abnormal global motion processing, although there are some inconsistent reports on the presence of deficits as will be discussed below. These include autism (Milne, Swettenham, Hansen, Campbell, Jeffries, & Plaisted, 2002; Pellicano, Gibson, Maybery, Durkin, & Badcock, 2005; Spencer, O'Brien, Riggs, Braddick, Atkinson, & Wattam-Bell, 2000), bipolar disorder (O'Bryan, Brenner, Hetrick, & O'Donnell, 2014), learning disorders such as dyslexia (Cornelissen, Richardson, Mason, Fowler, & Stein, 1995; Talcott, Hansen, Assoku, & Stein, 2000) and dyscalculia (Sigmundsson, Anholt, & Talcott, 2010), long-term MDMA drug use (White, Brown, & Edwards, 2014), pre-term birth (Guzzetta et al., 2009; Taylor, Jakobson, Maurer, & Lewis, 2009), prenatal exposure to alcohol (Chakraborty, Anstice, Jacobs, LagAsse, Lester, Wouldes, & Thompson, 2015; Gummel, Ygge, Benassi, & Bolzani, 2012), schizophrenia (Chen, Bidwell, & Holzman, 2005; Chen, Nakayama, Levy, Matthysse, & Holzman, 2003), and Williams syndrome (Atkinson et al., 2003; Atkinson et al., 1997; Palomares & Shannon, 2013).

1.3 Global motion perception in typical development

Psychophysical coherence thresholds for direction discrimination in random dot global motion tasks have been shown to be adult-like at ages as young as three months (measured via eye movements; Blumenthal, Bosworth, & Dobkins, 2013), three years (Parrish et al., 2005), or six years (Ellemberg, Lewis, Maurer, Brar, & Brent, 2002). Other studies have shown coherence thresholds to be immature at age two years (measured via eye movements; Yu et al., 2013) or five years (Ellemberg et al., 2004; Ellemberg et al., 2003; Ellemberg et al., 2010; Narasimhan & Giaschi, 2012), with adult-like performance reached by 12 years (Hadad, Maurer, & Lewis, 2011) or 14 years (Bogfjellmo et al., 2014). Similarly, motion-defined form tasks using random-dot stimuli have shown maturation by age 7 years (Hayward et al., 2011; Parrish et al., 2005), 10 years (Gunn et al., 2002), or 15 years (Schrauf, Wist, & Ehrenstein, 1999), depending on the stimulus.

There are many spatial and temporal parameters in a global motion stimulus that, when varied, can produce a change in coherence thresholds. When changes in parameters *differentially*

impact performance in children and adults, this is an important indicator of the trajectory of the developing motion system. In addition to implications for understanding the developing motion system, a consequence of this differential impact of stimulus parameters on coherence thresholds is that it may lead to discrepancies in the literature with respect to when motion perception is fully mature. This is likely why the literature provides such a wide range of estimates for the age at which global motion reaches maturity. Relevant parameters may include the density of a stimulus (typically measured in dots per square degree) and dot lifetime (the number of animation frames for which a signal dot continues in the signal direction before being replotted in a random direction). For example, while adult performance remains unchanged with changes in density, children perform more adult-like for more dense stimulus arrays (Narasimhan & Giaschi, 2012). Limiting the lifetime of signal dots will increase thresholds in control children (Manning, Charman, & Pellicano, 2015) and in adults (Festa & Welch, 1997; Pilly & Seitz, 2009), but no direct comparisons have been made between the age groups to determine if they are impacted to the same extent.

Dot speed is also important. For example, global motion perception is more immature for slow than for fast speeds (Bogfjellmo, Bex, & Falkenberg, 2014; Narasimhan & Giaschi, 2012). A similar effect of speed on the maturation of motion perception has been found for global motion using Gabor patterns (Ellemberg et al., 2004; Ellemberg et al., 2010), grating direction discrimination (Falkenberg, Simpson, & Dutton, 2014), motion-defined form (Hayward, Truong, Partanen, & Giaschi, 2011), radial flow (Joshi & Falkenberg, 2015), dot rotation (Kaufmann, 1995), and speed discrimination (Ahmed, Lewis, Ellemberg, & Maurer, 2005; Manning, Aagten-Murphy, & Pellicano, 2012). Minimum velocity thresholds decrease with age for tasks using moving bars (Aslin & Shea, 1990) or motion-defined form (Giaschi & Regan, 1997; Parrish et al., 2005), suggesting a prolonged fine-tuning of mechanisms underlying slow motion perception even when mastery of a task at higher speeds has occurred.

The speed of signal dot movement in deg/s, however, does not fully characterize the spatiotemporal displacement properties of a global motion stimulus. The speed of a motion stimulus depends on a ratio of spatial and temporal displacements, that is, the distance a dot is offset between each pair of animation frames (Δx), and the duration of a single animation frame before the next is displayed (Δt). Coherence thresholds in adults can vary when the underlying spatial (Δx) and temporal (Δt) displacement parameters are changed but their ratio, and hence

stimulus speed, remains the same (Arena, Hutchinson, & Shimozaki, 2012). Crucially, the effect of stimulus parameters on coherence thresholds can depend on the age of the observer. While coherence thresholds of young macaques and children also vary as a function of Δx and Δt displacement components, both groups show greater motion sensitivity for stimuli comprised of larger spatial displacements regardless of Δt (macaques: Kiorpes & Movshon, 2004; children: Meier & Giaschi, 2014). Consistent with this, Hou, Gilmore, Pettet, and Norcia (2009) found visually evoked potential (VEP) responses in 4-6 month old infants were maximal for large spatial displacements, suggesting the sensitivity of the developing motion system is tuned for faster speeds early in life. This finding indicates that development unfolds in a coarse-to-fine fashion such that sensitivity for large spatial displacements is mature early in life, while sensitivity to smaller spatial displacements, regardless of speed, is improved with development.

In previous work that I conducted for my Master's thesis comparing global motion coherence thresholds in children aged 4–6 years to adults (Meier & Giaschi, 2014), I demonstrated that some of the discrepant maturational age estimates can be accounted for by taking spatial displacement parameters into account. Children demonstrated greater immaturities for small displacements, which correspond to slow speeds, and more adult-like responses for large displacements, which correspond to faster speeds. This concept is demonstrated in Figure 1.3. This means that for a given speed, whether a child displays mature performance or not can depend on the Δx parameter of the motion stimulus. In addition to indicating that sensitive periods in development rely on the spatial and temporal frequency content of a motion sequence and not solely on motion speed, this result clarified some discrepancies in prior work that did not support the idea that slow speeds take longer to mature. For example, Hadad et al. (2011) found late maturation for both slow and fast speeds. However, they used small Δx displacements to create both speeds, which may explain why they did not capture any age-by-speed interactions. Parrish et al. (2005), on the other hand, found young children showed mature performance using a slow speed stimulus. This stimulus used a large Δx parameter, which may explain the early maturation described in this work.

Figure 1.3 Motion sensitivity as a function of spatial displacement, for children and adults.

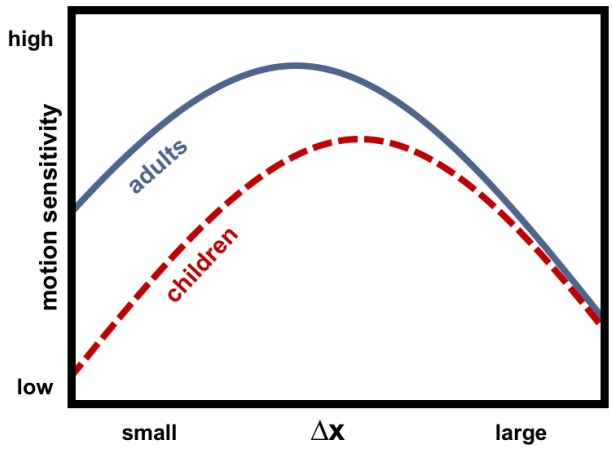

Note. In prior work (Meier & Giaschi, 2014), I demonstrated that children showed greater immaturities for small displacements and more adult-like responses for large displacements. This suggests a coarse-to-fine pattern of development for motion sensitivity, in which the visual system shows mature performance for stimuli that recruit neurons tuned for large displacements earlier in life, with performance for small displacements reaching maturity later in life.

Taken together, these findings indicate that mature performance is reached at a later age for smaller spatial displacements, but provide no indication of what this age might be. Additionally, the pattern of coherence thresholds obtained in my previous study (Meier & Giaschi, 2014) suggested that maturity at medium-to-small displacements may be reached earlier in life for stimuli presented with a shorter temporal displacement and further evidence is necessary to confirm whether or not this is the case. *To further describe the trajectory of motion development in humans, the first study of my dissertation, described in Chapter 3, was designed to track performance on a global motion direction discrimination task across age into young adulthood, as a function of different stimulus parameters.* I predicted that adult-like performance would be reached latest in childhood for stimuli using the smallest spatial displacement, and the shortest temporal displacement. Consistent with my prediction, I found that performance for the smallest displacement was reached in the middle teenage years. Maturational trajectory was the same for both temporal displacements I assessed.

1.4 Motion perception during abnormal development

Observers with amblyopia show deficits in global motion perception when monocularly viewing with the amblyopic eye (Aaen-Stockdale & Hess, 2008; Constantinescu, Schmidt, Watson, &

Hess, 2005; Hou, Pettet, & Norcia, 2008; Knox, Ledgeway, & Simmers, 2013; Simmers, Ledgeway, Hess, & McGraw, 2003; Simmers, Ledgeway, & Hess, 2005; Simmers, Ledgeway, Mansouri, Hutchinson, & Hess, 2006; Thompson et al., 2011). Global motion deficits cannot be fully accounted for by stimulus visibility due to poor acuity or contrast sensitivity deficits in the amblyopic eye (Simmers et al., 2005; Simmers et al., 2003; Hess, Mansouri, Dakin, & Allen, 2006; Aaen-Stockdale & Hess, 2008). Deficits in monocular viewing with the fellow eye have also been identified, but these are slightly attenuated relative to those measured in the amblyopic eye, at least in adults (Simmers et al., 2003; Simmers et al., 2006). Aaen-Stockdale, Ledgeway, and Hess (2007) found global motion deficits in both eyes of similar magnitude, but when contrast sensitivity deficits were controlled for in both eyes, persistent fellow eye deficits were smaller in magnitude than amblyopic eye deficits. The disruption of typical binocular development may lead to impaired motion processing in either eye, due to abnormal maturation of motion-responsive regions. For example, cells in macaque MT respond to motion presented to either eye (Kiorpes, Walton, O'Keefe, Movshon, & Lisberger, 1996; Maunsell & van Essen, 1983). This supports the notion that atypical development of binocularly-sensitive motion regions may be responsible for deficits observed in the amblyopic eye *and* the fellow eye.

Consistent with the principles of the last-in-first-out model of disruption during sensitive periods, children with amblyopia have shown speed-tuned deficits for slow, but not fast, motion-defined form tasks (Hayward et al., 2011). Similarly, speed-tuned deficits have been shown in global motion tasks for other visual developmental disorders (e.g., autism: Manning, Charman, & Pellicano, 2013; reading difficulties: Edwards et al., 2004; Kassaliete, Lacis, Fomins, & Krumina, 2015). Similar to the discrepancies reported in the typical development of global motion, motion perception in amblyopia has reported to be deficient in some studies, but relatively spared in others (e.g., Ellemberg et al., 2002; Ho et al., 2005; Ho & Giaschi, 2006; Wang et al., 2007). As noted above, changes in the spatio-temporal parameters of a global motion stimulus can differentially elicit changes in performance for children and adults. Likewise, differences in the dot displacement parameter Δx may explain why not all studies have shown global motion deficits in children with amblyopia. Figure 1.4 illustrates this concept. For example, no significant group difference in coherence thresholds between children with amblyopia and age-matched controls were found by Ho et al. (2005), Ho and Giaschi (2006), and Wang et al. (2007). Given that young children demonstrate mature performance for the global

motion stimulus used in these studies (Parrish et al., 2005), a lack of deficit in children with amblyopia may not be surprising. On the other hand, studies that have found elevated thresholds in both the amblyopic and fellow eyes of participants with amblyopia (e.g., Constantinescu et al., 2005; Simmers et al., 2003; Simmers et al., 2006) generally employ global motion stimuli with faster speeds. Macaques with amblyopia show motion sensitivity functions that are depressed overall, and shifted to larger Δx (corresponding to faster speeds; Kiorpes, Tang, & Movshon, 2006). If the aspects of motion perception that typically mature early are robust to the effects of amblyopia, these apparently discrepant findings may be resolved: deficits in global motion perception may only be detected, regardless of speed, with a stimulus that is sensitive to developmental differences.

Figure 1.4 Motion sensitivity as a function of spatial displacement, for children with typical and atypical visual development.

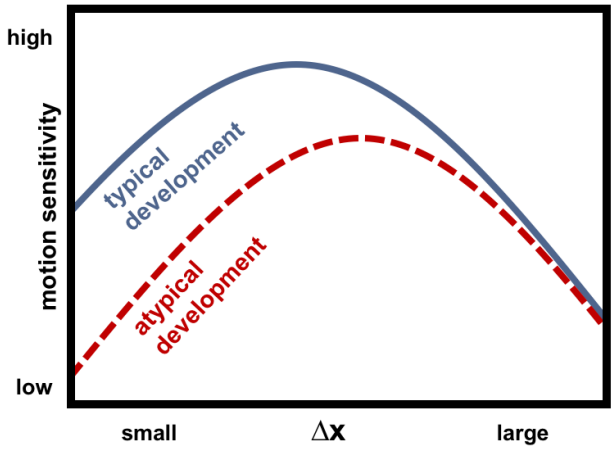

Note. Compare this figure with Figure 1.3, above. Children with amblyopia and other disorders that impact the development of vision may only show deficiencies in motion sensitivity for stimulus parameters that develop later in life.

The presence of motion perception deficits in amblyopia may also vary by clinical factors such as etiological subtype, binocular function and depth of amblyopia. Performance thresholds in aspects of spatial vision such as Vernier acuity have been shown to vary by subtype, such that participants with strabismic amblyopia tend to perform worse than participants with anisometropic amblyopia (e.g., Levi & Klein, 1982b), regardless of age of onset (Birch & Swanson, 2000). There is some evidence that children with anisometropic amblyopia perform poorer on global motion tasks than children with strabismic amblyopia (Ho et al., 2005; Ho et al.,

2006), whereas a study with macaques suggests greater deficits in strabismic amblyopia, particularly in the fellow eye at small values of Δx (Kiorpes et al., 2006). Other human studies have found no differences between subtypes on motion tasks (e.g., Giaschi, Chapman, Meier, Narasimhan, & Regan, 2015; Simmers et al., 2003; Simmers et al., 2005) and motion deficits have been shown across subtypes of anisometropic, strabismic, and ansio-strabismic amblyopia (e.g., Aaen-Stockdale & Hess, 2008; Simmers et al., 2006; Thompson et al., 2011), as well as deprivation amblyopia (Constantinescu et al., 2005). There is some suggestion that binocularity, rather than etiology, may be a better predictor of deficits in the amblyopic visual system (McKee, Levi, & Movshon, 2003). Poor stereoacuity in participants with amblyopia has been shown to correlate with motion perception deficits (e.g., Knox et al., 2013). However, it has also been shown to correlate with *better* global motion perception (e.g., Ho et al., 2005), whereas other studies showed no correlation (e.g., Ho et al., 2006). Finally, motion perception deficits may be indicative of deeper or more treatment-resistant amblyopia (Ho et al., 2005; Giaschi et al., 1992; Giaschi et al., 2015).

In the second study of my dissertation (Chapter 4), I explored the effects of stimulus parameters with different developmental trajectories on global motion direction discrimination thresholds in children with amblyopia. I also investigated clinical factors in amblyopia to assess whether a predictive relationship exists between these and deficits on global motion tasks. I predicted that performance deficits in amblyopia would match the immaturities studied in Chapter 3: compared to controls, these children would have elevated thresholds for stimuli using the smallest, but not the largest, spatial displacements. I found this to be the case for both amblyopic eye and for fellow eye viewing. I also hypothesized that motion deficits may be associated with clinical characteristics. However, none of the clinical measures assessed had any relationship with the severity of motion deficits on this task.

1.5 Non-motion factors limiting performance in global motion

Thus far, I have assumed that by manipulating the spatial and temporal parameters comprising the speed of a motion stimulus, I am probing the function of a mechanism that operates at a global motion processing stage. However, much information is processed prior to reaching motion integration regions of the brain, and the final two chapters of this dissertation are designed to rule out (or confirm) limitations at these earlier processing stages. In Chapter 5, I

consider the role of spatial integration in limiting performance. In Chapter 6, I investigate the extent to which an oculomotor factor, fixation stability, may account for poor performance.

1.5.1 Spatial factors

Spatial integration refers to the general ability to combine visual cues in a stimulus spanning a large area of the visual field into a cohesive percept. This information is distributed across multiple receptive fields, presumed to be subserved by facilitatory long-range lateral connections between cortical cells in V1 (Gilbert, 1998; Li, 1998). If children show limitations in spatial integration, a stage prior to global motion integration, then the immaturities and deficits shown in the studies above may not solely be a function of motion processing mechanisms.

Spatial integration shows long developmental trajectories, similar to motion perception: sensitivity for Glass patterns (detecting coherent structure from an array of dot pairs) becomes adult-like between the ages of 6–9 years (Lewis et al., 2004), and contour detection thresholds (detecting correlated orientations in an array of Gabor patches) improve until at least age 14 (Hadad et al., 2010; Kovács et al., 1999). In developing macaques, Glass pattern detection (Kiorpes, Price, Hall-Haro, & Movshon, 2012) and contour integration (Kiorpes & Bassin, 2003) mature between 2–3 years of age (equivalent to 8–12 human years). These longer developmental trajectories leave these visual functions susceptible to disruption in disorders such as amblyopia. For example, children with deprivation amblyopia show deficits in Glass pattern detection (Lewis et al., 2002), and adults with strabismic amblyopia show deficits in Glass pattern discrimination even after treatment (Joshi, Simmers, & Jeon, 2016). Additional studies in adults (Rislove et al., 2010) and macaques (Kiorpes, 2006) with amblyopia indicate these deficits appear selectively at small spatial scales. In all of these studies, Glass pattern perception is deficient in both eyes of observers with amblyopia compared to controls, though the deficits in the fellow eye are typically smaller in magnitude. Similarly, children (Chandna, Pennefather, Kovács, & Norcia, 2001; Chandna, Gonzalez-Martin, & Norcia, 2004), adults (Kovács et al., 2000; Levi et al., 2007), and macaques (Kozma & Kiorpes, 2003) with amblyopia all show deficits in contour integration, though there is some evidence that contour integration can improve with treatment for amblyopia (Chandna et al., 2004).

This evidence highlights the fact that spatial factors may potentially mitigate the apparent motion perception immaturities observed in children and the deficits observed in amblyopia.

Thus, it is important to consider manipulations of spatial aspects of motion stimuli that may impact performance by increasing the available motion energy (Adelson & Bergen, 1985) in a stimulus. Density is one such parameter. Barlow and Tripathy (1997) assessed performance for global motion stimuli from 1.7 to 111 dots/deg^2 and found only a very small improvement in thresholds (slope = -0.05) with increases in density. Thresholds in adults appear invariant to changes in density for a range of 1 to 30 (Narasimhan & Giaschi, 2012) or 1.5 to 12.2 (Talcott, Hansen, Assoku, & Stein, 2000) dots/deg^2. However, these studies also found that typically-developing children (Narasimhan & Giaschi, 2012) and adults diagnosed with dyslexia, a developmental disorder that can also disrupt motion perception (Talcott et al., 2000), perform better when presented with more dense displays when all other stimulus parameters are held constant. It is possible that stimuli with greater density are advantageous for performance in children and observers with visual dysfunction, while the performance advantage for adults plateaus at far lower densities. In this way, global motion immaturities and deficits may be exaggerated when assessments are made with very sparse displays. Dense dot displays, on the other hand, may yield mature performance. This could explain, in part, why Parrish et al. (2005) found adult-like performance in young children: in addition to large values of Δx, these stimuli were presented at a relatively high density of 32 dots/deg^2.

Another way to increase the available motion energy in a stimulus is through increasing the area covered by a motion stimulus. In my previous work (Meier & Giaschi, 2014) and in the experiments presented in Chapters 3, 4, and 6, I have used stimuli that are square patches measuring 7.7^2 deg, for total area covering 59.3 deg^2. In healthy adults, both motion detection and direction discrimination thresholds decrease logarithmically with increases in stimulus area between 0.25 to 16 deg^2 (Downing & Movshon, 1989). Barlow and Tripathy (1997) also noted a logarithmic decrease in direction discrimination thresholds as stimulus area was increased from 3 to 12 deg^2, with only small improvements for areas larger than this, up to 171 deg^2. From this evidence, it seems unlikely that adult performance would improve with stimulus areas larger than I have used previously. However, it is possible that effects of speed on coherence thresholds may interact with effects of stimulus area. If so, the developmental differences observed selectively for slow speeds in Meier and Giaschi (2014) and in Chapter 3 may be abolished if children are presented with larger stimulus areas. Pilly and Seitz (2009) determined that performance improvements from 8 to 18 deg^2 do not interact with speed, using speeds of 4 and 12 deg/s.

However, these are not as extreme as the slow (0.3 and 1 deg/s) and fast (10 and 30 deg/s) speeds I assessed previously. Minimum displacement thresholds for grating stimuli are unaffected by stimulus area unless the stimuli are presented in the periphery (Boulton, 1987), suggesting that perception of global motion using small Δx displacements may be unaffected by stimulus area. However, it has been established that maximum Δx displacement thresholds can increase as stimulus area increases (Baker & Braddick, 1982; Chang & Julesz, 1983; Eagle & Rogers, 1997), and as retinal eccentricity increases (Baker & Braddick, 1985a). This finding indicates that larger stimulus areas that cover more of the periphery may shift to or recruit additional motion mechanisms tuned to large or coarse displacements, and in turn, faster speeds. In fact, the size of a direction-selective receptive field in macaque MT is positively correlated with its maximum detectable spatial displacement (Mikami et al., 1986), and electrophysiological MT responses match psychophysical responses well at faster speeds (Newsome, Mikami, & Wurtz, 1986).

Taken together, these previous findings suggest that the healthy adults in my studies will show better performance with increased stimulus area for fast, but not slow, speeds (when speed is manipulated by keeping Δt constant and changing Δx). To my knowledge, no one has assessed the effect of area in children or in observers with amblyopia or other disorders that impact visual development. Therefore, it is unknown if stimulus area has a differential effect on performance in these populations. Given that increases in stimulus density can lead to improved performance in children, it is important to investigate whether increases in stimulus area may have a similar effect. *The third study of this dissertation (Chapter 5) is designed to determine whether adults show differential effects of area for slow and fast stimuli; and, more importantly, whether manipulating stimulus area has the same impact in children.* While I predict that the performance of children will be immature for slow but not fast speeds, I am specifically interested in whether stimulus area and age group have an interactive effect on coherence thresholds. I found that coherence thresholds in either age group did not change as a function of stimulus area for slow and medium speeds, but improved similarly as a function of area for the fast speed. Thus, stimulus area is not likely a mitigating factor for children's immature performance on slow-speed motion tasks.

1.5.2 Eye movements

Fixations are not perfectly stable. For example, microsaccades are small, high-velocity jerks of the eye that occur several times per second when a healthy observer is making a fixation. These movements are functional, since an image on a perfectly still retina will fade after a few hundred milliseconds, and they may also assist with corrective fixation control (for reviews see Martinez-Conde, Otero-Millan, & Macknik, 2013; Rolfs, 2009). Of interest to my dissertation is whether the fixation stability of an observer can impact the perception of global motion during direction-discrimination tasks. Studies with infants (Blumenthal et al., 2013) and two-year-olds (Yu et al., 2013) have used optokinetic responses to global motion stimuli as indicators of direction discrimination ability to assess coherence thresholds. Microsaccade activity predicts the direction of perceived motion in an ambiguous signal (Laubrock, Engbert, & Kliegl, 2008), suggesting that fixational eye movements may influence direction discrimination in global motion. However, no studies have directly investigated the effect of fixation stability on global motion coherence thresholds. Instability is likely to interfere with the alignment of smaller finely-tuned motion-sensitive receptive fields, whereas larger receptive fields making coarse matches between a dot in two positions over time may be robust to some retinal noise. Indeed, minimum Δx displacement thresholds for random dot patterns are correlated with fixation stability (Murakami, 2010; Tong, Lien, Cisarik, & Bedell, 2008). Thus, if fixation stability does affect coherence thresholds, it may have a selective impact on stimuli using the smallest spatial displacements, typically corresponding to slower speeds.

Fixation stability may underlie developmental differences on slow global motion tasks if stability becomes adult-like at a commensurate rate. Research on stability in children is sparse, however. A large-scale cross-sectional study of microsaccades during binocular visual search from age 4 to 66 years determined that the frequency of microsaccades increases very slightly with age ($\beta = 0.005$ Hz per year; Port, Trimberger, Hitzeman, Redick, & Beckerman, 2016), though a spline-fit to the data suggests the steepest increase in microsaccade frequency occurs between 4 and the late teenage years. Additionally, the density of fixations around a stationary fixation target increases between the ages of 4 and 15 years (Aring, Grönlund, Hellström, & Ygge, 2007). This suggests a similar trajectory for the stability of gaze and coherence thresholds on slow-speed global motion tasks. However, Seemiller, Port, and Candy (2018) found that the dispersion area of fixations to binocularly-presented random noise targets was similar for 4- to

10-week old infants and adults with healthy vision, and no studies have investigated the stability of fixation to moving stimuli in young children.

Poor fixation stability in amblyopia, on the other hand, has been well-established in the literature. Eye movement abnormalities have been documented in both anisometropic and strabismic amblyopia, which include increased latency and decreased precision when making saccades (McKee, Levi, Schor, & Movshon, 2016; Niechwiej-Szwedo, Goltz, Chandrakumar, Hirji, & Wong, 2010, Schor, 1975), abnormal vergence responses to disparity targets (Kenyon, Ciuffreda, & Stark, 1980; 1981), and abnormal patterns of smooth pursuit that depend on amblyopic subtype (Ciuffreda, Kenyon, & Stark, 1979; Raashid, Liu, Blakeman, Goltz, & Wong, 2016; Schor, 1975). Of importance to the current work, children and adults with amblyopia have poorer stability than control observers when viewing a stationary target with the amblyopic eye (Srebro, 1983; Subramanian, Jost, & Birch, 2013), including when viewing fixation targets binocularly (González, Wong, Niechwiej-Szwedo, Tarita-Nistor, & Steinbach, 2012). Stability in the fellow eye is usually equal, or slightly reduced, when compared to age-matched control eyes. Moreover, greater instability is associated with poorer visual acuity in the affected eye (Chung, Kumar, Li, & Levi, 2015; Shaikh, Otero-Millan, Kumar, & Ghasia, 2016) and poorer stereoacuity (Birch, Subramanian, & Weakley, 2013; Subramanian, Jost, & Birch, 2013). In fact, healthy observers wearing a +3 dioptre lens, which led to an acuity of 0.53 logMAR (approximately 20/67 Snellen), showed drastic decreases in fixation stability (Vikesdal & Langaas, 2016). Some authors have suggested that abnormal fixation patterns in amblyopia reflect an oculomotor adaptation in an attempt to increase contrast sensitivity (Shi et al., 2012), and others have found improved stability in the amblyopic eye when the contrast to each eye is psychophysically balanced to reduce interocular suppression (Raveendran, Babu, Hess, & Bobier, 2014). While fixation stability does improve with treatment-related increases in visual acuity for the amblyopic eye, fixation stability can remain abnormal in children who have completed treatment successfully (reaching at least 0 logMAR, or 20/20 Snellen; Carpineto et al., 2007).

Given that less stable fixation is predicted to have a more detrimental effect on the slower stimuli created with smaller Δx displacements, and a common trait in amblyopia is fixation instability, it is possible that deficits in motion perception may be a function of poor eye stability in the participants with amblyopia, rather than deficient motion mechanisms per se. While it is

already known that observers with amblyopia have less stable eye fixations, it is not known if the degree of instability is associated with the magnitude of global motion deficits. *The final study in my dissertation (Chapter 6) is designed to determine the relationship between fixation stability and motion coherence. I have investigated this relationship in healthy controls, to determine if an individual's fixation stability predicts their motion coherence threshold and whether fixation stability varies parametrically with stimulus coherence level.* I found no evidence that fixational stability is related to performance on a global motion task at either speed in healthy controls.

1.6 Dissertation overview

Chapter 2 describes the general research methods used in this dissertation. In Chapter 3, I examine the development of motion perception by expanding my previous work in 5-year-old children (Meier & Giaschi, 2014) to a visually healthy cross-section of participants aged 7 years through young adulthood in order to describe the maturational trajectory of global motion perception as a function of spatio-temporal stimulus parameters Δx and Δt. In Chapter 4, I assess the hypothesis that aspects of motion perception identified in Chapter 3 to reach maturity latest in development will show the greatest impairment in children with a history of amblyopia, while those that mature earlier in life will be spared. Next, I examine two spatial effects that may at least partially account for the immaturities and deficits in global motion perception described in Chapters 3 and 4 of this dissertation: the stimulus-driven effect of area (Chapter 5), and the observer-driven effect of fixation stability (Chapter 6). I conclude with a discussion in Chapter 7 that integrates the results described in this dissertation and contextualizes these findings in a broader framework.

Chapter 2: General methodology used in this paper

2.1 General methods

All work contained within this dissertation was carried out in accordance with the Code of Ethics of the World Medical Association (Declaration of Helsinki) and approved by the University of British Columbia's Children and Women's Clinical and Behavioural Ethics Board. Informed consent was obtained from adults or parents, and children gave written (or verbal, if under 7 years of age, as in Chapter 5) assent.

2.2 Participant recruitment

All healthy control participants in these studies were recruited from the community. These participants had normal or corrected-to-normal vision and no self- or parental-reported visual, developmental, or cognitive disorders. Children with a history of unilateral amblyopia and no developmental, cognitive, or additional visual disorders aside from strabismus were recruited from the Ophthalmology Clinic at BC Children's Hospital.

2.3 Visual acuity and stereoacuity

For each participant, visual acuity was assessed using the Regan high-contrast letter chart (Regan, 1988) and stereoacuity was assessed using the Randot Preschool Stereoacuity Test (Stereo Optical Co., Inc.). Children who could not reliably name letters were assessed with the Lea Symbols picture chart (Hyvärinen, Näsänen, & Laurinen, 1980). These data were used to exclude control participants with poor vision from data analysis. Inclusion criteria are listed for each study in the Chapters below.

2.4 Apparatus

An Intel Core i7 Macintosh MacBook Pro running MATLAB R2015a (The MathWorks, Inc.) equipped with the Psychophysics Toolbox extension version 3.0.12 (Brainard, 1997; Kleiner, Brainard, & Pelli, 2007; Pelli, 1997) was used to generate the stimuli for these experiments. Unless described otherwise, a BenQ XL2420T LED-backlit LCD monitor at a resolution of 1920

× 1080 and a 60 Hz refresh rate was used to present the stimuli. Participants were seated in a dimly-lit room at a viewing distance of 1 m. Responses were collected using a Gravis Gamepad Pro controller.

2.5 Stimuli

Unless described otherwise, the motion stimulus parameters were the same as those used in my previous study (Meier & Giaschi, 2014) and were chosen to approximate those of Kiorpes and Movshon (2004). Each stimulus consisted of an array of 64 white (260 cd/m^2) dots, 1 arcmin diameter, on a black (0.7 cd/m^2) background. Stimuli subtended a 7.7 x 7.7 deg square area in the centre of the screen, yielding a density of 1.1 dots/deg^2 in each frame (or 1.7% of area). Signal dots moved left or right. A white noise algorithm controlled dot movement: on each update of an animation frame, a dot was selected to be a signal dot with a probability equal to the coherence value, which could range from 0 to 1. The remaining dots were re-plotted in random locations. Thus, signal dot lifetime was determined probabilistically, such that the probability of each signal dot disappearing was equal to the stimulus coherence level on any given trial. Stimulus duration was 600 ms.

2.6 Procedure

Unless described otherwise, the procedure for measuring coherence thresholds began with a slideshow that presented instructions for how to play a space-themed game. The study used a two-alternative forced choice procedure in a direction discrimination task: participants were instructed to decide whether they saw a star field moving to the left towards one character, or to the right towards another character. The procedure for controlling stimulus coherence is described in section 2.7 below. For correct responses, a cartoon character and an auditory chime were presented; for incorrect responses, a different cartoon character was presented with no auditory feedback. Staircases were conducted sequentially, such that within a given block, only one threshold for one condition was being estimated with a single staircase.

2.7 Coherence threshold estimation

To estimate coherence thresholds, a hybrid approach was used (Hall, 1981; Leek, Hanna, & Marshall, 1992) in which a staircase was used to control stimulus levels and a psychometric

function was fit to the response data. In general, all psychophysical studies used a two-alternative forced choice procedure with a two-down, one-up staircase controlling stimulus coherence level. The first trial of each staircase began with a coherence of 1 (full coherence). For subsequent trials, coherence levels were decreased (made more difficult) when the participant answered correctly on two trials in a row, or increased (made easier) for one incorrect trial. Stimulus coherence was adjusted in steps of 0.1 for the first three response reversals after which the step size was halved at each reversal until a minimum step of 0.01 was reached. After a minimum of 40 trials, a staircase terminated after 10 response reversals or 50 trials, whichever occurred first. Response reversals at coherence values greater than 0.8 did not contribute to stopping rules in order to prevent early mistakes from impacting the range of coherence values reached by the staircase.

To calculate a coherence threshold for each condition, I fit a Weibull function (Watson & Pelli, 1983) to participants' coherence by accuracy data using a maximum-likelihood minimization bootstrap procedure. The coherence level at the slope of maximum inflection on the Weibull curve (α; 82% correct for a two-alternative forced-choice task; Strasburger, 2001) was defined as threshold. Coherence thresholds were bounded between 0 (completely random motion) and 1 (completely coherent motion). During threshold estimation, the slope (β) of the function was free to vary; initial guess value was set to 3.5. Lapse rate (λ) was fixed to 0.01. A chi-square goodness-of-fit test was used to assess the psychometric function fit for each threshold. Where this goodness-of-fit test failed, trial-by-trial data were inspected and re-fit after removing early mistakes at high coherence levels and/or trials reflecting a coherence level that was presented only once. If fit was not improved, the participant's threshold for this condition was removed from analysis.

Additional details about coherence threshold estimation are described in Appendix A.

Chapter 3: Typical maturation of global motion perception as a function of spatio-temporal stimulus parameters

3.1 Introduction

The goal of the current study was to investigate global motion maturation in children and adults with typical visual development between seven and 30 years of age. In particular, I was interested in quantifying the age at which global motion perception can be considered mature across six different combinations of spatial (Δx = 1, 5, and 30 arcmin) and temporal (Δt = 17 and 50 ms) stimulus parameters. This will expand upon our previous finding showing the effect of these stimulus parameters in children age 4 to 6 years (Meier & Giaschi, 2014), and also provide normative data for future studies involving children with developmental visual disorders.

3.2 Methods

3.2.1 Participants

Participants between the ages of seven and 30 years old were recruited from the community to participate in this study. Recruitment remained open for all age groups until a minimum of 12 participants per year of age were included up to age 17 years, and a minimum of 36 adult participants between age 17 to 30 years were included. Data from some adult participants were collected for a prior study (Meier & Giaschi, 2014) that used the same stimuli as in the current study. In total, 217 participants were recruited. For inclusion in the data analysis, a best-corrected monocular visual acuity score of 0.15 logMAR (1.4 arcmin resolution; equivalent to 20/28 Snellen) or better in both eyes, and stereoacuity of 60 arcsec or better (Birch et al., 2008) were required.

Twenty-four participants (aged 7.2–22.7 years, M = 14.9 years) were excluded for poor visual acuity and/or poor stereoacuity; and eleven participants (aged 7.1–23.4 years, M = 11.0 years) were excluded for failing to complete enough of the experiment within the hour either due to task misunderstanding or motivational difficulties. In all, data from 182 participants were used in the analysis. One participant had data missing from two of the six experimental conditions described below (age 16.3 years); thirteen participants had data missing from one of the six

conditions (age range 7.1 to 24.2 years), and the remaining 168 participants had data for all six conditions.

3.2.2 Stimuli and experimental conditions

The stimuli used in this experiment are described in section 2.5. Two factors were examined in this study: Δx, the spatial displacement of the dots between each pair of animation frames; and Δt, the duration of each frame. The six conditions assessed here are a subset of those assessed in Meier and Giaschi (2014): three Δx values (1, 5, and 30 arcmin) crossed with two Δt values (17 and 50 ms, equivalent to 60 and 20 Hz, respectively). This combination of parameters yielded signal dot speeds of 1, 5, and 30 deg/s in the Δt = 17 ms condition with a dot density over time of 66 dots/deg^2/sec (36 animation frames total), and 0.3, 1.7, and 10 deg/s in the Δt = 50 ms condition with a dot density over time of 22 dots/deg^2/sec (12 animation frames total). The total stimulus duration for all conditions was 600 ms.

3.2.3 Procedure

The procedure for measuring coherence thresholds is described in section 2.6. Prior to beginning experimental trials, eight trials of a practice staircase were conducted binocularly using the parameters of Δx =15 arcmin and Δt = 33 ms. Practice trials were repeated if accuracy was below 5/8 correct. Experimental trials were conducted monocularly with an eye patch covering the eye not being examined. A Latin square was used to determine the condition order for each participant to mitigate order and practice effects.

3.2.4 Data analysis

Our goal for this study was to estimate the age at which performance can be considered mature for each condition, and compare this across conditions. A common practice for determining whether performance can be considered mature is to create bins of ages (e.g., 7 years, 8 years, 9 years, and so on; or 7-8 years, 9-10 years, and so on) and compare each age bin to the adult data by conducting an analysis of variance with multiple-comparison follow-ups to determine significant differences between ages (e.g., Parrish et al., 2005; Hadad et al., 2011; Giaschi et al., 2013). In keeping with this practice and to allow for easy comparison to other papers, I first

present the results of an age-binned analysis of variance. Here, I binned participants into two-year age bands, which gave the following total number of participants per age group: 29 total 7-8 year olds; 35 total 9-10 year olds; 27 total 11-12 year olds; 26 total 13-14 year olds; 26 total 15-16 year olds; and 39 total adults aged 17-30 years old. With this number of participants, I had the ability to detect a medium-sized main effect of age (Cohen's $f = 0.27$) with a power (1-β) of 0.80. For context, the main effect of age in my prior work comparing 4- to 6-year-olds and adults (Meier & Giaschi, 2014) was large (Cohen's $f = 0.97$).

However, there are a few problems with the age-binning approach for our specific research question: quantifying the age at which global motion perception can be considered mature. First, accuracy and precision are lost when a continuous variable, in this case age, is turned into a categorical variable. Moreover, the selection of age bin widths is usually arbitrary and can impact the outcome of the analysis; for example, whether the "true" maturational age falls near the lower limit, middle, or upper limit of an age bin has implications for the calculated mean of the binned data. Finally, this approach does not allow us to directly compare ages of maturation across conditions – it would only allow us to make statements on whether or not children of younger ages appear adult-like for each condition.

For these reasons, I have used a non-parametric approach to estimate maturational age and used a bootstrapping procedure to construct confidence intervals around these estimates in order to compare maturational age across conditions. I have used LOESS smoothing (Cleveland & Devlin, 1988; Gijbels & Prosdocimi, 2010; Jacoby, 2000), a locally-weighted polynomial regression technique, to model our data by fitting a curve to our coherence thresholds as a function of age. While some authors have compared the *developmental rates* of performance across tasks by fitting exponential functions and comparing time constants (e.g., Parrish et al., 2005), this does not allow for direct estimation of maturation age. An additional advantage of the LOESS analysis strategy is that this data-driven approach allows us to assess age-related changes in coherence thresholds without imposing a functional form on any of the trends across all conditions, that is, without assuming any specific mathematical relationships between coherence thresholds and age. While I have selected this procedure because I presume that adults will have the lowest coherence thresholds, this is not a built-in assumption of the statistical model.

I conducted a one-way between-subjects analysis of variance (ANOVA) for each of the six conditions to test the effect of age on coherence thresholds, using a Welch (1951) correction

for heterogeneous variances where appropriate. Children were divided into two-year age bins (7-8 years, 9-10 years, 11-12 years, 13-14 years, and 15-16 years old) and participants 17 to 30 years old were binned into one adult group. Significant age effects were followed up with the Dunnett procedure (Dunnett, 1955; Dunnett, 1964) comparing coherence thresholds of each age bin to the adult bin, using a Welch-Satterthwaite adjustment (Satterthwaite, 1946; Welch, 1947) for degrees of freedom to correct for heterogeneous variances. Our LOESS fitting and bootstrapping procedures were implemented in R (version 3.3.1; R Core Team, 2013) using the *boot* package (version 1.3-18; Canty & Ripley, 2016; Davison & Hinkley, 1997). For each condition, I fit a LOESS curve to coherence thresholds as a function of age using a smoothing parameter of 0.50. Next, I determined the age at which the lowest coherence threshold was achieved in the *fitted* data. The value one standard error above this was taken as a LOESS threshold value, T. I have defined the age of maturation as the age at which performance reaches T. I compared the LOESS fit to T, and took the age at which the fitted values crossed T as our point estimate of the age of maturation. Finally, I constructed a 68% bootstrapped bias corrected and accelerated (BCa) confidence interval (Carpenter & Bithell, 2000; Efron, 1987) around this point estimate, in order to compare estimated ages across all six conditions. Note that the obtained confidence intervals are expected to be asymmetric.

3.3 Results

Mean coherence thresholds for each of the six age bins assessed in the analysis of variance are displayed in Figure 3.1. For stimuli using Δx = 1 arcmin, there was a significant effect of age for both Δt conditions (for Δt = 17 ms, $F(5, 77.2) = 17.12$, $p < .001$; for Δt = 50 ms: $F(5, 76.9) = 16.37$, $p < .001$). Follow-up tests indicated that children aged 7 to 14 years had significantly higher coherence thresholds than adults (for Δt = 17 ms, 7-8 years: Dunnett's $t(42.3) = 8.51$, $p < .05$; 9-10 years: $t(47.5) = 4.80$, $p < .05$; 11-12 years: $t(39.4) = 2.36$, $p < .05$, 13-14 years: $t(43.7) = 2.23$, $p < .05$; for Δt = 50 ms, 7-8 years: $t(33.4) = 7.11$, $p < .05$; 9-10 years: $t(47.2) = 4.73$, $p < .05$; 11-12 years: $t(38.0) = 2.45$, $p < .05$; 13-14 years: $t(37.2) = 3.42$, $p < .05$), and that coherence thresholds for 15-16 year olds were not different from adults (for Δt = 17 ms, 15-16 years: $t(50.8) = 0.82$, $p = .42$; for Δt = 50 ms, 15-16 years: $t(62.7) = 0.07$, $p = .94$). There was also a significant effect of age for stimuli using Δx = 5 arcmin for both Δt conditions (for Δt = 17 ms, $F(5, 74.5) = 6.08$, $p < .001$; for Δt = 50 ms, $F(5, 75.6) = 3.26$, $p = .010$). Follow-up tests

indicated that the 7-10 year olds, in both conditions, had significantly higher thresholds than adults (for Δt = 17 ms, 7-8 years: Dunnett's $t(30.5) = 4.00$, $p < .05$; 9-10 years: $t(42.9) = 2.55$, $p < .05$; for Δt = 50 ms, 7-8 years: $t(30.0) = 2.93$, $p < .05$; 9-10 years: $t(47.0) = 2.67$, $p < .05$). Thresholds for the children aged 11 to 16 were not different from adults (for Δt = 17 ms, 11-12 years: $t(32.8) = 1.36$, $p = .18$; 13-14 years: $t(37.5) = 1.92$, $p = .062$; 15-16 years: $t(59.1) = 1.24$, $p = .22$; for Δt = 50 ms, 11-12 years: $t(35.1) = 1.48$, $p = .15$; 13-14 years: $t(51.3) = 0.74$, $p = .46$ 15-16 years: $t(50.6) = 0.59$, $p = .56$). Finally, there was no effect of age for stimuli using Δx = 30 arcmin (for Δt = 17 ms, $F(5, 174) = 1.06$, $p = .38$; and for Δt = 50 ms, $F(5, 174) = 0.42$, $p = .83$). Notably, the variance in coherence thresholds was not significantly different across age groups for stimuli using Δx = 30 arcmin (by Levene's test using median-deviated scores: $F(5, 174) = 1.44$, $p = .21$; $F(4, 174) = 0.43$, $p = .82$; for Δt = 17 and 50 ms, respectively), supporting the notion that maturation is complete in this condition for all ages.

The results of the LOESS analysis were consistent with the age-binned analysis of variance, and provided point-estimates for the age at which motion perception can be considered mature for each condition. Coherence thresholds are plotted as a function of age, for each condition, in Figure 3.2. Age of maturation for the Δx = 1 arcmin conditions was estimated to be 15.7 (68% CI: 12.1 – 16.5) years and 15.9 (68% CI: 11.5 – 16.46) years for the Δt = 17 ms and 50 ms conditions, respectively. For the Δx = 5 arcmin conditions, age of maturation was estimated to be 10.7 (68% CI: 8.8 – 10.9) years and 12.4 (68% CI: 9.3 – 13.6) years for the Δt = 17 ms and 50 ms conditions, respectively. For both conditions using Δx = 30 arcmin, the model was unable to generate a point estimate or construct a confidence interval around age because the LOESS fit was below T at all ages. This indicates that performance stabilized at adult-like levels before age 7 for these conditions. For clearer comparison across conditions, Figure 3.3 displays these estimated ages. A maturational age was reached earliest in the Δx = 30 arcmin conditions, with maturation occurring sometime before age 7 years. The remaining conditions yielded mature performance later than 7 years: both Δx = 5 arcmin conditions yielded maturational ages in late childhood/early teenage years, and both Δx = 1 arcmin conditions yielded maturational ages in the late teenage years.

To determine if visual acuity was significantly correlated with coherence thresholds in each condition independent of any age effects, I partialled out the effect of participant age in correlations between logMAR visual acuity of the eye used to conduct the task, and coherence

thresholds in each of the six conditions, using a Holm-Bonferroni adjustment (Holm, 1979) for multiple comparisons. Partial correlations between acuity and the three Δx conditions (1, 5, and 30 arcmin, respectively) were 0.14, 0.00, and 0.03 in the Δt = 17 ms condition, and 0.16, 0.16, and -0.11 in the Δt = 50 ms. The largest correlation, 0.16, indicated that acuity explained less than 3% of variance in coherence thresholds for these conditions and was not statistically significant p = .48). Because all participants obtained a stereoacuity of 40 arcsec, with the exception of two younger children who obtained 60 arcsec, I was unable to assess a relationship between stereoacuity and coherence thresholds.

Figure 3.1 Mean coherence thresholds as a function of age.

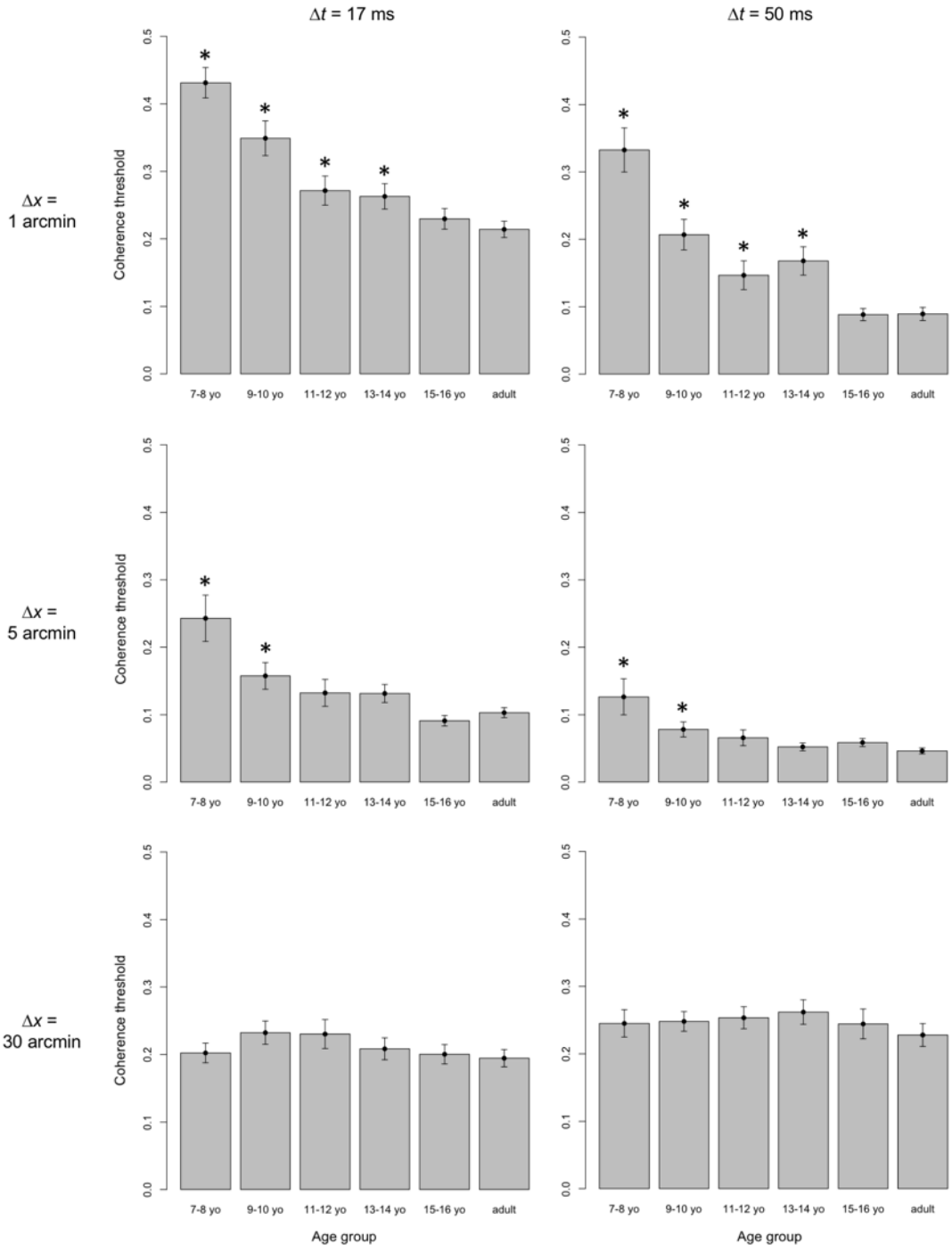

Note. Mean coherence thresholds as a function of two-year age bins for each of the six spatio-temporal stimulus parameter conditions. Error bars indicate standard error. Asterisks indicate age groups that were found to have significantly higher thresholds than the adult group. No significant effect of age was found in either of the Δx = 30 arcmin conditions (bottom two panels).

Figure 3.2 LOESS fits for coherence thresholds as a function of age.

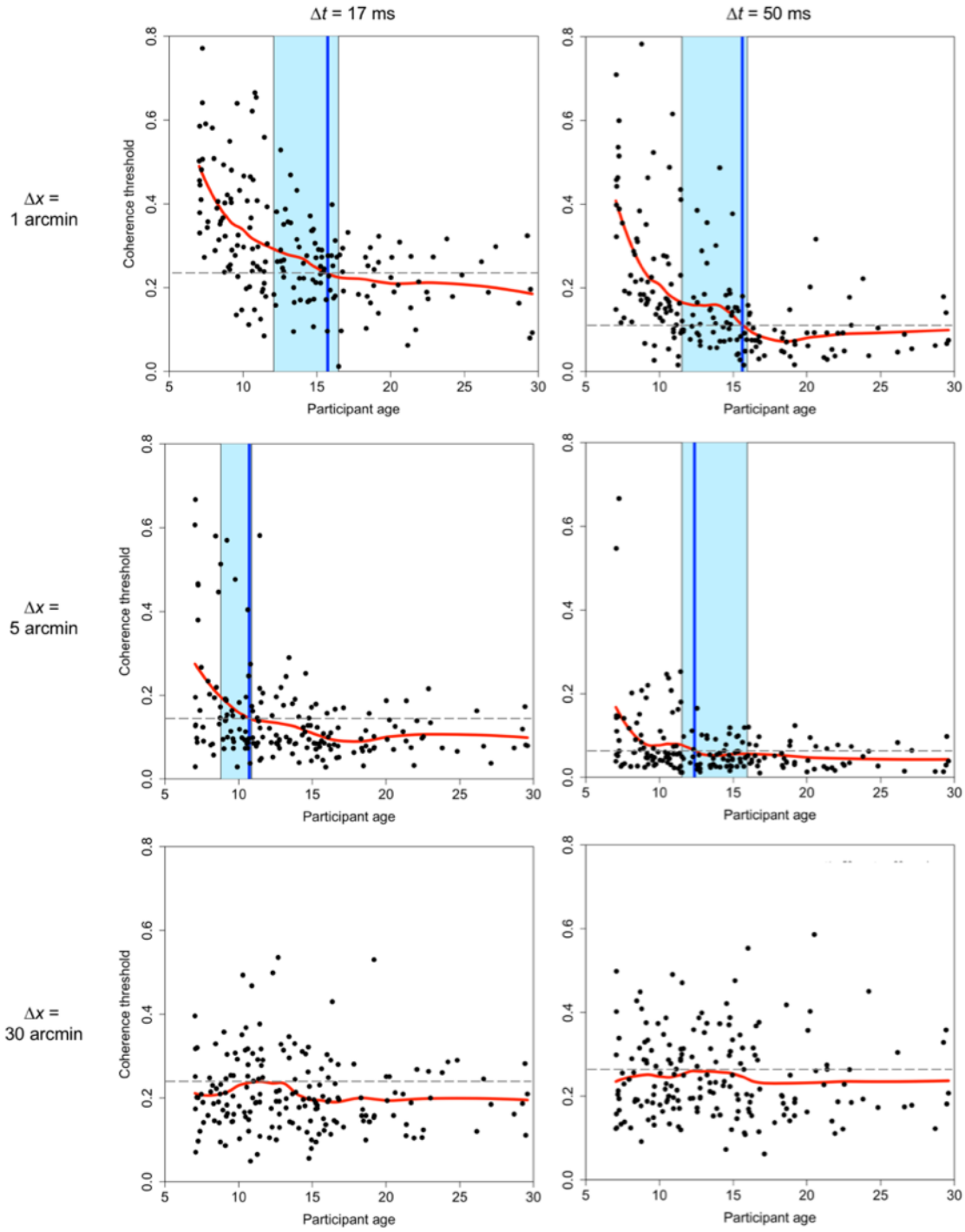

Note. Coherence thresholds as a function of age for each of the six spatio-temporal stimulus parameter conditions. Red lines indicate the model LOESS fit (span = 0.5). The horizontal dashed line represents T, the threshold that the LOESS fit must pass for performance to be adult-like. The age at which the LOESS fit passes T (see text section 3.2.4) is the estimated age of maturation. The point estimate of this age is indicated in dark blue; the shaded lighter blue area indicates the 68% confidence interval around this estimate. The model fits indicated that coherence thresholds for the Δx = 30 arcmin conditions (bottom two panels) were adult-like by age 7, so no age estimates are given.

Figure 3.3 Estimated age of maturation for each of the six spatio-temporal stimulus parameter conditions.

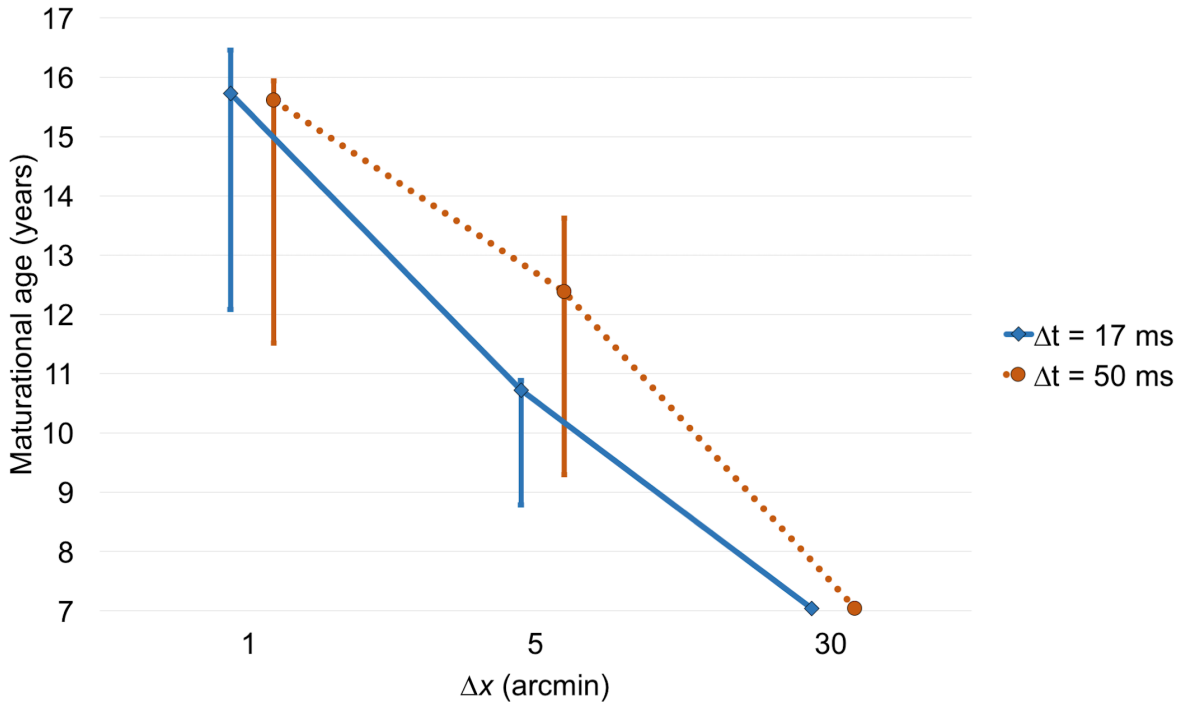

Note. The point estimate of each condition is plotted; error bars indicate the 68% confidence interval around this estimate. Model fits indicated that coherence thresholds for the Δx = 30 arcmin conditions were adult-like by age 7, the youngest age assessed in this dataset, so no confidence intervals are available.

3.4 Discussion

I found that adult-like performance was reached on global motion tasks by age 7 years for a large spatial displacement parameter (30 arcmin), but not reached until 10-12 years for medium (5 arcmin) or 15-16 years for small (1 arcmin) parameters. These results confirmed my prediction that performance on the smallest spatial displacements mature latest in life. I did not find any evidence that performance reaches maturity at an earlier age for longer (50 ms) rather than shorter (17 ms) temporal displacements.

The results of the current study are consistent with our previous work in younger children (4 – 6 years old; Meier & Giaschi, 2014) which found that young children demonstrated immature performance on global motion stimuli with small spatial displacements, but showed adult-like performance on stimuli with large spatial displacements. In that study, performance

was not determined by signal dot speed, since thresholds were mature on medium speeds using larger, but not smaller, displacements. My results are also consistent with research in developing macaques indicating that peak Δx for motion sensitivity decreases as a function of age, regardless of stimulus Δt, until around 3 years of age (Kiorpes & Movshon, 2004). The current study indicates a similar coarse-to-fine pattern of development in humans, with full maturity reached around age 16 years, a developmentally equivalent age for spatial visual function of approximately 4 years in macaques (following the 4:1 rule; Boothe, Dobson, & Teller, 1985).

While I did not conduct formal analyses on changes in variance across age groups and conditions, it is clear from inspection of Figures 3.1 and 3.2 that in the conditions where development is still occurring (small and medium spatial displacements), variation decreases with age. This likely reflects variation from a number of sources that impact development. Stages of development do not begin at precisely the same age; rather, as in many aspects of development, some children will mature earlier than their peers, while others will lag behind. Moreover, this may reflect differences in the slope of children's developmental trajectories, such that some children take more time to reach maturation than others. It is not possible to estimate this slope without conducting a longitudinal study, but doing so may assist in accounting for individual differences in coherence thresholds, particularly in younger children at risk for visual developmental disorders. It is also clear from the data that variance is stable, but highest, in the conditions with the largest displacements, where mature performance is observed for all ages. While I ruled out an influence of visual acuity, this variability may be related to individual differences in D_{max}, the largest displacement for which coherent motion is perceived; larger displacements are not perceived as motion. D_{max} has been shown to be adult-like by 7 years of age (Parrish et al., 2005), though this may also depend on stimulus parameters. In adults, D_{max} is reduced for stimuli with smaller elements (Morgan, Perry, & Fahle, 1997) and lower densities (Eagle & Rogers, 1996), so the large displacement for this condition may be nearing participants' maximum motion displacement limit.

The results of the current study provide a framework for generating predictions about which global dot motion stimuli will elicit the most differences between children and adults in a global motion task, resolving inconsistencies across previous studies. Blumenthal et al. (2013) found near-adult like coherence thresholds in 3-month-old infants using eye-movement responses to large-field stimuli of similar density with Δx = 25 arcmin (Δt = 13 ms), although

these optokinetic responses may not reflect the same processes underlying perceptually-based direction discrimination particularly before the first year of life (Mason, Braddick, & Wattam-Bell, 2003; Morrone, Atkinson, Cioni, Braddick, & Fiorentini, 1999). On the other hand, children aged two years had elevated thresholds compared to adults for stimuli using Δx = 7.8 arcmin displacements (Δt = 17 ms; Yu et al., 2013), and children up to age 11 years were immature on stimuli with Δx = 3 and 14 arcmin (Δt = 13 ms; Hadad et al., 2011). Parrish et al. (2005) found no significant differences between a group of 3 to 4-year-olds compared to adults for stimuli using Δx = 8.5 arcmin, which may not be consistent with the current data; however, with larger variance in the youngest age groups they may not have had the power to detect a small age effect (Hedge's g = 0.63). Moreover, their stimulus had a very long Δt of 107 ms. While the temporal displacement parameters assessed in the current study did not appear to have an effect on maturation of coherence thresholds, this may not be the case for very long (or even very short) Δt.

Chapter 4: The impact of amblyopia on global motion perception as a function of spatio-temporal stimulus parameters

4.1 Introduction

The purpose of this study was to determine the spatio-temporal parameters at which children with amblyopia demonstrate global motion perception deficits. I selected the same subset of the Δx and Δt combinations tested previously in typically-developing 4- to 6-year olds (Meier & Giaschi, 2014) as used in Chapter 3, and measured motion coherence thresholds for children with amblyopia and age-matched controls. Consistent with the last-in-first-out principle, I hypothesized that children with amblyopia would show selective deficits for parameter combinations that were found to be immature in Chapter 3. In addition to group differences, I sought to determine whether motion perception deficits in children with amblyopia were predicted by clinical factors such as etiological subtype, binocular function and depth of amblyopia. I assessed whether a relationship exists between motion deficits and amblyopic eye visual acuity, interocular visual acuity difference, and the number of months a child had undergone occlusion therapy.

4.2 Methods

4.2.1 Participants

4.2.1.1 Patient group

Children with a history of unilateral amblyopia and no developmental, cognitive, or additional visual disorders aside from strabismus were recruited for this study. Twenty-seven children participated in the study; data from one child with a developmental disorder and one child with deprivation amblyopia were discarded, and two children had attention-related difficulties with conducting the full procedure, leaving a total of 23 children with data available for analysis (*M* age = 10.7 years, *SD* = 2.3, *range* = 7.1 – 14.7).

Patient characteristics are listed in Table 4.1. The initial diagnosis of amblyopia was made by an ophthalmologist based on a best-corrected Snellen acuity of 20/30 or worse in the amblyopic eye, 20/25 or better in the fellow eye and a minimum two-line difference in Snellen acuity (equivalent to 0.2 logMAR) between the eyes. A participant was considered to have

anisometropic amblyopia if their visual acuity loss was accompanied by a spherical equivalent difference between the eyes ≥ 1 diopter or an astigmatic difference ≥ 1.5 diopter in the absence of any ocular manifest deviation (Weakley, 2001). The amblyopia subtype was considered to be strabismic if it occurred in the presence of either a heterotropia at distance and/or near or a history of strabismus surgery (Pediatric Eye Disease Investigator Group, 2003). Aniso-strabismic amblyopia was diagnosed if the participant met criteria for both anisometropic and strabismic amblyopia. Twelve of these children had anisometropic amblyopia, eight had strabismic amblyopia, and three had aniso-strabismic amblyopia. At the time of testing, most children had completed amblyopia treatment and several had normal visual acuity in the amblyopic eye; three children were still undergoing occlusion therapy.

Table 4.1 Patient characteristics for children with amblyopia included in data analysis.

		Visual acuity at testing (logMAR)					
Amblyopia subtype	Age (yrs)	Ambly-opic eye	Fellow eye	Refraction at time of testing	Stereo-acuity (arcsec)	Treatment history	Total number of deficits‡
aniso	7.1	0.11 (L)	0.05	R: -0.25 +0.50 x 85 L: +0.50 +0.75 x 90†	40	OT: 37 months	11
aniso	7.8	0.09 (L)	-0.11	R: plano +0.50 x 70 L: -0.25 + 1.75 x 90	40	OT: 42 months	2
aniso	8.2	0.21 (L)	-0.04	R: -0.25 +0.50 x 75 L: -3.25 +2.00 x 120	200	OT: 16 months	9
aniso	10.8	0.36 (L)	0.13	R: +0.75 L: +2.75 +0.75 x 90	NM	OT history unavailable	3
aniso	11.2	0.08 (L)	-0.15	R: plano +1.00 x 95 L: +2.75 +1.50 x 95	100	OT: 17 months	3
aniso	11.6	0.30 (L)	-0.20	R: plano L: +2.00 +2.20 x 90	200	OT: 15 months	4
aniso	11.6	0.43 (L)	-0.08	R: +1.00 L: +7.00 +1.75 x 100	NM	OT: 13 months *	8
aniso	12.0	0.29 (L)	-0.06	R: +1.25 +1.50 x 90 L: plano +4.50 x 85	40	OT: none	1
aniso	13.1	0.15 (R)	-0.20	R: +6.75 +1.75 x 100 L: +4.00 +1.00 x 100	200	OT: 84 months	1
aniso	13.2	-0.01 (L)	-0.09	R: plano L: plano + 1.50 x 90	40	OT: 6 months	4
aniso	14.4	0.18 (L)	-0.20	R: -0.25 L: +8.00	NM	OT: 50 months	2
aniso	14.7	0.01 (R)	-0.08	R: +1.00 L: plano	200	OT: 13 months	2
strab	7.5	0.29 (L)	0.05	R: +2.25 +0.75 x 90 L: +2.25 +0.50 x 85	200	1 surgery; OT: 43 months *	11
strab	7.6	0.10 (L)	0.05	R: +2.25 +1.00 x 95 L: +2.75 +0.75 x 100	NM	2 surgeries; OT: 23 months	5

strab	8.3	0.03 (L)	0.05	R: +2.50 +3.00 x 85 L: +2.25 +2.75 x 95	100	OT: 18 months	10
strab	9.0	0.11 (R)	0.00	R: +2.50 +2.00 x 100 L: +2.50 +1.25 x 80	800	1 surgery; OT: 56 months	2
strab	10.1	0.20 (R)	-0.03	R: +6.50 +2.25 x 100 L: +7.00 +2.00 x 80	100	1 surgery; OT: 10 months	9
strab	11.2	0.43 (R)	-0.03	R: +6.75 +1.00 x 110 L: +7.25 +1.00 x 110	200	1 surgery; OT: 24 months	7
strab	11.5	0.24 (L)	-0.04	R: +1.00 +2.25 x 90 L: +1.00 +2.50 x 90	NM	1 surgery; OT: 53 months	4
strab	13.6	0.36 (L)	0.00	R: +4.50 +3.75 x 80 L: +5.50 +3.50 x 90	NM	OT: 10 months	0
aniso-strab	9.0	0.15 (R)	-0.10	R: +2.50 +0.75 x 95 L: +3.00 +1.75 x 90	800	OT: 58 months *	8
aniso-strab	10.8	0.11 (L)	-0.04	R: +1.00 +1.75 x 20 L: +3.75 +2.00 x 135	NM	OT: 75 months	7
aniso-strab	11.0	0.30 (L)	-0.18	R: +2.00 L: +3.00 +0.50 x 90	NM	OT: 75 months	3

Note: aniso = anisometropic amblyopia; strab = strabismic amblyopia; (L) = left eye amblyopic; (R) = right eye amblyopic; NM = stereoacuity not measurable at the largest disparity tested (800 arcsec); OT = occlusion therapy, * = still undergoing occlusion therapy treatment, † = patient did not meet definition for anisometropia at time of testing but has a history of a 1.5 dioptre spherical equivalent difference between the eyes, ‡ = see text section 4.2.4 for details on how this measure is computed.

4.2.1.2 Control group

For each child with amblyopia, data from two age-matched control children were selected for analysis. These children were participants in the study described in Chapter 3. To be included in the study, control participants needed to have best-corrected monocular visual acuity scores on the Regan high-contrast letter chart (Regan, 1988) of 0.1 logMAR (minimum 1.25 arcmin resolution; equivalent to 20/25 Snellen) or better, and stereoacuity on the Randot Preschool Stereoacuity Test (Stereo Optical Co., Inc.) of 60 arcsec or better (Birch et al., 2008). Data from a total of 46 control children were included in the analysis (*M* age = 10.7, *SD* = 2.3, *range* = 7.0 – 14.8). For an additional analysis, I compared children with amblyopia to 23 *visual acuity*-matched controls. These data came from control children who passed the stereoacuity screening but did not necessarily have visual acuity better than 0.1 logMAR. Children with poor vision were typically those who had not had a recent update to their glasses prescription, or forgot to bring their glasses to the research appointment. None of these control children had a difference in visual acuity between their eyes greater than two lines.

4.2.2 Stimuli and experimental conditions

The stimulus used in the current study was similar to the stimulus used in our previous studies (Meier & Giaschi, 2014; Chapter 3) and is described in section 2.5. Two factors were crossed in the current study: Δx, the spatial displacement of the dots between each pair of animation frames (1, 5, or 30 arcmin); and Δt, the duration of each frame (17 or 50 ms). The same stimulus conditions were used as in Chapter 3. See section 3.2.2 for a full description.

4.2.3 Procedure

Procedures for assessing visual and stereoacuity are described in section 2.3, and for assessing coherence thresholds in sections 2.6 and 2.7. Participants completed eight trials of a practice staircase binocularly using the parameters Δx = 15 arcmin and Δt = 33 ms, then proceeded to the experimental conditions. The motion coherence thresholds used in analysis were obtained under monocular viewing conditions, for a total of 12 thresholds obtained per participant (six conditions per eye). The condition order for each child was determined using a Latin square to mitigate order and practice effects.

4.2.4 Data analysis

Coherence thresholds for each condition were determined by fitting a Weibull function to participants' responses (see section 2.7). Each control child had data from the eye with poorer visual acuity assigned to be compared to the amblyopic eye of the patients, and the other served as a control for the fellow eye. Where the two eyes of control children had equal visual acuity, random assignment was used. To assess group differences between patients and controls, four separate analyses of variance (ANOVAs) were conducted. For each eye (amblyopic and fellow) at each Δt condition (17 ms and 50 ms), an ANOVA using the between-subject factor group (patient, control) and the within-subjects factor Δx (1, 5, or 30 arcmin) was performed. Using estimates from our previous results (Meier & Giaschi, 2014), with the current sample I had adequate power (1-β = .80) to detect a medium-sized (f = 0.27) main effect of group, a small (f = 0.16) main effect of Δx, and a small (f = 0.16) interaction between these factors. Degrees of freedom were corrected with a Huynh-Feldt adjustment where Mauchly's test indicated the assumption of sphericity had been violated (α = .25). Significant interactions were probed with a simple main effects analysis investigating the effect of group at each Δx.

To assess individual differences in patients with amblyopia, I examined differences between subtypes, as well as bivariate correlations between patients' number of elevated coherence thresholds and their visual acuity and stereoacuity scores. A patient was considered to have an elevated coherence threshold if it fell above the upper limit of the 95% confidence interval around the control group's mean performance in the amblyopic control eye. This was calculated for each condition separately, so a patient could have up to 12 elevated thresholds in total. For differences between subtypes, I had power to detect only a large effect size (f = 0.61) with our patient sample. To assess individual differences in the total number of elevated coherence thresholds, I had power to detect a medium-to-large effect (r = |.41|).

4.3 Results

4.3.1 Participant characteristics

There was no difference between the patient and control groups on age, $t(67) = 0.09$, $p = .93$, or gender, $t(67) = 0.67$, $p = .50$. Eight children with amblyopia had no measurable stereopsis on the

Randot Preschool Stereoacuity Test; the remaining 15 children had significantly worse stereoacuity (M = 217 arcsec, SD = 246) than the control children (M = 40 arcsec, SD = 3), $t(14.0) = 2.78$, $p = .015$. Visual acuity in the amblyopic eye of patients (M = 0.196 logMAR, SD = 0.128) was significantly worse than the control "amblyopic" eyes (M = -0.068 logMAR, SD = 0.062; 2.6 line difference), $t(27.3) = 9.38$, $p < .001$. Visual acuity in the fellow eye of patients (M = -0.057 logMAR, SD = 0.089) was significantly different from the control "fellow" eyes (M = -0.099, SD = 0.062; 0.4 line difference), $t(31.3) = 1.91$, $p = 0.049$, but still within the normal range (better than 20/20 Snellen, on average).

4.3.2 Global motion perception in children with amblyopia vs. controls

Coherence thresholds for the amblyopic eye of patients compared to one eye of controls are displayed in Figure 4.1. For the Δt = 17 ms condition, there was a main effect of group, $F(1, 67) = 4.13$, $p = .046$, $f = 0.43$; a main effect of Δx, $F(2.0, 133.6) = 38.22$, $p < .001$, $f = 0.75$; and a group by Δx interaction, $F(2.0, 133.6) = 6.25$, $p = .003$, $f = 0.30$. A simple main effects analysis probing the interaction revealed a main effect of group at the two smallest Δx, such that children with amblyopia had elevated coherence thresholds compared to controls: for 1 arcmin, $F(1, 67) = 18.56$, $p < .001$, $d = 0.98$; and for 5 arcmin, $F(1, 67) = 4.65$, $p = .035$, $d = 0.54$. There was no significant effect of group at Δx = 30 arcmin, $F(1, 67) = 0.08$, $p = .79$. Results for the Δt = 50 ms condition were similar: there was a main effect of group, $F(1, 67) = 13.36$, $p = .001$, $f = 0.45$; a main effect of Δx, $F(1.8, 233.8) = 32.81$, $p < .001$, $f = 0.70$; and a group by Δx interaction, $F(1.8, 233.8) = 6.66$, $p = .002$, $f = 0.31$. As before, there was a simple main effect of group for Δx = 1 arcmin, $F(1, 67) = 16.23$, $p < .001$, $d = 0.93$; and for 5 arcmin, $F(1, 67) = 7.26$, $p = .009$, $d = 0.66$; but no significant effect of group at 30 arcmin, $F(1, 67) = 0.10$, $p = .75$.

Coherence thresholds for the fellow eye of patients compared to controls are displayed in Figure 4.2. For the Δt = 17 ms condition, there was a significant effect of group, $F(1, 67) = 4.13$, $p = .046$, $f = 0.25$; a main effect of Δx, $F(2, 134) = 32.98$, $p < .001$, $f = 0.70$; and a group by Δx interaction, $F(2, 134) = 5.77$, $p = .004$, $f = 0.29$. Simple main effects analysis revealed children with amblyopia had elevated thresholds for Δx = 1 arcmin, $F(1, 67) = 4.69$, $p = .034$, $d = 0.54$; and for Δx = 5 arcmin, $F(1, 67) = 8.62$, $p = .005$, $d = 0.71$. Thresholds were not significantly different in the Δx = 30 arcmin condition, $F(1, 67) = 0.01$, $p = .73$. For the Δt = 50 ms condition, only the main effect of Δx was significant, $F(1.8, 123.0) = 41.75$, $p < .001$, $f = 0.79$; the effect of

group was not significant, $F(1, 67) = 2.54$, $p = .12$, $f = 0.19$; nor was the group by Δx interaction, $F(1.8, 123.0) = 0.64$, $p = .52$, $f = 0.10$.

Figure 4.1 Mean motion coherence thresholds for the amblyopic eye in children with amblyopia and controls.

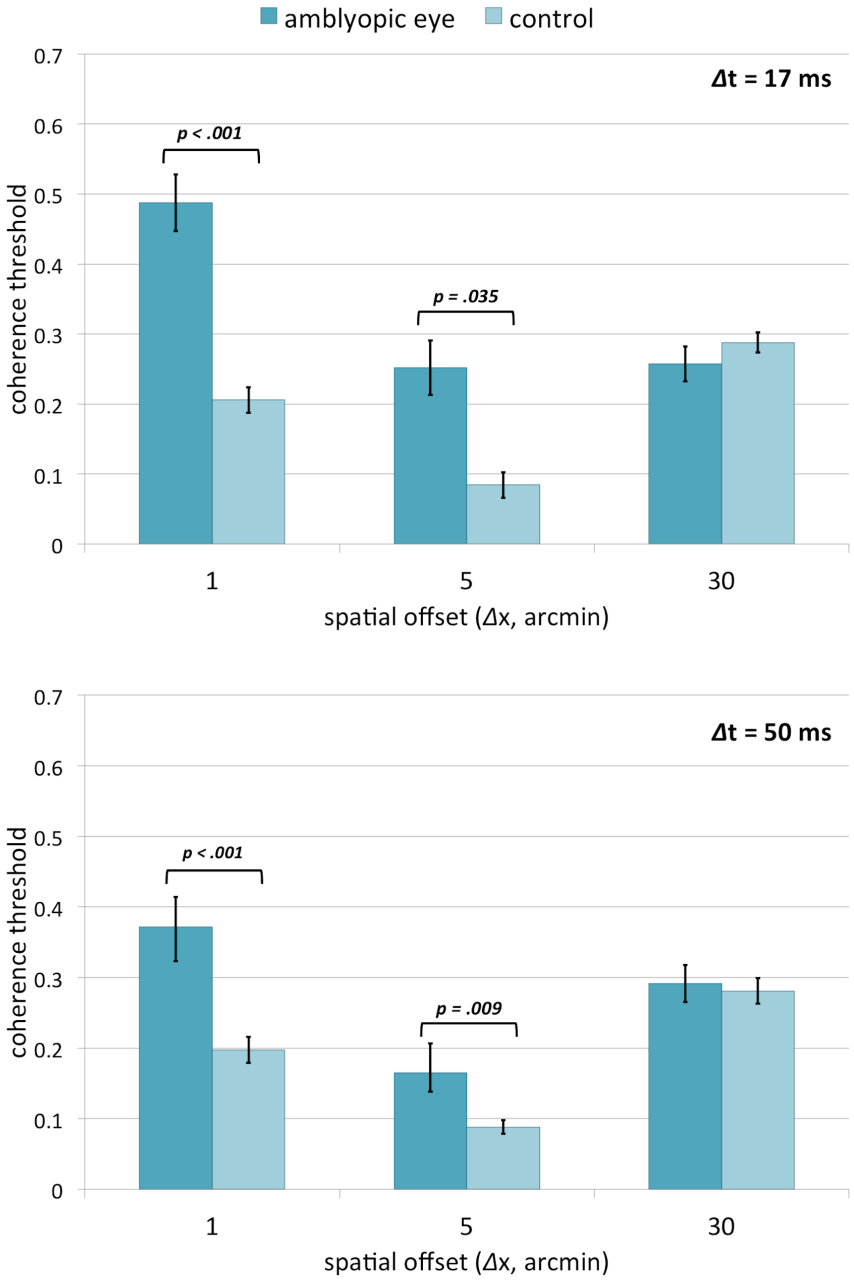

Note. Data are shown for the $\Delta t = 17$ ms condition (top) and 50 ms condition (bottom). Error bars indicate standard error.

Figure 4.2 Mean motion coherence thresholds for the fellow eye in children with amblyopia and controls.

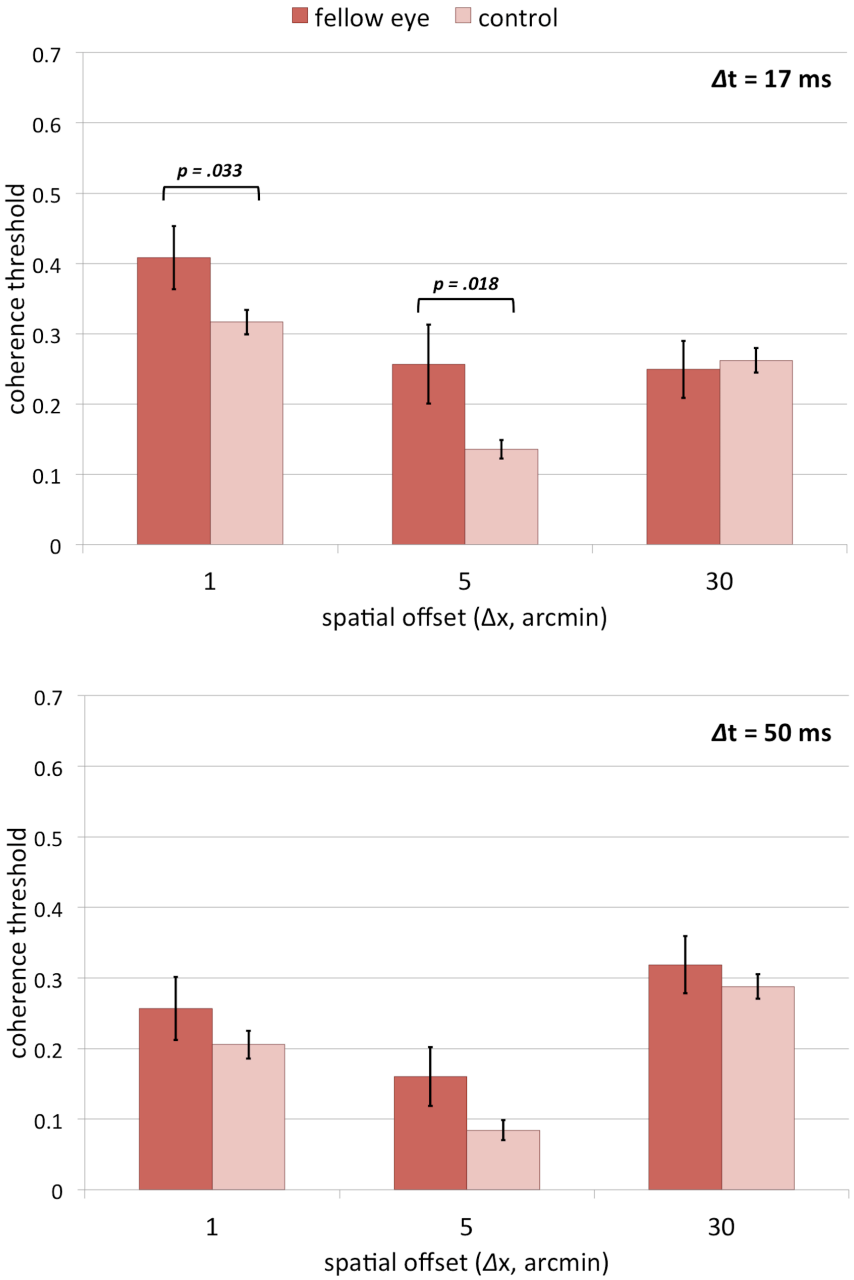

Note. Data are shown for the Δt = 17 ms condition (top) and 50 ms condition (bottom). Error bars indicate standard error.

Children with amblyopia have poorer visual acuity in their amblyopic eye compared to control children, and it is possible that acuity, rather than amblyopia per se, may be driving elevated thresholds. To rule out this potential confound, I compared thresholds in children with amblyopia to a group of visual acuity-matched control children. Some of these control children

had poor visual acuity; the acuity in the eyes selected for analysis (*range* = 0.025 – 0.400, *M* = 0.176 logMAR, *SD* = 0.119; 20/30 Snellen equivalent) was not significantly different from the amblyopic eyes of the patient group, $t(44) = 0.57$, $p = .57$, nor did they differ in mean age (*M* = 11.8 years old, *SD* = 3.0), $t(44) = 1.45$, $p = .15$. My analysis focuses on the condition where patients demonstrated deficits with the largest effect size (Δt = 17 ms, Δx = 1 arcmin). Children with amblyopia had significantly elevated thresholds compared to the acuity-matched control children, $t(44) = 3.41$, $p = .001$, confirming that reduced acuity alone is not likely responsible for the elevated motion coherence thresholds. In fact, these acuity-matched control children had the same coherence thresholds (*M* = 0.31, *SD* = .14) as the control children with 0.1 logMAR or better acuity in the current study (*M* = .32, *SD* = .13), confirming that global motion perception is not affected by visual acuity, at least for the range of acuities tested here.

In summary, children with amblyopia demonstrated group-level deficits at 1 and 5 arcmin spatial displacements, but not at the 30 arcmin displacement. In the amblyopic eye, this was true for both Δt values tested. This corresponds to amblyopic eye deficits for speeds of 1 and 5 deg/s (Δt = 17 ms) and 0.3 and 2 deg/s (Δt = 50 ms), but not speeds of 30 deg/s (Δt = 17 ms) or 10 deg/s (Δt = 50 ms). In the fellow eye, these deficits were only seen for the Δt = 17 ms condition (1 and 5 deg/s), but not the 50 ms condition (0.3 and 2 deg/s). Figure 4.3 displays coherence thresholds for the amblyopic, fellow, and control eyes plotted as a function of speed. Two points are apparent from this graph: first, motion sensitivity is greatest at the medium displacement (Δx = 5 arcmin; 2 and 5 deg/s), regardless of speed. Second, the pattern of deficits in both Δt conditions is similar: at Δx = 1 arcmin, both eyes show elevated thresholds, with the amblyopic eye showing greater deficits than the fellow eye; at Δx = 5 arcmin, the magnitude of the amblyopic and fellow eye deficits is nearly identical. Thus, the lack of a significant effect for the fellow eye in the Δt = 50 ms condition likely reflects a lack of power to detect a significant interaction. At Δx = 30 arcmin, children with amblyopia perform the same as controls.

Figure 4.3 Coherence thresholds as a function of speed.

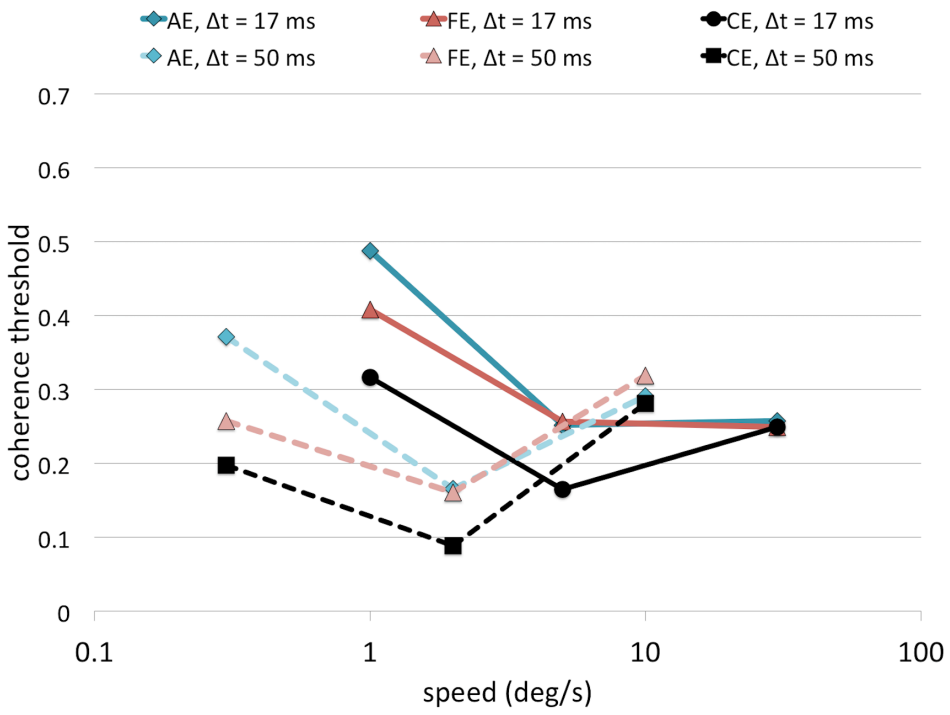

Note. Mean coherence thresholds for amblyopic eyes (AE), fellow eyes (FE), and control eyes (CE) are plotted as a function of signal dot speed. For clarity, error bars have been omitted, but they are shown in Figure 4.1 and Figure 4.2. Control data from the comparison to the amblyopic eye are plotted; control data for the fellow eye were similar.

4.3.3 Clinical factors and deficits in global motion perception

Mean coherence thresholds by amblyopia subtype are displayed in Figure 4.4. Because there were only three children with aniso-strabismic amblyopia, they were grouped with the strabismic amblyopia subtype. When coherence thresholds were averaged across the six conditions for each eye, there was no significant difference between the anisometropic amblyopia and the strabismic amblyopia groups for the amblyopic eye, $t(21) = 1.12$, $p = .27$, or the fellow eye, $t(21) = 0.92$, $p = .38$; nor were thresholds significantly different for any of the 12 conditions individually (all $p = .27$ or greater).

Figure 4.4 Coherence thresholds by amblyopia subtype.

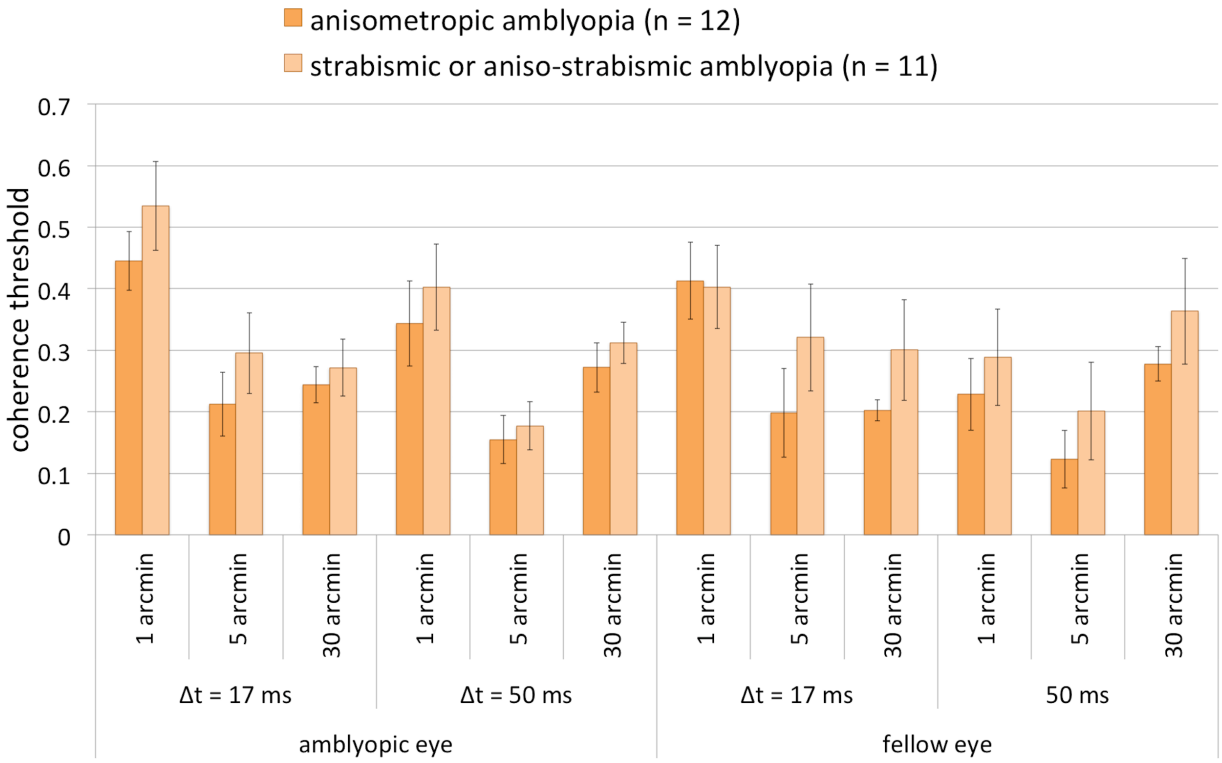

Note. Mean motion coherence thresholds for the children with anisometropic amblyopia and strabismic or aniso-strabismic amblyopia for all 12 conditions of the experiment. Error bars indicate standard error.

Figure 4.5 (top) shows the percentage of children in the amblyopia group with an elevated coherence threshold as a function of condition. The total number of elevated coherence thresholds in an individual child was taken as an indicator of deficit severity (Figure 4.5 bottom). Overall, children had between 0 and 11 total deficits ($M = 5.0$, $SD = 3.5$). There was no significant relationship between total number of deficits and whether a child had anisometropic or strabismic (including aniso-strabismic) amblyopia, $t(21) = 1.29$, $p = .21$.

Figure 4.5 Deficits in children with amblyopia.

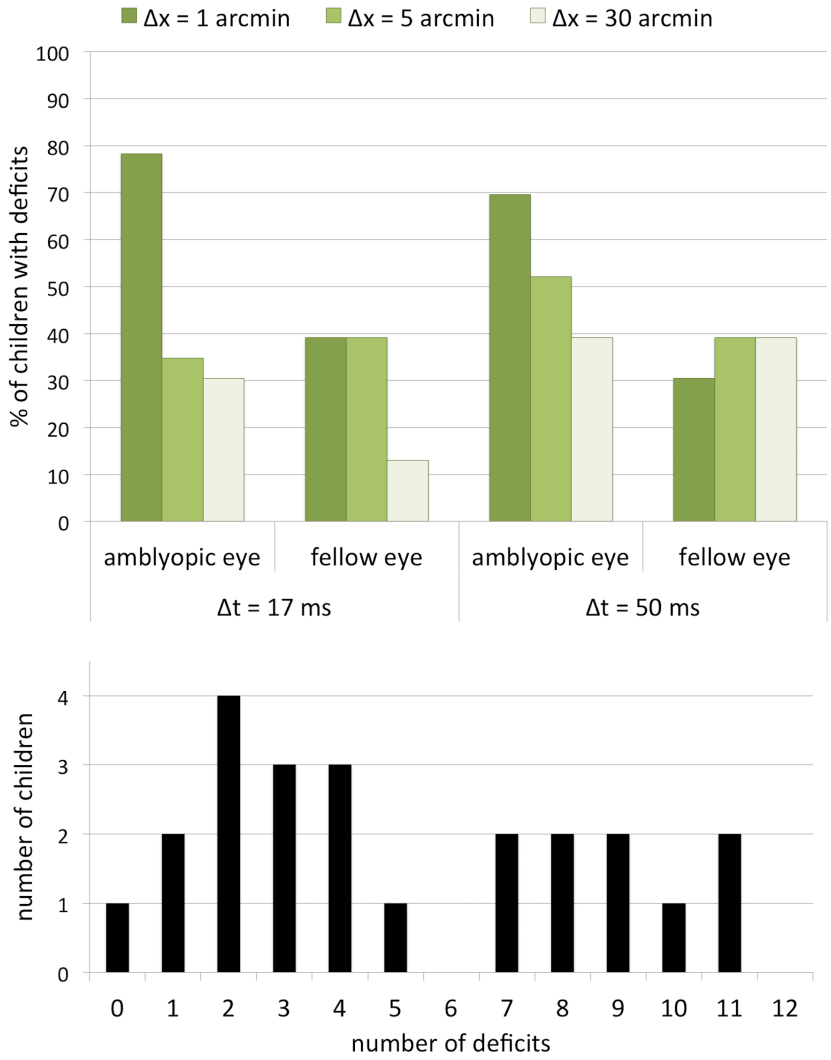

Note. The distribution of motion perception deficits (elevated thresholds) in children with amblyopia across conditions (top), and the frequency of the number of deficits in each patient (bottom).

To assess the relationship with stereoacuity, children with non-measurable acuity were assigned a value of 1600; there was no significant relationship between total number of deficits and stereoacuity scores on the Randot Preschool test, $r(21) = -0.23$, $p = .30$, including when subtype is controlled for, $r(20) = -0.34$, $p = .12$; nor was there a difference in mean number of deficits for the 8 children with no measurable stereoacuity vs. the 15 children with any measurable stereoacuity, $t(19.33) = 1.88$, $p = .25$.

Finally, indicators of greater depth of amblyopia were not associated with greater motion deficits: there was no significant correlation between total number of deficits and amblyopic eye

logMAR visual acuity, $r(21) = 0.01$, $p = .95$, interocular visual acuity difference, $r(21) = -0.24$, $p = .27$, or total months of prescribed occlusion therapy in the 20 children who had completed treatment at the time of testing, $r(18) = -0.15$, $p = .53$.

4.4 Discussion

The current study varied the spatial and temporal displacement parameters in a global motion stimulus to determine the spatio-temporal pattern of motion deficits in children with amblyopia. Consistent with my hypothesis, I found that, compared to age-matched controls, children with amblyopia between 7 and 14 years old had elevated coherence thresholds for stimuli on which 5-year-olds were previously found to be immature (Δx = 1 and 5 arcmin; Meier & Giaschi, 2014; Chapter 3). Coherence thresholds for stimuli on which 5-year-olds showed adult-like performance (Δx = 30 arcmin) were within the typical range. This effect was seen at both Δt = 17 and 50 ms when patients viewed the stimuli with the amblyopic eye. In the fellow eye, this effect was seen in the Δt = 17 ms condition only. The lack of an effect in the fellow eye at Δt = 50 ms was possibly due to a lack of power (see Figure 4.3). I found no consistent clinical predictors of the number of motion deficits observed in children with amblyopia.

4.4.1 Global motion perception in children with amblyopia vs. controls

I found that children with amblyopia demonstrated deficits in global motion perception for stimuli using small spatial displacements. This is also where young children show the greatest immaturities (Meier & Giaschi, 2014; Chapter 3). The current study extends the findings of Kiorpes et al. (2006), who found motion sensitivity deficits at small spatial scales in macaques with anisometropic or strabismic amblyopia, to children. Similar to young typically-developing macaques (Kiorpes & Movshon, 2004), the amblyopic macaques demonstrated a motion sensitivity tuning curve in the amblyopic eye that was shifted to greater values of Δx. El-Shamayleh, Kiorpes, Kohn, and Movshon (2010) assessed neural responses in MT to motion coherence stimuli in these macaques, and determined that this behavioural pattern was reflected in MT neuronal population responses. Compared to tuning curves for stimuli presented to the fellow eye, response magnitude for stimuli presented to the amblyopic eye was depressed and the peak was shifted towards faster speeds or coarser spatial scales. Similarly, Hou et al. (2008)

assessed VEPs in adults with mild strabismic amblyopia in response to global motion for a range of Δx parameters, and found that compared to controls, the response curve tuning of the amblyopic eye was shifted to larger spatial displacements. Although psychophysical coherence thresholds were not assessed in their participants, this reduced cortical sensitivity likely translates into elevated coherence thresholds over a selective range of small spatial scales, in accordance with the current data. Given VEPs in young infants show maximal responses to large spatial displacements (Hou et al., 2009), this is consistent with a deficit in aspects of visual function that mature later.

A reduction at high spatial frequencies is a characteristic feature of amblyopia (Bradley & Freeman, 1981; Hess & Howell, 1977; Levi & Harwerth, 1977), so it is quite possible the pattern of deficits observed here can be attributed to loss of sensitivity to high spatial frequencies in earlier stages of motion processing. I did not assess contrast sensitivity in the children with amblyopia in this study to determine whether a relationship exists in our participants. However, if this is the case, this frequency-selective deficit observed for translational motion may persist in other motion tasks. For example, when slow speeds are defined by smaller spatial displacements, children with amblyopia show higher minimum speed thresholds (Giaschi et al., 1992; Ho et al., 2005) and have higher coherence thresholds at slower speeds (Hayward et al., 2011) compared to controls for motion-defined form discrimination tasks embedded in random dot noise. Children with amblyopia also show higher minimum speed thresholds in a single object-tracking task that does not involve noise (Ho et al., 2006). This speed-tuning may not be independent across tasks, nor limited to tasks involving noise. I did not sample thresholds from a large enough spatio-temporal parameter space to comment on the overall reduction of motion sensitivity curves in children with amblyopia, but I predict a similar pattern to that of Kiorpes et al. (2006).

These results demonstrate that deficits in amblyopia may not be revealed by all global motion stimuli. Simmers et al. (2003; 2006) found global motion deficits in adults with amblyopia using Δx = 18 arcmin, Δt = 53 ms. The current study found deficits for displacements of Δx = 5, but not 30, arcmin. Taken together, these studies suggest stimuli with spatial displacements at least as small as 18 arcmin are sensitive enough to detect motion deficits. This may be, in part, a function of Δt. We previously found no global motion deficits in children with amblyopia using Δx = 7.6 arcmin (Ho et al., 2005; Ho & Giaschi, 2006; Wang et al., 2007), but this used Δt = 107 ms to create a slow speed (1.2 deg/s). A temporal displacement this long was

not tested in the current study. However, children show more mature performance in stimuli with longer Δt and the peak of the motion sensitivity curve shifts to smaller values of Δx with increases in Δt (Meier & Giaschi, 2014), so it is possible the pattern of disruption in amblyopia shifts similarly with longer values of Δt.

These results are potentially in conflict with those obtained by Knox et al. (2013). Similar to the current study, the effects of spatio-temporal parameters of a random-dot global motion stimulus were assessed, by either holding Δx constant and varying Δt, or vice versa. While coherence thresholds of control and amblyopia groups were not directly compared at each combination of parameters, an analysis is possible from the data provided in their Table 2. Adults with amblyopia demonstrated no deficits when tested using Δx = 2.4 arcmin, Δt = 27 ms. Results from the current study would predict a deficit at this small displacement, highlighting that additional stimulus parameters may be impacting observed deficits in amblyopia. A salient difference between tasks is the larger dot size and sparser display used by Knox et al. (58 arcmin diameter, 0.19 dots/deg^2) compared to those employed in the current study (1 arcmin diameter, 1.1 dots/deg^2). While little work has directly compared the impact of these differences on motion coherence thresholds, decreased density and increased dot size may engage high-level feature tracking mechanisms in maximum motion displacement (D_{max}) tasks (Sato, 1998; Smith & Ledgeway, 2001), which may also depend on spatial displacement rather than speed (Baker & Braddick, 1985b).

Finally, the hallmark of amblyopia is reduced visual acuity in one eye, so it is possible that visual acuity, and not amblyopia per se, limits global motion perception. Consistent with this possibility, children with amblyopia showed deficits for stimuli with very small spatial displacements (1 and 5 arcmin). Though prior work has shown that motion deficits persist in amblyopia even when stimulus visibility is guaranteed (e.g., Constantinescu et al., 2005; Simmers et al., 2006), the stimuli in the current study have not been controlled for visibility. While all but three of the patients who participated in the current study had completed occlusion therapy, mean visual acuity in the amblyopic eye was significantly worse than controls, and some patients with amblyopia showed poor acuity even after treatment (see Table 4.1). However, it is unlikely that poor visual acuity accounts for the deficits observed here, since children with amblyopia had global motion deficits in their fellow eyes with normal visual acuity. Moreover, children with amblyopia had significantly elevated coherence thresholds compared to a group of

acuity-matched control children, who performed identical to their better-acuity peers. While this is the first direct comparison between patients and controls on global motion thresholds matched for visual acuity, the lack of effect of visual acuity on coherence thresholds is consistent with prior work (Chakraborty et al., 2015). Similarly, coherence thresholds for global motion are unaffected by optical blur at least up to visual acuities as poor as 0.40 logMAR in adults wearing blurred lenses (Zwicker, Hoag, Edwards, Boden, & Giaschi, 2006), at least for the stimulus parameters showing early maturation used by Parrish et al. (2005).

4.4.2 Clinical factors and deficits in global motion perception

I did not find any significant predictors of the total number of global motion deficits for each child. I assessed etiological subtype, evidence of binocularity, and indicators of depth of amblyopia. The data collected in amblyopic macaques (Kiorpes et al., 2006) would predict a greater deficit in strabismic amblyopia, particularly in the fellow eye, but this was not observed in the current data. Differences in performance by subtype were very small and not statistically significant, nor were they indicative of such a pattern. Simmers et al (2003; 2006) found no difference in global motion thresholds for adults with strabismic or aniso-strabismic amblyopia; the current results confirm this finding and extend it to children with anisometropic amblyopia as well. Similar to Ho et al. (2006), I did not find a relationship between stereoacuity and number of motion perception deficits. Finally, the three indicators of depth of amblyopia I tested – amblyopic eye visual acuity, interocular visual acuity difference, and months spent undergoing occlusion therapy – did not predict motion deficits. It is possible that other indicators of depth of amblyopia, such as increased interocular suppression (Mansouri, Thompson, & Hess, 2008; Narasimhan, Harrison, & Giaschi, 2012) or a lack of coarse stereopsis (Giaschi, Lo, Narasimhan, Lyons, & Wilcox, 2013) may provide more direct or sensitive measures. Finally, it is possible that greater global motion perception deficits are not indicative of deeper amblyopia, but of differing down-stream effects following the impact of amblyopia. If this were the case, however, I might expect to see differences in subtype.

Most patients (87%) had completed occlusion therapy when they participated in this study, so these results largely reflect global motion processing in treated amblyopia. Few studies have examined the effect of occlusion therapy on global motion processes, so it is uncertain whether I should expect deficits in untreated children to be more severe. Treatment has been

shown to improve minimum oscillatory motion displacement thresholds (Simmers, Gray, McGraw, & Winn, 1999), with the greatest improvements occurring for patients with poorer initial thresholds, and not necessarily those showing the greatest recovery in other acuity measures. However, deficits in motion-defined form and multiple object tracking persist even with improvements in visual acuity (Giaschi et al., 2015). In line with this, the current results do not show a relationship between deficits and visual acuity outcomes, suggesting that gains in visual acuity following treatment are not sufficient for alleviating motion integration deficits. On the other hand, contrast sensitivity in amblyopia improves with treatment (Wali, Leguire, Rogers, & Bremer, 1991) so I may expect a similar improvement in motion sensitivity, though not all children treated with occlusion therapy achieve normal contrast sensitivity in either the amblyopic or the fellow eye (Chatzistefanou et al., 2005).

Chapter 5: The effect of stimulus area on global motion thresholds in children and adults

5.1 Introduction

In Chapter 3, I confirmed that global motion perception can mature as late as 16 years of age, depending on the stimulus parameters. Some aspects of spatial vision also reach maturity in adolescence (see section 1.5.1). This suggests protracted development in global motion tasks may depend on spatial-specific aspects of the motion stimulus. One way to selectively target spatial integration mechanisms in motion stimuli is increasing the area covered by a stimulus.

This study was designed to assess the effect of stimulus area on coherence thresholds. Maximum Δx displacement thresholds can increase as stimulus area increases (Baker & Braddick, 1982; Chang & Julesz, 1983; Eagle & Rogers, 1997), so I hypothesized that participants would show better performance for larger stimulus areas for stimuli with a large, but not small, Δx parameter (corresponding to fast, but not slow, speeds). Additionally, I aimed to determine whether children could achieve mature performance for the conditions previously found to show late maturation (Meier & Giaschi, 2014; Chapter 3) if stimulus area was increased. If so, the immature performance on global motion tasks described previously may be attributed to limitations in the mechanisms involved in spatial integration, rather than motion perception per se. To this end, I assessed performance for three stimulus speeds as a function of area in children and in adults.

5.2 Methods

5.2.1 Participants

Children (4–6 years old) and young adults (18–30 years old) were recruited from the community to participate in this study. No minimum acuity criteria were imposed, since the results of Chapter 4 indicated that this did not impact coherence thresholds in participants with healthy vision. However, since participants were requested to have up-to-date corrected vision, those with greater than 0.2 logMAR difference in acuity between the two eyes were excluded from analysis, as this can be a risk factor for, or indicative of, amblyopia. Because motion processing and stereopsis share common cortical networks (Born & Bradley, 2005), participants were

required to have stereoacuity scores within the normal limit for their age (200 arcsec for 4- and 5-year olds, 100 arcsec for 6-year olds, 40 arcsec for adults; Birch et al., 2008).

A total of 30 children were recruited to participate. However, three children (ages 4.0, 4.8, and 5.3) did not complete more than two or three conditions of the experiment, and their data were excluded from analysis. The remaining 27 children were between the ages of 4.2 and 6.9 years (M = 5.7, SD = 0.7) and had data for a total of six (one child), seven (one child), eight (three children) or all nine (the remaining 22 children) conditions of the experiment (described in section 5.2.2). A total of 28 adults were recruited. One adult was excluded for having a visual acuity difference between the two eyes that was larger than 0.2 logMAR. The remaining adults included in analysis were between the ages of 18.6 and 29.6 years (M = 23.8, SD = 3.5). Four of these adults had data for eight of the experimental conditions, and the remaining 23 adults had data for all nine conditions. No participants were excluded for poor stereoacuity.

5.2.2 Stimuli and experimental conditions

The stimuli used in this experiment are described in section 2.5. Two stimulus factors were examined: speed and area. As in Chapters 3 and 4, this study assessed performance for three spatial displacements (Δx = 1, 5, and 30 arcmin), but used only one temporal displacement (Δt = 17 ms). This combination of parameters yielded three speeds: slow (1 deg/s), medium (5 deg/s) and fast (30 deg/s). See section 3.2.2 for a full description of these conditions. Three stimulus areas were assessed: 3 × 3, 6 × 6, and 9 × 9 deg; for total areas of 9, 36, and 81 deg^2.

5.2.3 Procedure

Procedures for assessing visual and stereoacuity are described in section 2.3, and for assessing coherence thresholds in sections 2.6 and 2.7. Participants completed eight trials of a practice staircase binocularly using the parameters Δx = 15 arcmin and Δt = 33 ms at a stimulus area of 8 × 8 (64 deg^2) before proceeding to the experimental conditions. A total of 9 thresholds were obtained for each participant, one for each speed by area condition. Participants conducted the task monocularly using the eye with best visual acuity; if acuity between the eyes was equal, participants chose whichever eye was preferred. The order in which participants conducted each condition was determined using a Latin square.

5.2.4 Data analysis

A power analysis was conducted to determine the appropriate sample size for this study. Using estimates from the prior work comparing 4–6 year olds to adults (Meier & Giaschi, 2014), I calculated that 14 total participants were required to replicate the main effect of age (Cohen's f = 0.97) and 56 total participants were required to replicate the age by speed interaction (f = 0.30) with a power of 0.80. Based on the magnitude of this interaction, I also used f = 0.30 as the minimum meaningful effect size for detecting an age by stimulus area interaction in the current study. Thus, I determined I needed a total of 28 participants per age group for this experiment to detect significant interactions with age.

As before, coherence thresholds for each condition were determined by fitting a Weibull function to participants' responses (section 2.7). To quantify the effect of area, I obtained the slope of coherence thresholds as a function of the square root of the stimulus area for each participant. A negative value indicates that performance is better for larger stimulus areas. Figure 5.1 illustrates how these values are obtained for an adult participant. This area effect was used as a dependent variable in a subsequent ANOVA using the between-subjects factor age (child, adult) and the within-subjects factor speed (slow, medium, fast). Degrees of freedom were corrected with a Huynh-Feldt adjustment where Mauchly's test indicated the assumption of sphericity had been violated (α = .25).

The benefit of expressing the effect of area with a slope, rather than entering area as the third factor in the ANOVA, is two-fold. For practical reasons, an estimate of the area effect can still be obtained for participants who do not complete all three speeds for a given area; and so the ANOVA does not need to account for missing data. More importantly, quantifying the area effect in terms of a slope provides a directly interpretable value, and this value can be used in analyses of individual differences and meaningfully compared with other studies.

Figure 5.1 Area effect at each speed for one adult participant.

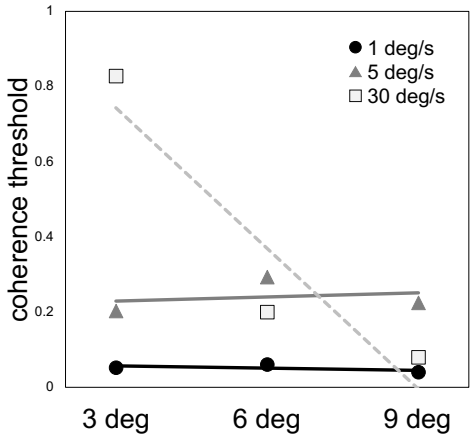

Note. For this adult participant, the area effect is 0.00 for 1 deg/s and 5 deg/s; and -0.12 for 30 deg/s. See text section 5.2.4 for a description of how these values are obtained.

Finally, I conducted a bivariate correlation between these slope values and participants' visual acuity to determine if differences in acuity may account for area effects as a function of speed. Given a sample size of 54, I had the power to detect a correlation of at least 0.27 in magnitude ($\alpha = 0.05$). Stereoacuity did not vary sufficiently in this healthy sample to obtain a meaningful correlation.

5.3 Results

In adults, mean visual acuity for the eye used to conduct the task was -0.115 logMAR (approximately 20/15 Snellen; ranging from -0.213 to -0.025, SD = 0.058). In children, mean visual acuity was 0.059 logMAR (approximately 20/23 Snellen; ranging from -0.075 to 0.288, SD = 0.101). This difference was significant, $t(41.4) = 7.80$, $p < .001$, but within the normal range.

Mean coherence thresholds for each speed by area condition are shown separately for children and adults in Figure 5.2, along with the mean fitted slopes quantifying the area effect. This area effect for each speed in each age group is re-plotted in Figure 5.3. There was a significant effect of speed, $F(1.8, 91.4) = 142.50$, $p < .001$; but no significant effect of age group, $F(1, 52) = 0.99$, $p = 0.32$, nor a speed by age group interaction, $F(1.8, 91.4) = 2.17$, $p = 0.13$. Follow-up of the significant speed effect using Bonferroni-adjusted pairwise comparisons indicated that the area effect for 30 deg/s was significantly different from the effects at 1 and 5

deg/s, both $p < .001$, but the area effects at 1 and 5 deg/s were not different from each other ($p = .43$). The effect at 30 deg/s ($M = -0.093$, 95% CI: [-0.105, -0.81]) was significantly less than zero, $t(53) = 15.76$, $p < .001$, indicating that performance was better for larger stimulus areas at this speed. The effects at 1 deg/s ($M = -0.004$, 95% CI: [-0.012, 0.003]) and 5 deg/s ($M = 0.003$, 95% CI: [-0.003, 0.010]), were not significantly different from zero, $t(53) = 1.12$ and 1.00, $p = 0.27$ and 0.32, respectively, indicating that performance did not differ as a function of stimulus size for these slower speeds.

The correlations between area effect and the visual acuity of the eye used for the task across all 54 participants were 0.04, 0.21, and 0.14 for the 1, 5, and 30 deg/s conditions respectively (all $p \geq 0.14$, uncorrected), indicating no significant role for visual acuity.

Figure 5.2 Coherence thresholds as a function of area for each speed.

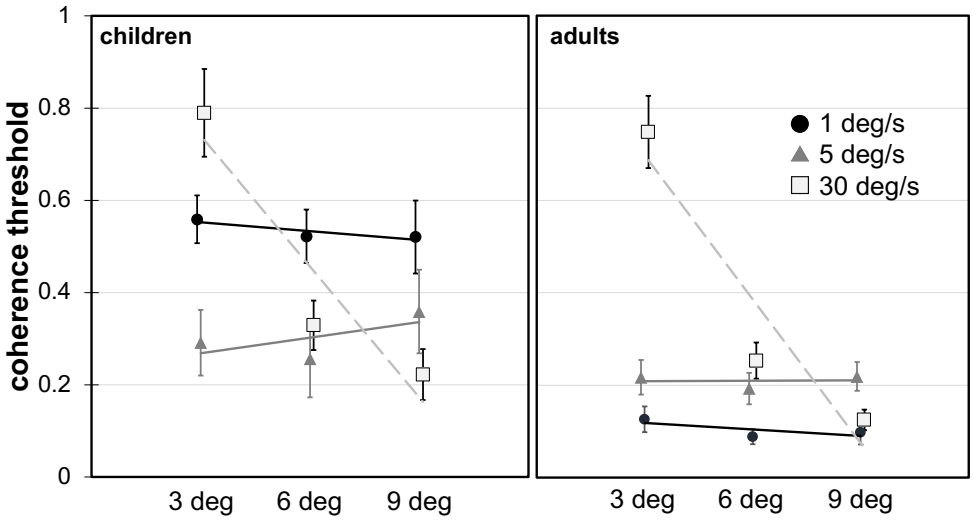

Note. Error bars indicate 95% CI, determined individually for each mean. Linear fits describe the mean area effect at each speed; standard errors for the area effect are displayed in Figure 5.3.

Figure 5.3 Effect of area by speed for both age groups.

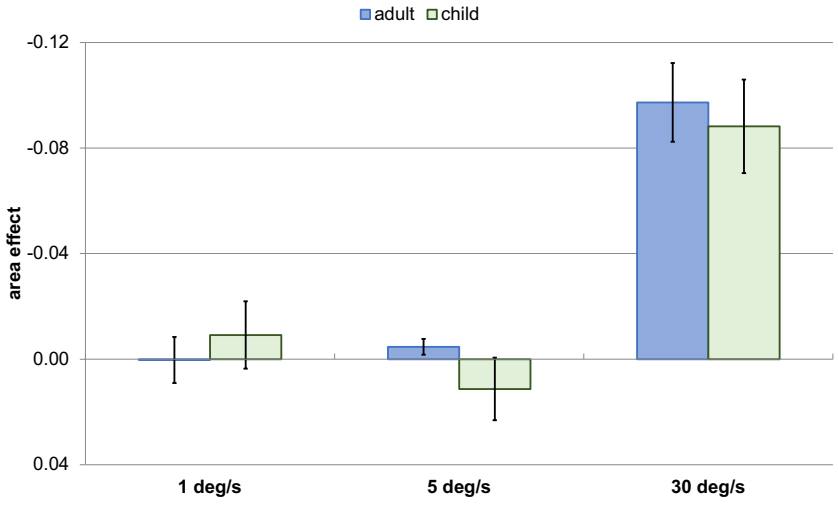

Note. Error bars indicate standard error, determined individually for each age group. A value of 0 reflects no effect of area on coherence thresholds. A negative value indicates coherence thresholds are lower (improve) for larger stimulus area.

5.4 Discussion

I assessed coherence thresholds in young children and adults as a function of stimulus area for three speeds (1, 5, and 30 deg/s; created with spatial displacements of Δx = 1, 5, and 30 arcmin). My previous work has indicated that young children show immature performance at the slowest, but not fastest, speeds assessed in the current study (Meier & Giaschi 2014; Chapter 3). The results of this study confirm these immaturities are not limited by the spatial extent of stimulus area. Consistent with my hypothesis, I found an area effect at the fastest speed (30 deg/s) only. The effect of area was the same for children and adults, regardless of speed.

While this work assesses motion coherence thresholds as a function of Δx and stimulus area, prior work on the impact of stimulus area in motion perception has assessed the largest spatial displacement in a two-frame animation that is perceived as motion (maximum displacement thresholds, commonly termed D_{max}). My data are consistent with this work. For example, Baker and Braddick (1982) determined maximum displacement thresholds vary strongly as a function of stimulus area. At 81 deg^2, the largest area assessed in my study, the limit approached 40 arcmin; at 36 deg^2 the limit was around 30 arcmin, and at 9 deg^2, the smallest area assessed in my study, they found maximum displacement limits around 20 arcmin.

The poorer performance at smaller areas for the fast speed stimulus is likely a result of these limitations. Discrimination becomes difficult at 36 deg^2 for stimuli with Δx = 30 arcmin, because signal dot displacements are approaching the two-frame D_{max}. Even greater difficulty is observed at 9 deg^2, where 30 arcmin displacements are larger than two-frame D_{max}. Participants are still able to conduct the task, likely due to sequential recruitment mechanisms that increase D_{max} by taking advantage of multiple animation frames (McKee & Welch, 1985). However, the task is clearly difficult: the mean increase in coherence thresholds is 0.48 between 36 and 9 deg^2. Inspection of the linear fit for the data at 30 deg/s in Figure 5.2 suggests that this area effect is unlikely to truly be linear, consistent with previous literature (Baker & Braddick, 1982; Nakayama & Silverman, 1984). With only three data points per participant, a non-linear fit could not be accurately estimated for this data. It is not surprising that area effects were not observed for the speeds created using smaller displacements (1 and 5 deg/s). In fact, results from Baker & Braddick (1982) predict that an area effect would not be apparent for these speeds in the current study unless stimulus areas below 1 deg^2 were assessed.

In this study, I found that although children show immature performance compared to adults for some spatio-temporal stimulus conditions, the pattern of immaturity does not vary as a function of stimulus area. Previous research has suggested that children's performance may be limited by an immaturity in sampling efficiency (Bogfjellmo et al., 2014; Falkenberg et al., 2014), that is, the ability to make full use of the information available in a motion stimulus. If this is the case, it does not appear that increasing the area covered by a stimulus improves sampling efficiency in children. The results of the current study indicate that the immaturities observed at small Δx described in my previous studies (Meier & Giaschi, 2014; Chapter 3) cannot be accounted for by limitations in spatial integration that selectively impact children's performance, at least when indexed by stimulus area. Moreover, these results indicate that a difference in stimulus area across studies is unlikely to underlie any inconsistent results across studies of global motion maturation.

.

Chapter 6: The relationship between fixation stability and motion perception in healthy controls

6.1 Introduction

In Chapter 4, I demonstrated that global motion perception is impaired in participants with amblyopia whether they are viewing with the amblyopic or fellow eye. This selective deficit is for stimuli created with small Δx displacements. Poor fixational stability is a common trait in amblyopia. In section 1.5.2, I hypothesized that if poor fixational stability leads to poor performance on a global motion task, it would selectively impact stimuli created with small Δx displacements, which typically correspond to slow speeds.

This study is designed to determine whether there is any relationship between fixational stability and performance on a motion perception task in observers with healthy vision, and whether this relationship holds only for slow speeds. Understanding the nature of this relationship in controls will help inform the results of a future study designed to investigate this link in observers with amblyopia.

6.2 Methods

6.2.1 Participants

Twenty-six healthy young adults were recruited from the community to participate in this study. Participants were not excluded for poor vision or poor stereoacuity, because variation on these characteristics is useful for the goals of this study. However, data from two participants were removed for an excessive number of trials with no data (see section 6.2.5.1). A total of 24 healthy young adults (17 female; 19.6 – 35.9 years old; *M* age = 28.1 years, *SD* = 4.9) were included in this study.

6.2.2 Apparatus

In addition to the apparatus described in section 2.4, an Eyelink 1000+ (SR Research Ltd) video-based eye-tracker was used to monitor monocular gaze position at 1000 Hz. Participants' heads were stabilized with a chin rest positioned 1 m from the monitor.

6.2.3 Stimuli and experimental conditions

The stimuli used in this experiment are described in section 2.5. Two speed conditions were presented, using the parameters Δt = 17 ms for both conditions, and Δx = 1 arcmin (slow: 1 deg/s) or Δx = 30 arcmin (fast: 30 deg/s). The 1 deg/s stimulus corresponds to a condition from the previous studies where immature performance (Chapter 3) or deficits in performance (Chapter 4) were observed; the fast stimulus corresponds to a condition from these studies where no differences in performance were observed. Additionally, a third control condition was included in which dots appeared on the screen for the same duration (600 ms), but remained stationary.

6.2.4 Procedure

The general procedure used for this experiment is similar to that described in section 2.6, with the addition of an eye-tracking component. Before beginning experimental trials, participants first conducted 8 binocular practice trials using the parameters Δx = 15 arcmin and Δt = 33 ms. All subsequent trials were conducted monocularly with the gaze position of the viewing eye being recorded while the non-viewing eye was occluded with an opaque eye patch. A gaze-contingent display was used to ensure participants were viewing the centre of the display at the beginning of each trial: if they were not, the next trial would not advance. In the motion conditions, participants were asked to decide if the stimulus moved left or right and press the corresponding button on the response pad; in the stationary condition, participants were asked to make a response even though there was no movement by pressing a direction button of their choice. Condition order across participants (left or right eye; slow, fast, or stationary stimulus) was balanced using a Latin square.

In this experiment, coherence was controlled similar to the previous experiments as described in sections 2.6 and 2.7, but with the following changes. First, each motion staircase consisted of 70 (rather than 40) trials and did not terminate early after a given number of response reversals. Additionally, a minimum step size of 0.05 (rather than 0.01) was used, so that trials of a given coherence level were more likely to be repeated than would be with a smaller step. Participants completed each eye × condition pairing twice, so that in the slow and fast motion conditions, there were 140 trials of data from two staircases for each eye. In the

stationary condition, each run consisted of 50 trials conducted once for each eye.

6.2.5 Data analysis

Based on the estimates from the healthy adult data described in Chapter 3, a total of 12 participants were necessary to detect a difference in coherence thresholds for the fast and slow condition ($f = 0.52$) with a power of 0.80. A sample size of double this amount, 24, allows for the detection of a large effect predicting coherence thresholds from performance ($R^2 = 0.33$, non-directional).

In order to examine the influence of visual acuity on fixation stability, and for future comparison to participants with amblyopia, data from the two eyes were kept separate for analysis. Participants' eyes were grouped into "worst acuity" and "best acuity" eye to act as controls for the amblyopic and fellow eye, respectively. One participant had equal acuity between the two eyes, and the left eye was selected at random to be labeled the eye with best acuity.

6.2.5.1 Eye movement measures

Trials that contained any blinks or dropped samples were excluded from further analysis. Two of the 26 participants were excluded for dropping more than 15% of all trials they conducted. The remaining participants had very few trials with missing data ($M = 2\%$ of all trials per participant).

Gaze data were pre-processed offline using custom MATLAB scripts. First, a second-order low pass Butterworth filter with cut-off frequencies of 20 and 40 Hz, for position and velocity respectively, was applied to the raw gaze data. Then, for each trial, the 95% bivariate contour ellipse area (BCEA) was determined (Castet & Crossland, 2012). The BCEA is a value that quantifies an elliptical area around which 95% of gaze positions fall, following the equation:

$$BCEA = \pi\chi^2 s_H s_V \sqrt{1 - r_{H,V}^2} \tag{6.1}$$

where χ^2 is the chi-square value corresponding to the percentile of interest (in this case, 95%), and H and V are vectors of the horizontal and vertical gaze positions for a trial. A larger BCEA

value reflects less stable fixation during a trial than a smaller BCEA value. By convention, the $\log_{10}$ BCEA for each trial is calculated for final analysis to mitigate skewness in this variable.

After calculating these trial-by-trial measures, three participant-level stability measures were extracted to compare against behavioural measures: stability during high coherence trials, during threshold coherence trials, and during stationary trials. A participant's mean $\log_{10}$ BCEA for high coherence stimuli was calculated for trials with coherence levels between 0.8 and 0.9. All participants obtained 100% accuracy on these trials aside from one who obtained 95% accuracy, confirming direction discrimination for high coherence stimuli was not difficult. Mean $\log_{10}$ BCEA for trials presented at threshold coherence was defined as trials with coherence levels spanning 0.05 above and below a participant's calculated threshold (for example, for a threshold of 0.21 this includes trials with coherence of 0.16 to 0.26). Participants' mean accuracy on the trials used in this analysis was 79% (*SD* = 2.1), indicating the +/- span of 0.05 was appropriate to capture near-threshold conditions. Mean BCEA was also calculated for all stationary trials; this condition had no psychophysical accuracy measures.

6.3 Results

6.3.1 Vision assessment

Participants' mean best-eye visual acuity was -0.11 logMAR (*SD* = .07; approximately 20/16 Snellen; ranging from -0.20 to 0.05 logMAR) and mean worst-eye visual acuity was -0.04 logMAR (*SD* = 0.10, approximately 20/18 logMAR; ranging from -0.19 to 0.28 logMAR). The acuity difference was significant, $t(23) = 4.93$, $p < .001$. Participants' mean acuity difference between the eyes was 0.07 logMAR (equivalent to 0.7 lines of an eye chart), ranging from 0.00 (no difference) to 0.26 logMAR (equivalent to 2.6 lines on an eye chart). One participant had stereoacuity of 100 arcsec; two had stereoacuity of 60 arcsec; and the remaining 21 participants had stereoacuity of 40 arcsec. This was not enough variation to conduct further analyses using stereoacuity, although visual inspection of the data indicated that the participant with a stereoacuity of 100 arcsec was not abnormal on any measures reported.

6.3.2 Behavioural performance

Mean coherence thresholds are plotted in Figure 6.1 for each speed, separated by eye with best and worst visual acuity. There was no effect of eye, $F(1, 23) = 2.39$, $p = .14$, and a significant effect of speed, such that thresholds were higher for slow than for fast motion stimuli, $F(1, 23) = 19.17$, $p < .001$. There was a significant interaction between the two, $F(1, 23) = 6.02$, $p = .022$, such that the difference in thresholds between the two eyes was greater for slow (.034) than it was for fast (.001) motion. As expected, coherence thresholds did not significantly correlate with visual acuity in any of these four conditions (all $p \geq .12$).

Figure 6.1 Mean coherence thresholds for the two motion conditions in the experiment, separated by eye with the best- and worst visual acuity.

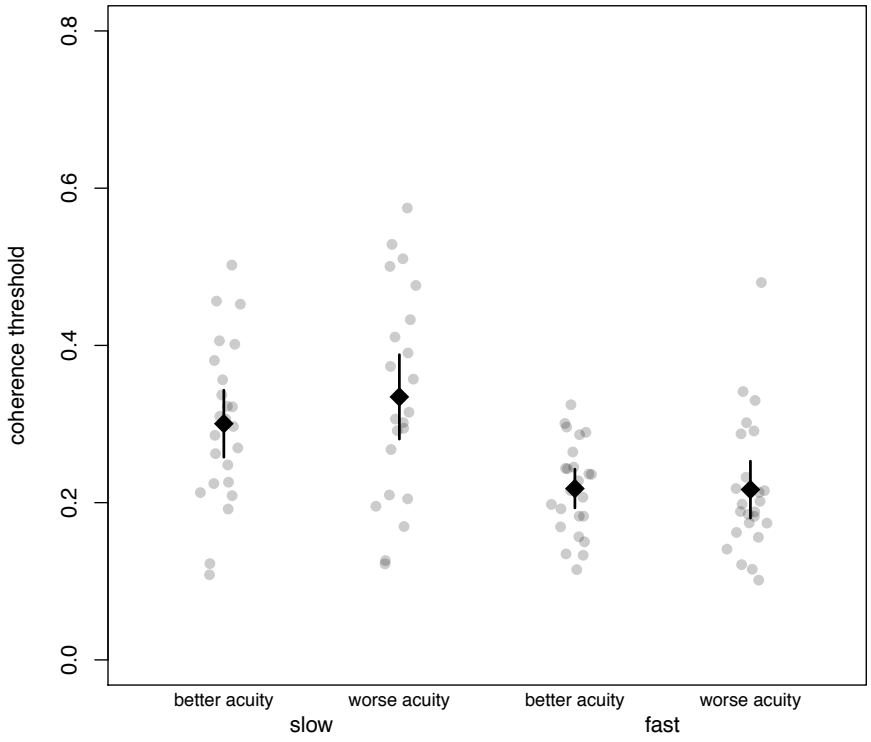

Note. Error bars represent 95% confidence intervals. Grey dots represent individual participants.

6.3.3 Stability measures

Stability on stationary trials, trials at high coherence, and trials near the participants' thresholds are shown in Figure 6.2, separated by eyes with best (top) and worst (bottom) acuity. A three-way within-subjects analysis of variance was conducted to examine the effects of speed (slow,

fast), coherence (high coherence, threshold coherence), and eye (best acuity, worst acuity) on mean $\log_{10}$ BCEA values. This revealed a significant effect of speed, $F(1, 23) = 11.08$, $p = .003$; a significant effect of coherence, $F(1, 23) = 13.04$, $p = .001$; and a coherence by speed interaction, $F(1, 23) = 22.94$, $p < .001$, such that fixation was less stable on high coherence trials than threshold coherence trials for fast stimuli, but not slow stimuli. There was no significant effect of eye, $F(1, 23) = 0.25$, $p = .62$; nor any interaction between eye and speed, $F(1, 23) = 0.24$, $p = .63$, eye and coherence, $F(1, 23) = 0.70$, $p = .41$, or eye, speed, and coherence, $F(1, 23) = 0.01$, $p = .93$, indicating that, at least for the range of acuities obtained in these participants, eye acuity did not impact stability. Similarly, there was no significant difference between eyes with best and worst acuity for stability on stationary trials, $F(1, 23) = 0.30$, $p = .59$. Finally, to compare the stationary condition to all other conditions, pairwise Bonferroni-corrected comparisons, collapsing across eye, were conducted. These indicated that fixation was less stable in the stationary condition compared to all motion conditions (M difference = 0.24 to 0.26, all $p \leq .036$) except for the high coherence stimuli in the fast condition (M difference = 0.02, $p = .99$).

Figure 6.2 Mean $\log_{10}$ BCEA for the stationary condition, and for the high and threshold coherence stimuli for each speed.

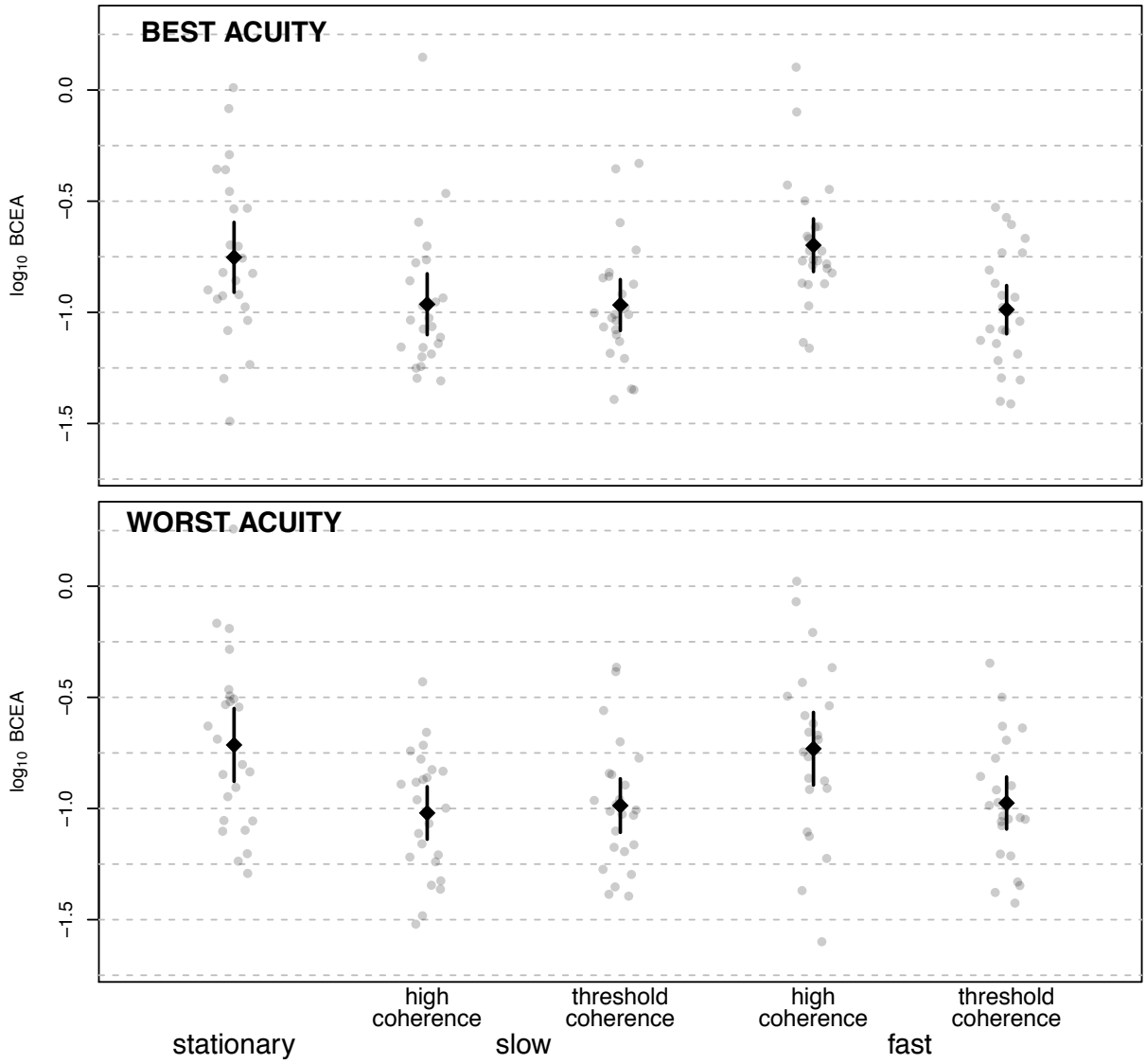

Note. Top: data from the best-acuity eyes of participants. Bottom: data from the worst-acuity eyes of participants. Error bars represent 95% CI. Grey dots represent individual participants.

6.3.4 The relationship between stability and performance

To confirm that visual acuity was not related to eye stability for either motion speed, I investigated the bivariate relationships between visual acuity and eye stability on threshold and high coherence trials. These are displayed in Figure 6.3. No significant relationships between acuity and stability were revealed, all $p \geq .17$ (uncorrected). The relationship between visual acuity and stability in the stationary conditions is also shown in Figure 6.3. These correlations were larger in magnitude ($r = 0.34$ and 0.33 for best and worst acuity eyes, respectively) but not

significantly greater than zero (p = 0.11 and 0.12). Thus, the measurements used in subsequent analyses have used the average of the left and right eye for each participant.

To determine if participants' eye stability was associated with their coherence threshold, correlations were calculated between participants' coherence threshold and mean stability measures (for high and threshold-level coherence trials) for each speed. The correlations are presented in Figure 6.4. None of these correlations were significant (all $p \geq .17$).

Figure 6.3 Correlations between visual acuity and stability.

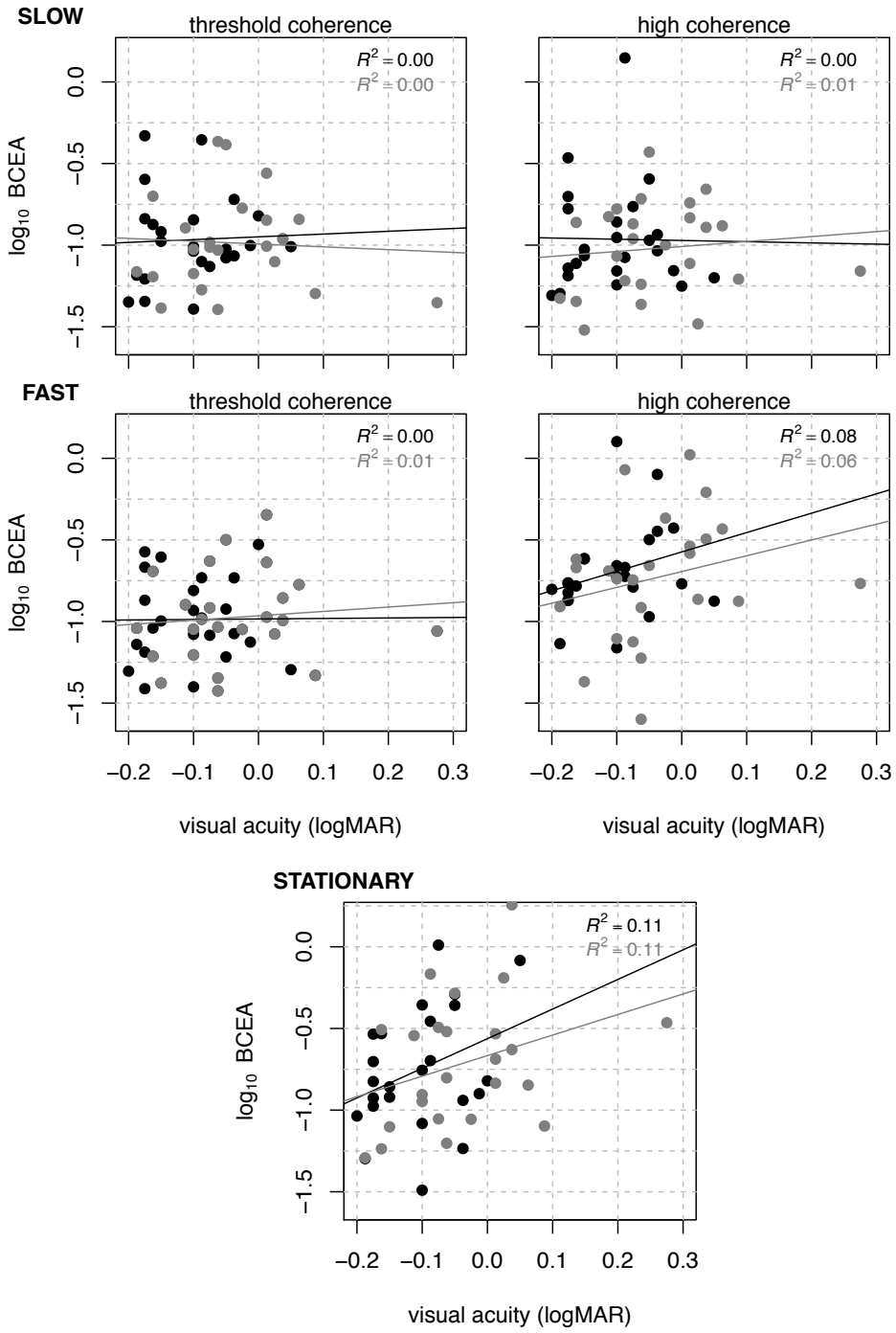

Note. Each plot displays acuity for participants' eye with best (black) and worst (grey) visual acuity, along with linear fits for each eye. Lower values indicate better visual acuity or greater stability. Top row, data collected in the slow condition; middle row, data collected in the fast condition. Left column shows stability on trials at threshold coherence; right column shows stability on trials at high coherence. Bottom shows stability on stationary trials.

Figure 6.4 Correlations between stability (log_{10} BCEA) and performance (coherence threshold).

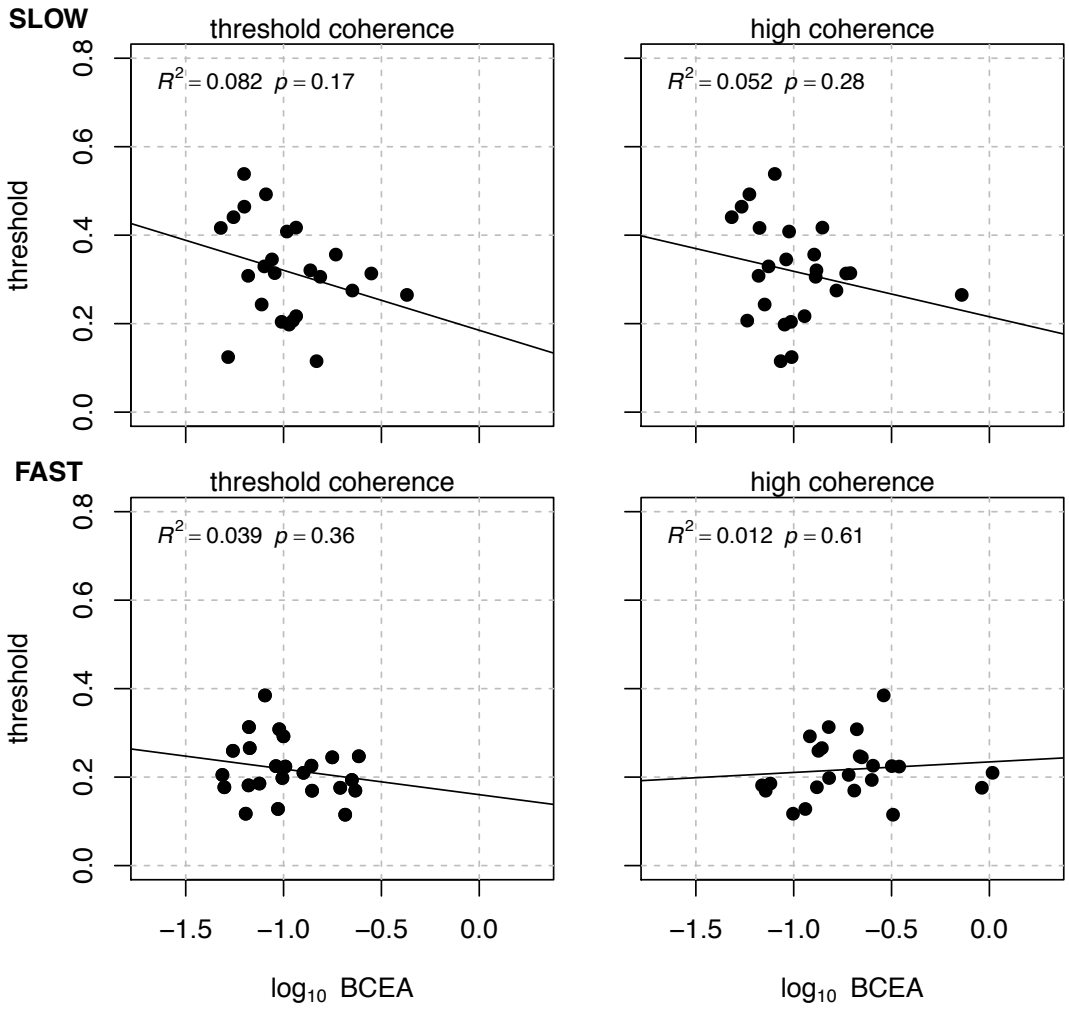

Note. Lower values indicate more stable fixation (BCEA), and better performance (threshold). Top row, data collected in the slow condition; bottom row, data collected in the fast condition. Left column shows stability on trials at threshold coherence; right column shows stability on trials at high coherence.

6.4 Discussion

The primary goal of this study was to determine whether unstable fixation could account for poor performance on a global motion task. I hypothesized that if a relationship could be established, poor fixational stability would have a greater impact on performance at slow, rather than fast, signal dot speeds. I found that stability did not predict participants' performance on the global motion task at either speed.

Fixation was most stable when participants were viewing slow dots at high or threshold coherence, and fast dots at threshold coherence. The decreased stability observed for the fast,

high coherence stimuli may reflect the fact that this condition contains the strongest motion signals, which could be inducing small eye movements in the horizontal plane. Optokinetic nystagmus (OKN) responses to moving dot fields are typically suppressed when a fixation target is provided, though suppression of OKN is not immediate (Wyatt & Pola, 1984). These stimuli are likely too small and too short in duration to induce OKN responses, but may still be inducing eye drift in the direction of the signal dots. As stimulus coherence decreases, the signal driving drift in the direction of the stimulus weakens, and fixations become less dispersed. The velocity limits for OKN depend on a range of spatio-temporal stimulus parameters, but the slow speed of 1 deg/s is expected to be below the lower velocity limit (Schor & Narayan, 1981). Thus, slow-speed signal dots are unlikely to be moving fast enough to induce drift responses, even at high coherence. The current study is the first to compare fixational stability for a stationary pattern to stability for a random dot motion stimulus. The decreased stability when participants viewed a stationary dot pattern relative to the remaining motion stimuli may reflect the decreased attentional demands in this condition, where participants do not need to make a direction-discrimination decision. It is possible that the more engaging act of conducting a task promotes greater diligence in maintaining fixation. In smooth pursuit, for example, the variability of position errors is reduced when participants conduct an *n*-back colour-naming task on the pursuit target (Stubbs et al., 2017), indicating that increased attention can enhance oculomotor performance. Surprisingly, no studies have investigated this question for the maintenance of fixation, as far as I am aware. This could be resolved for the current study by presenting global motion stimuli in a passive viewing condition.

Previous studies have typically recorded fixation to stationary targets for a duration of at least a few seconds. In the current study, stability was assessed during 600 ms stimulus presentations. For the stationary and high coherence fast stimuli, $\log_{10}$ BCEA was around -0.73 deg^2; for the remaining conditions, $\log_{10}$ BCEA was around -0.98 deg^2. These estimates are slightly more stable than other studies, which have reported mean $\log_{10}$ BCEA values of -0.59 deg^2 in adults fixating for 15 seconds (González et al., 2012); and -0.46 deg^2 in children fixating for 45 seconds (Shaikh et al., 2016). Additional studies have reported mean BCEA, so it not possible to precisely recover $\log_{10}$ BCEA for comparison, but relative to the estimates reported here, other studies have reported more stable fixation during 30 seconds of viewing in adults (Chung et al., 2015) or less stable fixation during 30 seconds of viewing in children (Birch et al.,

2013). Participants with amblyopia in all of these studies have poorer fixational stability than controls. González et al. (2012) estimated mean $\log_{10}$ BCEA as -0.52 deg^2 in fellow eyes, and -0.20 deg^2 in amblyopic eyes; whereas Shaikh et al. (2016) showed children with amblyopia had mean stability values ranging from -0.05 to 0.32 deg^2 in the fellow eye and 0.07 to 0.73 deg^2 in the amblyopic eye, with greater instability observed in the observers with the most severe amblyopia. Chung et al. (2015) found fixation instability was greatest for the amblyopic eye in strabismic amblyopia, and Birch et al. (2013) demonstrated fixation stability was worse for children with elevated or nil stereoacuity. Thus, while the current study found fixational stability is generally in agreement with the controls reported in other studies, fixational stability for observers with amblyopia may be outside the range captured here.

I found that visual acuity was not associated with coherence thresholds or fixational stability in any condition. A lack of correlation with coherence thresholds is consistent with the data reported in the previous Chapters of this dissertation. To my knowledge, no data have been published to address such a link between acuity and stability in healthy adults, even during stationary target viewing. Using lenses to induce poor visual acuity in healthy observers does not impact coherence thresholds (Zwicker et al., 2006), but can cause unstable fixation (Vikesdal & Langaas, 2016). Significant relationships between poor stability and poor acuity in observers with amblyopia have been reported (Birch et al., 2013; Chung et al.2015; Subramanian et al., 2013), but these studies did not report analyses on control participants to determine if this relationship held in healthy observers. González, Lillakas, Greenwald, Gallie, and Steinbach (2014) found a significant relationship between stability and *interocular* visual acuity, a common index of amblyopia severity. Taken together, these results indicate that elevated coherence thresholds and greater instability observed in participants with amblyopia are due to the neural consequences of amblyopia, rather than poor visual acuity per se.

Fixation stability cannot account for performance on a global motion task in adults with healthy vision, indicating that fixation instability alone is unlikely to account for poor performance on global motion tasks with slow signal dots. It remains worth assessing whether this finding holds for observers with amblyopia. If a relationship between stability and performance had been established in controls, this would suggest that motion perception deficits in amblyopia are simply a consequence of degraded input to the visual system. Instead, if a relationship between these variables is observed in participants with amblyopia, this may be

indicative of a common factor underlying these deficits. Preliminary results from ten adults with a history of amblyopia are presented in Appendix B. These data are consistent with the notion that poor performance on global motion tasks is not accounted for by poor fixation stability in amblyopia.

Chapter 7: General Discussion

7.1 Summary of findings

The primary goal of this dissertation was to investigate the sensitive periods underlying the typical development of global motion perception, and the sensitive period for damage as a consequence of amblyopia, a visual disorder that occurs after birth but before the age of 6 years. I tested the "last-in-first-out" model of development (Levi & Carkeet, 1993; Lewis & Maurer, 2009) that proposes the aspects of motion perception that take longer to mature will be most susceptible to disruption by visual dysfunction that onsets early in life, and those that mature early will be unaffected. I studied the development of global motion perception by varying spatial (Δx) and temporal (Δt) stimulus parameters to probe behavioural indicators of maturation or disorder.

In Chapter 3, I assessed the developmental trajectory of global motion perception as a function of Δx, for two Δt parameters, in people 7 to 30 years of age. I employed a non-parametric technique that allowed me to estimate the maturational age for performance in each condition more precisely than the common practice of running age-binned analyses of variance, and compare these ages across conditions with the use of confidence intervals. Based on my prior work in 4- to 6-year-olds showing the greatest immaturities at the smallest Δx parameters (Meier & Giaschi, 2014), I hypothesized that maturation would be reached at a later age for the smallest Δx tested. Consistent with my prediction, I found that adult-like performance was reached before age 7 for the largest Δx, by 10-12 years for the medium Δx, and as late as 15-16 years for the smallest Δx. I found no evidence to suggest maturation occurred as a function of Δt or speed (the $\Delta x/\Delta t$ ratio). This work helped to resolve inconsistent reports on maturational age in the literature (e.g., Blumenthal et al., 2013; Bogfjellmo et al., 2014; Ellemberg et al., 2010; Hadad et al., 2011; Narasimhan & Giaschi, 2012; Parrish et al., 2005; Yu et al., 2013) by providing a cohesive framework for incorporating a wide variety of age estimates. More importantly, these findings implicate a coarse-to-fine pattern of development in humans, such that sensitive periods are closed sooner in life for larger spatial displacements, but extend to the middle teenage years for stimuli with the smallest displacements.

In Chapter 4, I assessed the pattern of performance deficits in children aged 7 to 14 years old with a history of amblyopia, compared to age-matched control children with healthy vision. I

used the same stimuli as in Chapter 3. I hypothesized that children with amblyopia would have elevated motion coherence thresholds only for those parameters that showed late maturation in Chapter 3. Consistent with the last-in-first-out model, children with amblyopia showed deficits for stimuli using the small and medium Δx, but not the largest Δx. As before, there was no significant impact of Δt or stimulus speed. These deficits were apparent whether children were viewing with the amblyopic eye or with the fellow eye. No clinical predictors of poor performance could be identified in the children with amblyopia: etiological subtype, evidence of binocularity, and indicators of amblyopia severity (amblyopic eye visual acuity, interocular visual acuity difference, and months spent undergoing treatment) did not show any relationship with the severity of motion deficits. These findings provide a framework for understanding selective motion perception deficits in amblyopia, and highlight the importance of using stimuli that are properly tuned for assessing deficits in visual disorder. Crucially, these findings are consistent with the coarse-to-fine development of motion perception described above. This work indicates that the sensitive period for damage is over sooner in life for mechanisms underlying the perception of larger spatial displacements, but those underlying the smallest displacements remain susceptible to visual disruption by amblyopia.

In Chapters 5 and 6, I examined two factors that may influence motion coherence thresholds as a function of Δx. In Chapter 5, I varied the area of the motion stimulus. I hypothesized that coherence thresholds would show a relationship with stimulus area such that larger areas led to better performance (lower thresholds), but only for large Δx displacements. I predicted this would be the case for adults, but investigated whether young children would show this area effect at large *and* small Δx stimuli. Consistent with my prediction, there was an effect of area for large Δx only. This was the case for both adults and children. These results allowed me to rule out the possibility that the immature performance observed in children in my previous work (Meier & Giaschi, 2014; Chapter 3) could be due to the spatial limitations of the stimulus, rather than immaturities in the mechanisms underlying motion perception. In Chapter 6, I measured fixational stability in adults while they performed a global motion task using a small and a large Δx. I investigated whether there was a relationship between unstable fixation and poor performance. I hypothesized that if a relationship did exist, it would be for stimuli with small Δx only, because the larger receptive fields responsible for computing motion comprised of larger Δx would be less susceptible to small changes in the retinal position of the dots. However,

I found no relationship between fixational stability and performance in healthy control adults for stimuli of either speed. This indicates that poor fixation stability alone does not cause poor performance on a global motion task in healthy adult observers.

In the next section, I elaborate on the broader context and implications of the research described in this dissertation.

7.2 Discussion

The results of this dissertation support a coarse-to-fine progression of direction-tuned mechanisms for the development of global motion perception. Sensitivity to spatial displacements in childhood may be achieved by a local displacement-tuned mechanism in early visual areas, optimized to large spatial displacements (useful for detection of ecologically-relevant fast motion) that refines to smaller displacements with development (Introduction, Figure 1.3). This may be a function of V1: simple cells in V1 have receptive fields that are displacement-tuned, while neurons in MT are largely speed-tuned (Priebe, Cassanello & Lisberger, 2003; Priebe, Lisberger & Movshon, 2006). V1 sensitivity may limit the downstream development of global, speed-tuned processes in higher visual regions such as V5/MT+ that are slowly fine-tuned as the output of V1 matures. In support of this, magnetic resonance imaging in young macaques indicates BOLD responses in V1 are present as young as three months, but V5/MT+ responses do not emerge until at least one year (Kourtzi, Augath, Logothetis, Movshon, & Kiorpes, 2006). Visual evoked potentials (VEPs) to motion stimuli are displacement-tuned over occipital cortex in infants, similar to adults; unlike adults, however, infants do not show speed-tuned responses over parietal regions (Hou et al., 2009). The late maturation of global motion perception described in this dissertation may reflect the improvement of global motion processing as motion processing fully matures in V5/MT+ and other regions downstream of early visual cortex.

Rather than maturation within a single region, however, late maturation for slow speeds or small displacements in behavioural tasks may also reflect the pruning of connections among V5/MT+ and associated regions in response to visual experience. Biagi, Crespi, Toestti, and Morrone (2015) found that 7-week-old human infants demonstrated adult-like selectivity for coherent flow stimuli in V5/MT+, but functional connectivity between V1 and V5/MT+ was decreased compared to adults. These diffuse connections may become more adult-like as visual

experience becomes more adult-like. When an adult walks while carrying an infant, head-centred and retinal flow speeds for the infant are approximately 10 deg/s faster than for the adult (Raudies & Gilmore, 2014). The visual world of infants changes as they develop from sitting to crawling to walking, and a child's height, locomotion speed, or head posture can all contribute to different experiences of optic flow patterns (Gilmore, Raudies, & Jayaraman, 2015) with fast translational flow making up a large portion of early visual experience. The VEP responses of infants indicate that they are most sensitive to coherent translational motion (Gilmore, Hou, Pettet, & Norcia, 2007) and fast speeds (Hou et al., 2009). While VEPs to different flow patterns in children aged 4 to 8 years show many adult-like properties, speed-selective responses do not show a mature distribution (Gilmore, Thomas, & Fesi, 2016). Thus, the coarse-to-fine pattern of development shown in the current study may reflect cortical changes that arise in response to changes in the visual environment.

The current work indicates that the motion sensitivity tuning curve in amblyopia is shifted to greater values of Δx compared to age-matched controls, similar to the pattern of results we see in young children compared to adults (Introduction, Figure 1.4). Aaen-Stockdale and Hess (2008) have suggested that such a shift in sensitivity may arise, in part, from deficits in striate cortical areas that are frequency-selective, while an overall reduction in sensitivity is likely due to deficits in a broadband global motion integration mechanism that lies downstream of V1. In other words, the pattern of global motion deficits observed in amblyopia is determined in two independent stages: limitations at early stages of processing truncate the range of spatial displacements to which the amblyopic motion perception system is sensitive, and limitations at later stages of processing decrease the maximum sensitivity of the system. Consistent with deficits at the first stage, Kiorpes et al. (2006) found the shift to larger spatial displacements in motion sensitivity was accompanied by similar shifts in the peak of the contrast sensitivity function in amblyopic macaques. Consistent with deficits at the second stage, overall reductions in sensitivity were not strongly related for contrast and motion, suggesting the latter stage motion deficits are independent of deficits in contrast sensitivity. This also implies that later stages of global motion processing are likely to be not only independent of contrast sensitivity, but also of other motion tasks. Accordingly, deficits for other random-dot motion discrimination tasks (e.g., radial, rotational, maximum motion displacement, and motion-defined form) are not strongly correlated with deficits in translational global motion tasks (Aaen-Stockdale et al., 2007; Ho et

al., 2005; Simmers et al., 2006), although a comprehensive study designed to evaluate this hypothesis is warranted.

The finding that global motion deficits were identified for both the amblyopic and fellow eye is informative. Although the visual acuity of the fellow eye is not typically affected by amblyopia, the cortical consequences of amblyopia imply the entire binocular visual system is atypically developed. I found deficits in the fellow eye that were attenuated relative to those in the amblyopic eye, particularly at smaller spatial scales. Hou et al. (2008) found that the fellow eyes of observers with amblyopia showed a similar overall reduction in sensitivity compared to control eyes; however, fellow eyes did not show similar shifts in sensitivity tuning to larger Δx displacements. This may help explain the smaller magnitude of fellow eye deficits, compared to amblyopic eye deficits, found in Chapter 4: both eyes are impacted by deficits in overall motion sensitivity at the second stage described in the paragraph above, but only the amblyopic eye is limited by the first-stage deficits that are associated with parallel shifts in sensitivity for contrast and motion. On the other hand, the fellow eye of children and adults with amblyopia can also show contrast sensitivity deficits, particularly at high spatial frequencies (Chatzistefanou et al., 2005; Leguire, Rogers, & Bremer, 1990; Lewis, Maurer, Tytla, Bowering, & Brent, 1992; Wali et al., 1991; see Meier & Giaschi, 2017 for review), so if the shape of the motion sensitivity curve is limited by spatial frequency input to the fellow eye at the first stage, this is not reflected in the fellow eye tuning curves reported by Hou et al. (2008). The smaller magnitude of fellow eye deficits may also be attributed to a greater proportion of MT cells that are sensitive to fellow eye input in an amblyopic visual system. El-Shamayleh et al. (2010) found that while most cells are driven by the fellow eye, only about half of MT cells were driven by the amblyopic eye. In control macaques, nearly all MT cells can be driven by either eye (Kiorpes, Walton, O'Keefe, Movshon, & Lisberger, 1996; Maunsell & van Essen, 1983). Given the binocular nature of motion integration mechanisms, the deficits observed in both eyes of children with amblyopia likely reflect the abnormally monocular nature of MT responses following early disruption of binocular development.

During development, a child's experience of the visual environment can be disrupted by a number of developmental disorders that have an impact on vision. Many studies have measured this impact on motion perception, but different conclusions on whether motion perception has been disrupted in a variety of disorders have been reported. In addition to amblyopia, these also

include disorders such as autism (e.g., deficits: Milne et al., 2002; Pellicano et al, 2005; no deficits: Jones et al., 2011), dyslexia (e.g., deficits: Cornelissen, Hansen, Hutton, Evangelinou, & Stein, 1998; Talcott et al., 2000; no deficits: Tsermentseli, O'Brien, & Spencer, 2008; White et al., 2006); and Williams syndrome (deficits: Atkinson et al., 2003; Atkinson et al., 1997; Palomares & Shannon, 2013; no deficits: Nakamura, Kaneoke, Watanabe, & Kakigi, 2002; Reiss, Hoffman, & Landau, 2005). The mechanisms underlying motion perception are not all-or-none, however, as demonstrated by the differential maturational ages reported in Chapter 3. The results of Chapter 4 demonstrate that children with amblyopia show age-typical performance for stimuli using Δx = 30 arcmin, but elevated thresholds on 5 and 1 arcmin stimuli. Consistent with this, children with autism have shown deficits for stimuli using Δx = 1.5 arcmin, but not 6 arcmin (Manning et al., 2013), and children with dyslexia have shown deficits on Δx = 1.5 but not 46 arcmin stimuli (Edwards et al., 2004). Thus, while the findings described in this dissertation were conducted using amblyopia as a model of visual development, investigation into the generalizability of this model to other disorders is a worthwhile task.

References

Aaen-Stockdale, C., & Hess, R. F. (2008). The amblyopic deficit for global motion is spatial scale invariant. *Vision Research*, *48*, 1965-1971. doi:10.1016/j.visres.2008.06.012

Aaen-Stockdale, C., Ledgeway, T., & Hess, R. F. (2007). Second-order optic flow deficits in amblyopia. *Investigative Ophthalmology & Visual Science*, *48*, 5532-5538.

Adelson, E. H., & Bergen, J. R. (1985). Spatiotemporal energy models for the perception of motion. *Journal of the Optical Society of America A*, *2*, 284-299.

Ahmed, I. J., Lewis, T. L., Ellemberg, D., & Maurer, D. (2005). Discrimination of speed in 5-year-olds and adults: are children up to speed? *Vision Research*, *45*, 2129-2135. doi:10.1016/j.visres.2005.01.036

Albright, T. D. (1984). Direction and orientation selectivity of neurons in visual area MT of the macaque. *Journal of Neurophysiology*, *52*, 1106-1130.

Arena, A., Hutchinson, C. V., & Shimozaki, S. S. (2012). The effects of age on the spatial and temporal integration of global motion. *Vision Research*, *58*, 27-32. doi:10.1016/j.visres.2012.02.004

Aring, E., Grönlund, M. A., Hellström, A., & Ygge, J. (2007). Visual fixation development in children. *Graefe's Archive for Clinical & Experimental Ophthalmology*, *245*, 1659-1665. doi:10.1007/s00417-007-0585-6

Aslin, R. N., & Shea, S. L. (1990). Velocity thresholds in human infants. *Developmental Psychology*, *26*, 589-598.

Atkinson, J., & Braddick, O. (1992). Visual segmentation of oriented textures by infants. *Behavioural Brain Research*, *49*, 123-131.

Atkinson, J., Braddick, O., Anker, S., Curran, W., Andrew, R., Wattam-Bell, J., & Braddick, F. (2003). Neurobiological models of visuospatial cognition in children with Williams syndrome: measures of dorsal-stream and frontal function. *Developmental Neuropsychology*, *23*, 139-172. doi:10.1080/87565641.2003.9651890

Atkinson, J., French, J., & Braddick, O. (1981). Contrast sensitivity function of preschool children. *British Journal of Ophthalmology*, *65*, 525-529.

Atkinson, J., King, J., Braddick, O., Nokes, L., Anker, S., & Braddick, F. (1997). A specific deficit of dorsal stream function in Williams' syndrome. *Neuroreport*, *8*, 1919-1922.

Attebo, K., Mitchell, P., Cumming, R., Smith, W., Jolly, N., & Sparkes, R. (1998). Prevalence and causes of amblyopia in an adult population. *Ophthalmology*, *105*, 154-159.

Baker, C. L., & Braddick, O. J. (1982). The basis of area and dot number effects in random dot motion perception. *Vision Research*, *22*, 1253-1259.

Baker, C. L. J., & Braddick, O. J. (1985a). Eccentricity-dependent scaling of the limits for short-range apparent motion perception. *Vision Research*, *25*, 803-812.

Baker, C. L. J., & Braddick, O. J. (1985b). Temporal properties of the short-range process in apparent motion. *Perception*, *14*, 181-192.

Barlow, H., & Tripathy, S. P. (1997). Correspondence noise and signal pooling in the detection of coherent visual motion. *Journal of Neuroscience, 17*, 7954-7966.

Beazley, L. D., Illingworth, D. J., Jahn, A., & Greer, D. V. (1980). Contrast sensitivity in children and adults. *British Journal of Ophthalmology*, *64*, 863-866. doi:10.1136/bjo.64.11.863

Bedell, H. E., & Flom, M. C. (1981). Monocular spatial distortion in strabismic amblyopia. *Investigative Ophthalmology & Visual Science*, *20*, 263-268.

Bedell, H. E., Flom, M. C., & Barbeito, R. (1985). Spatial aberrations and acuity in strabismus and amblyopia. *Investigative Ophthalmology & Visual Science*, *26*, 909-916.

Biagi, L., Crespi, S. A., Tosetti, M., & Morrone, M. C. (2015). BOLD Response Selective to Flow-Motion in Very Young Infants. *PLoS Biology*, *13*, e1002260. doi:10.1371/journal.pbio.1002260

Birch, E., & Petrig, B. (1996). FPL and VEP measures of fusion, stereopsis and stereoacuity in normal infants. *Vision Research*, *36*, 1321-1327.

Birch, E. E., Subramanian, V., & Weakley, D. R. (2013). Fixation instability in anisometropic children with reduced stereopsis. *Journal of the American Association for Pediatric Ophthalmology & Strabismus*, *17*, 287-290. doi:10.1016/j.jaapos.2013.03.011

Birch, E. E., & Swanson, W. H. (2000). Hyperacuity deficits in anisometropic and strabismic amblyopes with known ages of onset. *Vision Research*, *40*, 1035-1040.

Birch, E., Williams, C., Drover, J., Fu, V., Cheng, C., Northstone, K., . . . Adams, R. (2008). Randot Preschool Stereoacuity Test: normative data and validity. *Journal of American Association for Pediatric Ophthalmology & Strabismus*, *12*, 23-26. doi:10.1016/j.jaapos.2007.06.003

Blumenthal, E. J., Bosworth, R. G., & Dobkins, K. R. (2013). Fast development of global motion processing in human infants. *Journal of Vision*, *13*, 8. doi:10.1167/13.13.8

Boets, B., De Smedt, B., & Ghesquiere, P. (2011). Coherent motion sensitivity predicts individual differences in subtraction. *Research in Developmental Disabilities*, *32*, 1075-1080. doi:10.1016/j.ridd.2011.01.024

Boets, B., Vandermosten, M., Cornelissen, P., Wouters, J., & Ghesquière, P. (2011). Coherent motion sensitivity and reading development in the transition from prereading to reading stage. *Child Development*, *82*, 854-869. doi:10.1111/j.1467-8624.2010.01527.x

Bogfjellmo, L. G., Bex, P. J., & Falkenberg, H. K. (2014). The development of global motion discrimination in school aged children. *Journal of Vision*, *14*, 1-12. doi:10.1167/14.2.19

Bonneh, Y. S., Sagi, D., & Polat, U. (2004). Local and non-local deficits in amblyopia: acuity and spatial interactions. *Vision Research*, *44*, 3099-3110. doi:10.1016/j.visres.2004.07.031

Boothe, R. G., Dobson, V., & Teller, D. Y. (1985). Postnatal development of vision in human and nonhuman primates. *Annual Review of Neuroscience*, *8*, 495-545. doi:10.1146/annurev.ne.08.030185.002431

Born, R. T., & Bradley, D. C. (2005). Structure and function of visual area MT. *Annual Review of Neuroscience*, *28*, 157-189. doi:10.1146/annurev.neuro.26.041002.131052

Boulton, J. C. (1987). Two mechanisms for the detection of slow motion. *Journal of the Optical Society of America A*, *4*, 1634-1642.

Braddick, O. J., O'Brien, J. M. D., Wattam-Bell, J., Atkinson, J., Hartley, T., & Turner, R. (2001). Brain areas sensitive to coherent visual motion. *Perception*, *30*, 61-72. doi:10.1068/p3048

Braddick, O., & Qian, N. (2001). The organization of global motion and transparency. In J. M. Zanker & J. Zeil (Eds.), *Motion Vision: Computational, Neural, and Ecological Constraints*. Berlin Heidelberg New York: Springer Verlag.

Bradley, A., & Freeman, R. D. (1981). Contrast sensitivity in anisometropic amblyopia. *Investigative Ophthalmology & Visual Science*, *21*, 467-476.

Bradley, D. C., Qian, N., & Andersen, R. A. (1995). Integration of motion and stereopsis in middle temporal cortical area of macaques. *Nature*, *373*, 609-611. doi:10.1038/373609a0

Brainard, D. H. (1997). The Psychophysics Toolbox. *Spatial Vision*, *10*, 433-436. doi:10.1163/156856897x00357

Bremmer, F., Schlack, A., Shah, N. J., Zafiris, O., Kubischik, M., Hoffmann, K., . . . Fink, G. R. (2001). Polymodal motion processing in posterior parietal and premotor cortex: a human fMRI study strongly implies equivalencies between humans and monkeys. *Neuron*, *29*, 287-296.

Buckingham, T., Watkins, R., Bansal, P., & Bamford, K. (1991). Hyperacuity thresholds for oscillatory movement are abnormal in strabismic and anisometropic amblyopes. *Optometry & Vision Science*, *68*, 351-356.

Caca, I., Cingu, A. K., Sahin, A., Ari, S., Dursun, M. E., Dag, U., . . . Palanci, Y. (2013). Amblyopia and refractive errors among school-aged children with low socioeconomic status in southeastern Turkey. *Journal of Pediatric Ophthalmology & Strabismus*, *50*, 37-43. doi:10.3928/01913913-20120804-02

Canty, A., & Ripley, B. (2016). Boot: Bootstrap R (S-Plus) functions. *R package version 1.3-18*.

Cardin, V., & Smith, A. T. (2010). Sensitivity of human visual and vestibular cortical regions to egomotion-compatible visual stimulation. *Cerebral Cortex*, *20*, 1964-1973. doi:10.1093/cercor/bhp268

Carkeet, A., Levi, D. M., & Manny, R. E. (1997). Development of Vernier acuity in childhood. *Optometry & Vision Science*, *74*, 741-750.

Carpenter, J., & Bithell, J. (2000). Bootstrap confidence intervals: when, which, what? A practical guide for medical statisticians. *Statistics in Medicine*, *19*, 1141-1164.

Carpineto, P., Ciancaglini, M., Nubile, M., Di Marzio, G., Toto, L., Di Antonio, L., & Mastropasqua, L. (2007). Fixation patterns evaluation by means of MP-1 microperimeter in microstrabismic children treated for unilateral amblyopia. *European Journal of Ophthalmology*, *17*, 885-890. doi:10.5301/EJO.2008.2464

Castet, E., & Crossland, M. (2012). Quantifying eye stability during a fixation task: A review of definitions and methods. *Seeing & Perceiving*, *25*, 449-469. doi:10.1163/187847611X620955

Chakraborty, A., Anstice, N. S., Jacobs, R. J., LaGasse, L. L., Lester, B. M., Wouldes, T. A., & Thompson, B. (2015). Prenatal exposure to recreational drugs affects global motion perception in preschool children. *Scientific Reports*, *5*, 16921. doi:10.1038/srep16921

Chakraborty, A., Anstice, N. S., Jacobs, R. J., Paudel, N., LaGasse, L. L., Lester, B. M., . . . Thompson, B. (2015). Global motion perception is independent from contrast sensitivity for coherent motion direction discrimination and visual acuity in 4.5-year-old children. *Vision Research*, *115*, 83-91. doi:10.1016/j.visres.2015.08.007

Chandna, A., Gonzalez-Martin, J. A., & Norcia, A. M. (2004). Recovery of contour integration in relation to logMAR visual acuity during treatment of amblyopia in children. *Investigative Ophthalmology & Visual Science*, *45*, 4016-4022. doi:10.1167/iovs.03-0795

Chandna, A., Pennefather, P. M., Kovács, I., & Norcia, A. M. (2001). Contour integration deficits in anisometropic amblyopia. *Investigative Ophthalmology & Visual Science*, *42*, 875-878.

Chang, J. J., & Julesz, B. (1983). Displacement limits for spatial frequency filtered random-dot cinematograms in apparent motion. *Vision Research*, *23*, 1379-1385.

Chatzistefanou, K. I., Theodossiadis, G. P., Damanakis, A. G., Ladas, I. D., Moschos, M. N., & Chimonidou, E. (2005). Contrast sensitivity in amblyopia: the fellow eye of untreated and successfully treated amblyopes. *Journal of the American Association for Pediatric Ophthalmology & Strabismus*, *9*, 468-474. doi:10.1016/j.jaapos.2005.05.002

Chen, Y., Bidwell, L. C., & Holzman, P. S. (2005). Visual motion integration in schizophrenia patients, their first-degree relatives, and patients with bipolar disorder. *Schizophrenia Research*, *74*, 271-281. doi:10.1016/j.schres.2004.04.002

Chen, Y., Nakayama, K., Levy, D., Matthysse, S., & Holzman, P. (2003). Processing of global, but not local, motion direction is deficient in schizophrenia. *Schizophrenia Research*, *61*, 215-227. doi:10.1016/S0920-9964(02)00222-0

Chia, A., Dirani, M., Chan, Y. H., Gazzard, G., Au Eong, K. G., Selvaraj, P., . . . Saw, S. M. (2010). Prevalence of amblyopia and strabismus in young Singaporean Chinese children. *Investigative Ophthalmology & Visual Science*, *51*, 3411-3417. doi:10.1167/iovs.09-4461

Chung, S. T., Kumar, G., Li, R. W., & Levi, D. M. (2015). Characteristics of fixational eye movements in amblyopia: Limitations on fixation stability and acuity. *Vision Research, 114*, 87-99. doi:10.1016/j.visres.2015.01.016

Cleveland, W. S., & Devlin, S. J. (1988). Locally weighted regression: An approach to regression analysis by local fitting. *Journal of the American Statstical Association*, 596-610.

Constantinescu, T., Schmidt, L., Watson, R., & Hess, R. F. (2005). A residual deficit for global motion processing after acuity recovery in deprivation amblyopia. *Investigative Ophthalmology & Visual Science*, *46*, 3008-3012. doi:10.1167/iovs.05-0242

Cornelissen, P. L., Hansen, P. C., Hutton, J. L., Evangelinou, V., & Stein, J. F. (1998). Magnocellular visual function and children's single word reading. *Vision Research*, *38*, 471-482.

Cornelissen, P., Richardson, A., Mason, A., Fowler, S., & Stein, J. (1995). Contrast sensitivity and coherent motion detection measured at photopic luminance levels in dyslexics and controls. *Vision Research*, *35*, 1483-1494.

Ciuffreda, K. J., Kenyon, R. V., & Stark, L. (1979). Abnormal saccadic substitution during small-amplitude pursuit tracking in amblyopic eyes. *Investigative Ophthalmology & Visual Science*, *18*, 506-516.

Davison, A. C., & Hinkley, D. V. (1997). *Bootstrap methods and their applications.* Cambridge: Cambridge University Press.

Derefeldt, G., Lennerstrand, G., & Lundh, B. (1979). Age variations in normal human contrast sensitivity. *Acta Ophthalmologica*, *57*, 679-690.

Derrington, A. M., Allen, H. A., & Delicato, L. S. (2004). Visual mechanisms of motion analysis and motion perception. *Annual Review of Psychology*, *55*, 181-205. doi:10.1146/annurev.psych.55.090902.141903

Downing, C. J., & Movshon, J. A. (1989). Spatial and temporal summation in the detection of motion in stochastic random dot displays. *Supplement to Investigative Ophthalmology and Visual Science*, *30*.

Dumoulin, S. O., Baker, C. L., Hess, R. F., & Evans, A. C. (2003). Cortical specialization for processing first- and second-order motion. *Cerebral Cortex*, *13*, 1375-1385. doi:10.1093/cercor/bhg085

Dunnett, C. W. (1955). A multiple comparison procedure for comparing several treatments with a control. *Journal of the American Statistical Association*, *50*, 1096-1121.

Dunnett, C. W. (1964). New tables for multiple comparisons with a control. *Biometrics*, *20*, 482-491.

Eagle, R. A., & Rogers, B. J. (1996). Motion detection is limited by element density not spatial frequency. *Vision Research*, *36*, 545-558.

Eagle, R. A., & Rogers, B. J. (1997). Effects of dot density, patch size and contrast on the upper spatial limit for direction discrimination in random-dot kinematograms. *Vision Research*, *37*, 2091-2102.

Edwards, V. T., Giaschi, D. E., Dougherty, R. F., Edgell, D., Bjornson, B. H., Lyons, C., & Douglas, R. M. (2004). Psychophysical indexes of temporal processing abnormalities in children with developmental dyslexia. *Developmental Neuropsychology*, *25*, 321-354. doi:10.1207/s15326942dn2503_5

Efron, B. (1987). Better bootstrap confidence intervals. *Journal of the American Statistical Association*, *82*, 171-185.

El-Shamayleh, Y., Kiorpes, L., Kohn, A., & Movshon, J. A. (2010). Visual motion processing by neurons in area MT of macaque monkeys with experimental amblyopia. *Journal of Neuroscience*, *30*, 12198-12209. doi:10.1523/JNEUROSCI.3055-10.2010

Ellemberg, D., Lewis, T. L., Maurer, D., Brar, S., & Brent, H. P. (2002). Better perception of global motion after monocular than after binocular deprivation. *Vision Research*, *42*, 169-179.

Ellemberg, D., Lewis, T. L., Maurer, D., Lee, B., Ledgeway, T., Guilemot, J. P., & Lepore, F. (2010). The effect of displacement on sensitivity to first- and second-order global motion in 5-year-olds and adults. *Seeing & Perceiving*, *23*, 517-532.

Ellemberg, D., Lewis, T. L., Meghji, K. S., Maurer, D., Guillemot, J. P., & Lepore, F. (2003). Comparison of sensitivity to first- and second-order local motion in 5-year-olds and adults. *Spatial Vision, 16*, 419-428.

Ellemberg, D., Lewis, T. L., Dirks, M., Maurer, D., Ledgeway, T., Guillemot, J.-P., & Lepore, F. (2004). Putting order into the development of sensitivity to global motion. *Vision Research*, *44*, 2403-2411. doi:10.1016/j.visres.2004.05.006

Falkenberg, H. K., Simpson, W. A., & Dutton, G. N. (2014). Development of sampling efficiency and internal noise in motion detection and discrimination in school-aged children. *Vision Research*, *100*, 8-17. doi:10.1016/j.visres.2014.04.001

Fern, K. D., & Manny, R. E. (1986). Visual acuity of the preschool child: a review. *American Journal of Optometry & Physiological Optics*, *63*, 319-345.

Festa, E. K., & Welch, L. (1997). Recruitment mechanisms in speed and fine-direction discrimination tasks. *Vision Research, 37*, 3129-3143.

Fox, R., Aslin, R. N., Shea, S. L., & Dumais, S. T. (1980). Stereopsis in human infants. *Science*, *207*, 323-324.

Freeman, R. D., & Bradley, A. (1980). Monocularly deprived humans: nondeprived eye has supernormal vernier acuity. *Journal of Neurophysiology*, *43*, 1645-1653.

Fronius, M., Sireteanu, R., & Zubcov, A. (2004). Deficits of spatial localization in children with strabismic amblyopia. *Graefe's Archive for Clinical & Experimental Ophthalmology*, *242*, 827-839. doi:10.1007/s00417-004-0936-5

Gattass, R., & Gross, C. G. (1981). Visual topography of striate projection zone (MT) in posterior superior temporal sulcus of the macaque. *Journal of Neurophysiology*, *46*, 621-638.

Gattass, R., Nascimento-Silva, S., Soares, J. G., Lima, B., Jansen, A. K., Diogo, A. C., . . . Fiorani, M. (2005). Cortical visual areas in monkeys: location, topography, connections, columns, plasticity and cortical dynamics. *Philosophical Transactions: Biolgocial Sciences*, *360*, 709-731. doi:10.1098/rstb.2005.1629

Giaschi, D., Chapman, C., Meier, K., Narasimhan, S., & Regan, D. (2015). The effect of occlusion therapy on motion perception deficits in amblyopia. *Vision Research*, *114*, 122-134. doi:10.1016/j.visres.2015.05.015

Giaschi, D., Lo, R., Narasimhan, S., Lyons, C., & Wilcox, L. M. (2013). Sparing of coarse stereopsis in stereodeficient children with a history of amblyopia. *Journal of Vision*, *13*, 1-15. doi:10.1167/13.10.17

Giaschi, D., Narasimhan, S., Solski, A., Harrison, E., & Wilcox, L. M. (2013). On the typical development of stereopsis: fine and coarse processing. *Vision Research*, *89*, 65-71. doi:10.1016/j.visres.2013.07.011

Giaschi, D., & Regan, D. (1997). Development of motion-defined figure-ground segregation in preschool and older children, using a letter-identification task. *Optometry & Vision Science*, *74*, 761-767.

Giaschi, D. E., Regan, D., Kraft, S. P., & Hong, X. H. (1992). Defective processing of motion-defined form in the fellow eye of patients with unilateral amblyopia. *Investigative Ophthalmology & Visual Science*, *33*, 2483-2489.

Gijbels, I., & Prosdocimi, I. (2010). Loess. *WIREs Computational Statistics*, *2*, 590-599. doi:10.1002/wics.104

Gilaie-Dotan, S. (2016). Visual motion serves but is not under the purview of the dorsal pathway. *Neuropsychologia*, *89*, 378-392. doi:10.1016/j.neuropsychologia.2016.07.018

Gilbert, C. D. (1998). Adult cortical dynamics. *Physiological Reviews*, *78*, 467-485.

Gilmore, R. O., Hou, C., Pettet, M. W., & Norcia, A. M. (2007). Development of cortical responses to optic flow. *Visual Neuroscience*, *24*, 845-856. doi:10.1017/S0952523807070769

Gilmore, R. O., Raudies, F., & Jayaraman, S. (2015). *What accounts for developmental shifts in optic flow sensitivity?* Proceedings from Proceedings of the 5th International Conference on Development and Learning and on Epigenetic Robotics.

Gilmore, R. O., Thomas, A. L., & Fesi, J. (2016). Children's brain responses to optic flow vary by pattern type and motion speed. *PLoS One*, *11*, e0157911. doi:10.1371/journal.pone.0157911

González, E. G., Lillakas, L., Greenwald, N., Gallie, B. L., & Steinbach, M. J. (2014). Unaffected smooth pursuit but impaired motion perception in monocularly enucleated observers. *Vision Research*, *101*, 151-157. doi:10.1016/j.visres.2014.06.014

González, E. G., Wong, A. M., Niechwiej-Szwedo, E., Tarita-Nistor, L., & Steinbach, M. J. (2012). Eye position stability in amblyopia and in normal binocular vision. *Investigative Ophthalmology & Visual Science*, *53*, 5386-5394. doi:10.1167/iovs.12-9941

Gummel, K., Ygge, J., Benassi, M., & Bolzani, R. (2012). Motion perception in children with foetal alcohol syndrome. *Acta Paediatrica*, *101*, e327-32. doi:10.1111/j.1651-2227.2012.02700.x

Gunn, A., Cory, E., Atkinson, J., Braddick, O., Wattam-Bell, J., Guzzetta, A., & Cioni, G. (2002). Dorsal and ventral stream sensitivity in normal development and hemiplegia. *Neuroreport*, *13*, 843-847.

Guzzetta, A., Tinelli, F., Del Viva, M. M., Bancale, A., Arrighi, R., Pascale, R. R., & Cioni, G. (2009). Motion perception in preterm children: role of prematurity and brain damage. *Neuroreport*, *20*, 1339-1343. doi:10.1097/WNR.0b013e328330b6f3

Hadad, B., Maurer, D., & Lewis, T. L. (2010). The effects of spatial proximity and collinearity on contour integration in adults and children. *Vision Research*, *50*, 772-778. doi:10.1016/j.visres.2010.01.021

Hadad, B. S., Maurer, D., & Lewis, T. L. (2011). Long trajectory for the development of sensitivity to global and biological motion. *Developmental Science*, *14*, 1330-1339. doi:10.1111/j.1467-7687.2011.01078.x

Hall, J. L. (1981). Hybrid adaptive procedure for estimation of psychometric functions. *Journal of the Acoustical Society of America*, *69*, 1763-1769. doi:10.1121/1.385912

Hayward, J., Truong, G., Partanen, M., & Giaschi, D. (2011). Effects of speed, age, and amblyopia on the perception of motion-defined form. *Vision Research*, *51*, 2216-2223. doi:10.1016/j.visres.2011.08.023

Heron, G., Dholakia, S., Collins, D. E., & McLaughlan, H. (1985). Stereoscopic threshold in children and adults. *American Journal of Optometry & Physiological Optics*, *62*, 505-515.

Helfrich, R. F., Becker, H. G., & Haarmeier, T. (2013). Processing of coherent visual motion in topographically organized visual areas in human cerebral cortex. *Brain Topography*, *26*, 247-263. doi:10.1007/s10548-012-0226-1

Hess, R. F., Campbell, F. W., & Greenhalgh, T. (1978). On the nature of the neural abnormality in human amblyopia; neural aberrations and neural sensitivity loss. *Pflugers Archiv*, *377*, 201-207.

Hess, R. F., & Demanins, R. (1998). Contour integration in anisometropic amblyopia. *Vision Research*, *38*, 889-894.

Hess, R. F., Demanins, R., & Bex, P. J. (1997). A reduced motion aftereffect in strabismic amblyopia. *Vision Research*, *37*, 1303-1311.

Hess, R. F., & Howell, E. R. (1977). The threshold contrast sensitivity function in strabismic amblyopia: evidence for a two type classification. *Vision Research*, *17*, 1049-1055.

Hess, R. F., Mansouri, B., Dakin, S. C., & Allen, H. A. (2006). Integration of local motion is normal in amblyopia. *Journal of the Optical Society of America A*, *23*, 986-992.

Ho, C. S., & Giaschi, D. E. (2006). Deficient maximum motion displacement in amblyopia. *Vision Research*, *46*, 4595-4603. doi:10.1016/j.visres.2006.09.025

Ho, C. S., & Giaschi, D. E. (2007). Stereopsis-dependent deficits in maximum motion displacement in strabismic and anisometropic amblyopia. *Vision Research*, *47*, 2778-2785. doi:10.1016/j.visres.2007.07.008

Ho, C. S., & Giaschi, D. E. (2009). Low- and high-level motion perception deficits in anisometropic and strabismic amblyopia: evidence from fMRI. *Vision Research*, *49*, 2891-2901. doi:10.1016/j.visres.2009.07.012

Ho, C. S., Giaschi, D. E., Boden, C., Dougherty, R., Cline, R., & Lyons, C. (2005). Deficient motion perception in the fellow eye of amblyopic children. *Vision Research*, *45*, 1615-1627. doi:10.1016/j.visres.2004.12.009

Ho, C. S., Paul, P. S., Asirvatham, A., Cavanagh, P., Cline, R., & Giaschi, D. E. (2006). Abnormal spatial selection and tracking in children with amblyopia. *Vision Research*, *46*, 3274-3283. doi:10.1016/j.visres.2006.03.029

Høeg, T. B., Moldow, B., Ellervik, C., Klemp, K., Erngaard, D., la Cour, M., & Buch, H. (2015). Danish Rural Eye Study: the association of preschool vision screening with the prevalence of amblyopia. *Acta Ophthalmologica*, *93*, 322-329. doi:10.1111/aos.12639

Holm, S. (1979). A simple sequentially rejective multiple test procedure. *Scandinavian Journal of Statistics*, *6*, 65-70.

Holmes, J. M., & Clarke, M. P. (2006). Amblyopia. *Lancet*, *367*, 1343-1351. doi:10.1016/S0140-6736(06)68581-4

Horton, J. C., & Hocking, D. R. (1997). Timing of the critical period for plasticity of ocular dominance columns in macaque striate cortex. *Journal of Neuroscience*, *17*, 3684-3709.

Hou, C., Gilmore, R. O., Pettet, M. W., & Norcia, A. M. (2009). Spatio-temporal tuning of coherent motion evoked responses in 4-6 month old infants and adults. *Vision Research*, *49*, 2509-2517. doi:10.1016/j.visres.2009.08.007

Hou, C., Pettet, M. W., & Norcia, A. M. (2008). Abnormalities of coherent motion processing in strabismic amblyopia: Visual-evoked potential measurements. *Journal of Vision*, *8*, 2.1-212. doi:10.1167/8.4.2

Howell, E. R., Mitchell, D. E., & Keith, C. G. (1983). Contrast thresholds for sine gratings of children with amblyopia. *Investigative Ophthalmology & Visual Science*, *24*, 782-787.

Hubel, D. H., & Wiesel, T. N. (1970). The period of susceptibility to the physiological effects of unilateral eye closure in kittens. *Journal of Physiology*, *206*, 419-436.

Hyvärinen, L., Näsänen, R., & Laurinen, P. (1980). New visual acuity test for pre-school children. *Acta Ophthalmologica*, *58*, 507-511.

Jacoby, W. G. (2000). Loess: A nonparametric, graphical tool for depicting relationships between variables. *Electoral Studies*, *19*, 577-613.

Jones, C. R., Swettenham, J., Charman, T., Marsden, A. J., Tregay, J., Baird, G., . . . Happe, F. (2011). No evidence for a fundamental visual motion processing deficit in adolescents with autism spectrum disorders. *Autism Research*, *4*, 347-357. doi:10.1002/aur.209

Joshi, M. R., & Falkenberg, H. K. (2015). Development of radial optic flow pattern sensitivity at different speeds. *Vision Research*, *110*, 68-75. doi:10.1016/j.visres.2015.03.006

Joshi, M. R., Simmers, A. J., & Jeon, S. T. (2016). Concurrent Investigation of Global Motion and Form Processing in Amblyopia: An Equivalent Noise Approach. *Investigative Ophthalmology & Visual Science*, *57*, 5015-5022. doi:10.1167/iovs.15-18609

Kassaliete, E., Lacis, I., Fomins, S., & Krumina, G. (2015). Reading and coherent motion perception in school age children. *Annals of Dyslexia*, *65*, 69-83. doi:10.1007/s11881-015-0099-6

Katz, L. M., Levi, D. M., & Bedell, H. E. (1984). Central and peripheral contrast sensitivity in amblyopia with varying field size. *Documenta Ophthalmologica*, *58*, 351-373.

Kaufmann, F. (1995). Development of motion perception in early infancy. *European Journal of Pediatrics*, *154*, S48-53.

Kelly, S. L., & Buckingham, T. J. (1998). Movement hyperacuity in childhood amblyopia. *British Journal of Ophthalmology*, *82*, 991-995.

Kenyon, R. V., Ciuffreda, K. J., & Stark, L. (1981). Dynamic vergence eye movements in strabismus and amblyopia: asymmetric vergence. *British Journal of Ophthalmology*, *65*, 167-176. doi:10.1136/bjo.65.3.167

Kenyon, R. V., Ciuffreda, K. J., & Stark, L. (1980). Dynamic vergence eye movements in strabismus and amblyopia: symmetric vergence. *Investigative Ophthalmology & Visual Science*, *19*, 60-74.

Kim, E., Enoch, J. M., Fang, M. S., Lakshminarayanan, V., Kono, M., Strada, E., & Srinivasan, R. (2000). Performance on the three-point Vernier alignment or acuity test as a function of age: measurement extended to ages 5 to 9 years. *Optometry & Vision Science*, *77*, 492-495.

Kiorpes, L. (2006). Visual processing in amblyopia: animal studies. *Strabismus*, *14*, 3-10. doi:10.1080/09273970500536193

Kiorpes, L., & Bassin, S. A. (2003). Development of contour integration in macaque monkeys. *Visual Neuroscience*, *20*, 567-575.

Kiorpes, L., & Movshon, J. A. (2004). Development of sensitivity to visual motion in macaque monkeys. *Visual Neuroscience*, *21*, 851-859. doi:10.1017/S0952523804216054

Kiorpes, L., Price, T., Hall-Haro, C., & Movshon, J. A. (2012). Development of sensitivity to global form and motion in macaque monkeys (Macaca nemestrina). *Vision Research*, *63*, 34-42. doi:10.1016/j.visres.2012.04.018

Kiorpes, L., Tang, C., & Movshon, J. A. (2006). Sensitivity to visual motion in amblyopic macaque monkeys. *Visual Neuroscience*, *23*, 247-256. doi:10.1017/S0952523806232097

Kiorpes, L., Walton, P. J., O'Keefe, L. P., Movshon, J. A., & Lisberger, S. G. (1996). Effects of early-onset artificial strabismus on pursuit eye movements and on neuronal responses in area MT of macaque monkeys. *Journal of Neuroscience*, *16*, 6537-6553.

Kleiner, M., Brainard, D., & Pelli, D. (2007). What's new in Psychtoolbox-3? *Perception*, *36*, ECVP Abstract Supplement. doi:doi:10.1068/v070821

Knox, P. J., Ledgeway, T., & Simmers, A. J. (2013). The effects of spatial offset, temporal offset and image speed on sensitivity to global motion in human amblyopia. *Vision Research*, *86*, 59-65. doi:10.1016/j.visres.2013.04.003

Kothe, A. C. (1990). The component of gaze selection/control in the development of visual acuity in children. *Optometry and Vision Science*, *67*, 770-778.

Kourtzi, Z., Augath, M., Logothetis, N. K., Movshon, J. A., & Kiorpes, L. (2006). Development of visually evoked cortical activity in infant macaque monkeys studied longitudinally with fMRI. *Magnetic Resonance Imaging*, *24*, 359-366. doi:10.1016/j.mri.2005.12.025

Kovács, I., Kozma, P., Feher, A., & Benedek, G. (1999). Late maturation of visual spatial integration in humans. *Proceedings of the National Academy of Sciences USA*, *96*, 12204-12209.

Kovács, I., Polat, U., Pennefather, P. M., Chandna, A., & Norcia, A. M. (2000). A new test of contour integration deficits in patients with a history of disrupted binocular experience during visual development. *Vision Research*, *40*, 1775-1783.

Kozma, P., & Kiorpes, L. (2003). Contour integration in amblyopic monkeys. *Visual Neuroscience*, *20*, 577-588.

Krug, K., & Parker, A. J. (2011). Neurons in dorsal visual area V5/MT signal relative disparity. *Journal of Neuroscience*, *31*, 17892-17904. doi:10.1523/JNEUROSCI.2658-11.2011

Laubrock, J., Engbert, R., & Kliegl, R. (2008). Fixational eye movements predict the perceived direction of ambiguous apparent motion. *Journal of Vision, 8*, 13.1-1317. doi:10.1167/8.14.13

Leat, S. J., Pierre, J. S., Hassan-Abadi, S., & Faubert, J. (2001). The moving Dynamic Random Dot Stereosize test: development, age norms, and comparison with the Frisby, Randot, and Stereo Smile tests. *Journal of Pediatric Ophthalmology & Strabismus*, *38*, 284-294.

Leek, M. R., Hanna, T. E., & Marshall, L. (1992). Estimation of psychometric functions from adaptive tracking procedures. *Perception & Psychophysics, 51*, 247-256.

Leguire, L. E., Rogers, G. L., & Bremer, D. L. (1990). Amblyopia: the normal eye is not normal. *Journal of Pediatric Ophthalmology & Strabismus*, *27*, 32-8; discussion 39.

LeVay, S., Wiesel, T. N., & Hubel, D. H. (1980). The development of ocular dominance columns in normal and visually deprived monkeys. *Journal of Comparative Neurology*, *191*, 1-51. doi:10.1002/cne.901910102

Levi, D., & Carkeet, A. (1993). Amblyopia: A consequence of abnormal visual development. In K. Simons (Ed.), *Early visual development, normal and abnormal* (pp. 391-408). New York: Oxford University Press.

Levi, D. M., & Harwerth, R. S. (1977). Spatio-temporal interactions in anisometropic and strabismic amblyopia. *Investigative Ophthalmology & Visual Science*, *16*, 90-95.

Levi, D. M., & Klein, S. (1982a). Hyperacuity and amblyopia. *Nature*, *298*, 268-270. doi:10.1038/298268a0

Levi, D. M., & Klein, S. (1982b). Differences in vernier discrimination for grating between strabismic and anisometropic amblyopes. *Investigative Ophthalmology & Visual Science*, *23*, 398-407.

Levi, D. M., & Klein, S. A. (1985). Vernier acuity, crowding and amblyopia. *Vision Research*, *25*, 979-991.

Levi, D. M., Waugh, S. J., & Beard, B. L. (1994). Spatial scale shifts in amblyopia. *Vision Research*, *34*, 3315-3333.

Levi, D. M., Yu, C., Kuai, S. G., & Rislove, E. (2007). Global contour processing in amblyopia. *Vision Research*, *47*, 512-524. doi:10.1016/j.visres.2006.10.014

Lewis, T. L., Ellemberg, D., Maurer, D., Dirks, M., Wilkinson, F., & Wilson, H. R. (2004). A window on the normal development of sensitivity to global form in Glass patterns. *Perception*, *33*, 409-418. doi:10.1068/p5189

Lewis, T. L., Ellemberg, D., Maurer, D., Wilkinson, F., Wilson, H. R., Dirks, M., & Brent, H. P. (2002). Sensitivity to global form in glass patterns after early visual deprivation in humans. *Vision Research*, *42*, 939-948.

Lewis, T. L., & Maurer, D. (2005). Multiple sensitive periods in human visual development: evidence from visually deprived children. *Developmental Psychobiology*, *46*, 163-183. doi:10.1002/dev.20055

Lewis, T. L., & Maurer, D. (2009). Effects of early pattern deprivation on visual development. *Optometry & Vision Science*, *86*, 640-646. doi:10.1097/OPX.0b013e3181a7296b

Lewis, T. L., Maurer, D., Tytla, M. E., Bowering, E. R., & Brent, H. P. (1992). Vision in the "good" eye of children treated for unilateral congenital cataract. *Ophthalmology*, *99*, 1013-1017.

Li, Z. (1998). A neural model of contour integration in the primary visual cortex. *Neural Computation*, *10*, 903-940.

Manning, C., Aagten-Murphy, D., & Pellicano, E. (2012). The development of speed discrimination abilities. *Vision Research*, *70*, 27-33. doi:10.1016/j.visres.2012.08.004

Manning, C., Charman, T., & Pellicano, E. (2013). Processing slow and fast motion in children with autism spectrum conditions. *Autism Research*, *6*, 531-541. doi:10.1002/aur.1309

Manning, C., Charman, T., & Pellicano, E. (2015). Brief Report: Coherent Motion Processing in Autism: Is Dot Lifetime an Important Parameter? *Journal of Autism & Developmental Disorders, 45*, 2252-2258. doi:10.1007/s10803-015-2365-1

Mansouri, B., Thompson, B., & Hess, R. F. (2008). Measurement of suprathreshold binocular interactions in amblyopia. *Vision Research*, *48*, 2775-2784. doi:10.1016/j.visres.2008.09.002

Martinez-Conde, S., Otero-Millan, J., & Macknik, S. L. (2013). The impact of microsaccades on vision: towards a unified theory of saccadic function. *Nature Reviews Neuroscience*, *14*, 83-96. doi:10.1038/nrn3405

Mason, A. J. S., Braddick, O. J., & Wattam-Bell, J. (2003). Motion coherence thresholds in infants—different tasks identify at least two distinct motion systems. *Vision Research*, *43*, 1149-1157. doi:10.1016/S0042-6989(03)00077-4

Maunsell, J. H., & van Essen, D. C. (1983). Functional properties of neurons in middle temporal visual area of the macaque monkey. II. Binocular interactions and sensitivity to binocular disparity. *Journal of Neurophysiology*, *49*, 1148-1167.

Mayer, D. L., Beiser, A. S., Warner, A. F., Pratt, E. M., Raye, K. N., & Lang, J. M. (1995). Monocular acuity norms for the Teller Acuity Cards between ages one month and four years. *Investigative Ophthalmology & Visual Science*, *36*, 671-685.

McKee, S. P., Levi, D. M., & Movshon, J. A. (2003). The pattern of visual deficits in amblyopia. *Journal of Vision*, *3*, 380-405. doi:10:1167/3.5.5

McKee, S. P., Levi, D. M., Schor, C. M., & Movshon, J. A. (2016). Saccadic latency in amblyopia. *Journal of Vision*, *16*, 3. doi:10.1167/16.5.3

McKee, S. P., & Welch, L. (1985). Sequential recruitment in the discrimination of velocity. *JOSA A*, *2*, 243-251.

Meier, K., & Giaschi, D. (2014). The maturation of global motion perception depends on the spatial and temporal offsets of the stimulus. *Vision Research*, *95*, 61-67. doi:10.1016/j.visres.2013.12.007

Meier, K., & Giaschi, D. (2017). Unilateral amblyopia affects two eyes: Fellow eye deficits in amblyopia. *Investigative Ophthalmology & Vision Science*, *58*, 1779-1800.

Mikami, A., Newsome, W. T., & Wurtz, R. H. (1986). Motion selectivity in macaque visual cortex. II. Spatiotemporal range of directional interactions in MT and V1. *Journal of Neurophysiology*, *55*, 1328-1339.

Milne, E., Swettenham, J., Hansen, P., Campbell, R., Jeffries, H., & Plaisted, K. (2002). High motion coherence thresholds in children with autism. *Journal of Child Psychology and Psychiatry*, *43*, 255-263.

Milner, A. D., & Goodale, M. A. (2006). *The visual Brain in Action (2nd ed.).* Oxford: Oxford University Press.

Mitchell, D. E., Kennie, J., & Kung, D. (2009). Development of global motion perception requires early postnatal exposure to patterned light. *Current Biology*, *19*, 645-649. doi:10.1016/j.cub.2009.02.038

Morgan, M. J., Perry, R., & Fahle, M. (1997). The spatial limit for motion detection in noise depends on element size, not on spatial frequency. *Vision Research*, *37*, 729-736.

Morrone, M. C., Atkinson, J., Cioni, G., Braddick, O. J., & Fiorentini, A. (1999). Developmental changes in optokinetic mechanisms in the absence of unilateral cortical control. *Neuroreport*, *10*, 2723-2729.

Movshon, J. A., & Kiorpes, L. (1988). Analysis of the development of spatial contrast sensitivity in monkey and human infants. *Journal of the Optical Society of America A*, *5*, 2166-2172.

Multi-ethnic Pediatric Eye Disease Study Group. (2008). Prevalence of amblyopia and strabismus in African American and Hispanic children ages 6 to 72 months the multi-ethnic pediatric eye disease study. *Ophthalmology*, *115*, 1229-1236.e1. doi:10.1016/j.ophtha.2007.08.001

Murakami, I. (2010). Eye movements during fixation as velocity noise in minimum motion detection: Fixational eye movements and motion detection. *Japanese Psychological Research*, *52*, 54-66. doi:10.1111/(ISSN)1468-5884

Mussap, A. J., & Levi, D. M. (2000). Amblyopic deficits in detecting a dotted line in noise. *Vision Research*, *40*, 3297-3307.

Nakamura, M., Kaneoke, Y., Watanabe, K., & Kakigi, R. (2002). Visual information process in Williams syndrome: intact motion detection accompanied by typical visuospatial dysfunctions: Visual cognition in Williams syndrome. *European Journal of Neuroscience*, *16*, 1810-1818. doi:10.1046/j.1460-9568.2002.02227.x

Nakayama, K., & Silverman, G. H. (1984). Temporal and spatial characteristics of the upper displacement limit for motion in random dots. *Vision Research*, *24*, 293-299.

Narasimhan, S., & Giaschi, D. (2012). The effect of dot speed and density on the development of global motion perception. *Vision Research*, *62*, 102-107. doi:10.1016/j.visres.2012.02.016

Narasimhan, S., Harrison, E. R., & Giaschi, D. E. (2012). Quantitative measurement of interocular suppression in children with amblyopia. *Vision Research*, *66*, 1-10. doi:10.1016/j.visres.2012.06.007

Newsome, W. T., Mikami, A., & Wurtz, R. H. (1986). Motion selectivity in macaque visual cortex. III. Psychophysics and physiology of apparent motion. *Journal of Neurophysiology*, *55*, 1340-1351.

Niechwiej-Szwedo, E., Goltz, H. C., Chandrakumar, M., Hirji, Z. A., & Wong, A. M. (2010). Effects of anisometropic amblyopia on visuomotor behavior, I: saccadic eye movements. *Investigative Ophthalmology & Visual Science*, *51*, 6348-6354. doi:10.1167/iovs.10-5882

Norcia, A. M., Pei, F., Bonneh, Y., Hou, C., Sampath, V., & Pettet, M. W. (2005). Development of sensitivity to texture and contour information in the human infant. *Journal of Cognitive Neuroscience*, *17*, 569-579. doi:10.1162/0898929053467596

O'Bryan, R. A., Brenner, C. A., Hetrick, W. P., & O'Donnell, B. F. (2014). Disturbances of visual motion perception in bipolar disorder. *Bipolar Disorders*, *16*, 354-365. doi:10.1111/bdi.12173

Orban, G. A., Fize, D., Peuskens, H., Denys, K., Nelissen, K., Sunaert, S., . . . Vanduffel, W. (2003). Similarities and differences in motion processing between the human and macaque brain: evidence from fMRI. *Neuropsychologia*, *41*, 1757-1768. doi:10.1016/S0028-3932(03)00177-5

Palomares, M., & Shannon, M. T. (2013). Global dot integration in typically developing children and in Williams syndrome. *Brain & Cognition*, *83*, 262-270. doi:10.1016/j.bandc.2013.09.003

Parrish, E. E., Giaschi, D. E., Boden, C., & Dougherty, R. (2005). The maturation of form and motion perception in school age children. *Vision Research*, *45*, 827-837. doi:10.1016/j.visres.2004.10.005

Pediatric Eye Disease Investigator Group. (2003). A randomized trial of patching regimens for treatment of moderate amblyopia in children. *Archives of Ophthalmology*, *121*, 603-611. doi:10.1001/archopht.121.5.603

Pelli, D. G. (1997). The VideoToolbox software for visual psychophysics: transforming numbers into movies. *Spatial Vision*, *10*, 437-442.

Pellicano, E., Gibson, L., Maybery, M., Durkin, K., & Badcock, D. R. (2005). Abnormal global processing along the dorsal visual pathway in autism: a possible mechanism for weak visuospatial coherence. *Neuropsychologia*, *43*, 1044-1053. doi:10.1016/j.neuropsychologia.2004.10.003

Pilly, P. K., & Seitz, A. R. (2009). What a difference a parameter makes: a psychophysical comparison of random dot motion algorithms. *Vision Research*, *49*, 1599-1612. doi:10.1016/j.visres.2009.03.019

Pitzalis, S., Sereno, M. I., Committeri, G., Fattori, P., Galati, G., Patria, F., & Galletti, C. (2010). Human v6: the medial motion area. *Cerebral Cortex*, *20*, 411-424. doi:10.1093/cercor/bhp112

Port, N. L., Trimberger, J., Hitzeman, S., Redick, B., & Beckerman, S. (2016). Micro and regular saccades across the lifespan during a visual search of "Where's Waldo" puzzles. *Vision Research, 118*, 144-157. doi:10.1016/j.visres.2015.05.013

Priebe, N. J., Cassanello, C. R., & Lisberger, S. G. (2003). The neural representation of speed in macaque area MT/V5. *Journal of Neuroscience, 23*, 5650-5661.

Priebe, N. J., Lisberger, S. G., & Movshon, J. A. (2006). Tuning for spatiotemporal frequency and speed in directionally selective neurons of macaque striate cortex. *Journal of Neuroscience*, *26*, 2941-2950. doi:10.1523/JNEUROSCI.3936-05.2006

Raashid, R. A., Liu, I. Z., Blakeman, A., Goltz, H. C., & Wong, A. M. (2016). The initiation of smooth pursuit is delayed in anisometropic amblyopia. *Investigative Ophthalmology & Vision Science*, *57*, 1757-1764. doi:10.1167/iovs.16-19126

Raudies, F., & Gilmore, R. O. (2014). Visual motion priors differ for infants and mothers. *Neural Computation*, *26*, 2652-2668. doi:10.1162/NECO_a_00645

Raveendran, R. N., Babu, R. J., Hess, R. F., & Bobier, W. R. (2014). Transient improvements in fixational stability in strabismic amblyopes following bifoveal fixation and reduced interocular suppression. *Ophthalmic Physiology & Optics*, *34*, 214-225. doi:10.1111/opo.12119

Regan, D. (1988). Low contrast letter charts and sinewave grating tests in ophthalmological and neurological disorders. *Clinical Vision Science*, *2*, 235-250.

Reiss, J. E., Hoffman, J. E., & Landau, B. (2005). Motion processing specialization in Williams syndrome. *Vision Research*, *45*, 3379-3390. doi:10.1016/j.visres.2005.05.011

Rentschler, I., & Hilz, R. (1985). Amblyopic processing of positional information. Part I: Vernier acuity. *Experimental Brain Research*, *60*, 270-278.

Rislove, E. M., Hall, E. C., Stavros, K. A., & Kiorpes, L. (2010). Scale-dependent loss of global form perception in strabismic amblyopia. *Journal of Vision*, *10*, 25. doi:10.1167/10.12.25

Robaei, D., Kifley, A., Rose, K. A., & Mitchell, P. (2008). Impact of amblyopia on vision at age 12 years: findings from a population-based study. *Eye*, *22*, 496-502. doi:10.1038/sj.eye.6702668

Robaei, D., Rose, K. A., Ojaimi, E., Kifley, A., Martin, F. J., & Mitchell, P. (2006). Causes and associations of amblyopia in a population-based sample of 6-year-old Australian children. *Archives of Ophthalmology*, *124*, 878-884. doi:10.1001/archopht.124.6.878

Rolfs, M. (2009). Microsaccades: small steps on a long way. *Vision Research, 49*, 2415-2441. doi:10.1016/j.visres.2009.08.010

Sato, T. (1998). Dmax: Relations to low- and high-level motion processes. In T. Watanabe (Ed.), *High-level motion processing, computational, neurobiological* (pp. 115-151). Boston: MIT Press.

Satterthwaite, F. E. (1946). An approximate distribution of estimates of variance components. *Biometrics*, *2*, 110-114.

Schenk, T., Mai, N., Ditterich, J., & Zihl, J. (2000). Can a motion-blind patient reach for moving objects? *European Journal of Neuroscience*, *12*, 3351-3360.

Schenk, T., & McIntosh, R. D. (2010). Do we have independent visual streams for perception and action? *Cognitive Neuroscience*, *1*, 52-62. doi:10.1080/17588920903388950

Schrauf, M., Wist, E. R., & Ehrenstein, W. H. (1999). Development of dynamic vision based on motion contrast. *Experimental Brain Research*, *124*, 469-473.

Schor, C. (1975). A directional impairment of eye movement control in strabismus amblyopia. *Investigative Ophthalmology & Visual Science*, *14*, 692-697.

Schor, C., & Narayan, V. (1981). The influence of field size upon the spatial frequency response of optokinetic nystagmus. *Vision Research*, *21*, 985-994.

Secen, J., Culham, J., Ho, C., & Giaschi, D. (2011). Neural correlates of the multiple-object tracking deficit in amblyopia. *Vision Research*, *51*, 2517-2527. doi:10.1016/j.visres.2011.10.011

Seemiller, E. S., Port, N. L., & Candy, T. R. (under revision). The gaze stability of 4- to 10-week-old human infants. Journal of Vision.

Shaikh, A. G., Otero-Millan, J., Kumar, P., & Ghasia, F. F. (2016). Abnormal fixational eye movements in amblyopia. *PLoS One*, *11*, e0149953. doi:10.1371/journal.pone.0149953

Shi, X. F., Xu, L. M., Li, Y., Wang, T., Zhao, K. X., & Sabel, B. A. (2012). Fixational saccadic eye movements are altered in anisometropic amblyopia. *Restorative Neurology & Neuroscience*, *30*, 445-462. doi:10.3233/RNN-2012-129000

Sigmundsson, H., Anholt, S. K., & Talcott, J. B. (2010). Are poor mathematics skills associated with visual deficits in temporal processing? *Neuroscience Letters*, *469*, 248-250. doi:10.1016/j.neulet.2009.12.005

Simmers, A. J., & Bex, P. J. (2004). The representation of global spatial structure in amblyopia. *Vision Research*, *44*, 523-533.

Simmers, A. J., Gray, L. S., McGraw, P. V., & Winn, B. (1999). Functional visual loss in amblyopia and the effect of occlusion therapy. *Investigative Ophthalmology & Visual Science*, *40*, 2859-2871.

Simmers, A. J., Ledgeway, T., & Hess, R. F. (2005). The influences of visibility and anomalous integration processes on the perception of global spatial form versus motion in human amblyopia. *Vision Research*, *45*, 449-460. doi:10.1016/j.visres.2004.08.026

Simmers, A. J., Ledgeway, T., Hess, R. F., & McGraw, P. V. (2003). Deficits to global motion processing in human amblyopia. *Vision Research*, *43*, 729-738. doi:10.1016/S0042-6989(02)00684-3

Simmers, A. J., Ledgeway, T., Mansouri, B., Hutchinson, C. V., & Hess, R. F. (2006). The extent of the dorsal extra-striate deficit in amblyopia. *Vision Research*, *46*, 2571-2580. doi:10.1016/j.visres.2006.01.009

Sireteanu, R., & Rieth, C. (1992). Texture segregation in infants and children. *Behavioural Brain Research*, *49*, 133-139.

Skoczenski, A. M., & Norcia, A. M. (2002). Late maturation of visual hyperacuity. *Psychological Science*, *13*, 537-541.

Smith, A. T., Greenlee, M. W., Singh, K. D., Kraemer, F. M., & Hennig, J. (1998). The processing of first- and second-order motion in human visual cortex assessed by functional magnetic resonance imaging (fMRI). *Journal of Neuroscience*, *18*, 3816-3830.

Smith, A. T., & Ledgeway, T. (2001). Motion detection in human vision: a unifying approach based on energy and features. *Proceedings Biological Science*, *268*, 1889-1899. doi:10.1098/rspb.2001.1727

Snowden, R. J., & Verstraten, F. A. J. (1999). Motion transparency: Making models of motion perception transparent. *Trends in Cognitive Sciences*, *3*, 369-377.

Spencer, J., O'Brien, J., Riggs, K., Braddick, O., Atkinson, J., & Wattam-Bell, J. (2000). Motion processing in autism: evidence for a dorsal stream deficiency. *Neuroreport*, *11*, 2765-2767.

Srebro, R. (1983). Measurements of eccentricity of fixation in normals and in amblyopes by evoked potentials. *Vision Research*, *23*, 1527-1532.

Stubbs, J. L., Corrow, S. L., Kiang, B., Panenka, W. J., & Barton, J. J. S. (2018). The effects of enhanced attention and working memory on smooth pursuit eye movement. *Experimental Brain Research*, *236*, 485-495. doi:10.1007/s00221-017-5146-6

Strasburger, H. (2001). Converting between measures of slope of the psychometric function. *Perception & Psychophysics, 63*, 1348-1355.

Subramanian, V., Jost, R. M., & Birch, E. E. (2013). A quantitative study of fixation stability in amblyopia. *Investigative Ophthalmology & Visual Science*, *54*, 1998-2003. doi:10.1167/iovs.12-11054

Sunaert, S., Van Hecke, P., Marchal, G., & Orban, G. A. (1999). Motion-responsive regions of the human brain. *Experimental Brain Research*, *127*, 355-370.

Takai, Y., Sato, M., Tan, R., & Hirai, T. (2005). Development of stereoscopic acuity: longitudinal study using a computer-based random-dot stereo test. *Japanese Journal of Ophthalmology*, *49*, 1-5. doi:10.1007/s10384-004-0141-4

Talcott, J. B., Hansen, P. C., Assoku, E. L., & Stein, J. F. (2000). Visual motion sensitivity in dyslexia: evidence for temporal and energy integration deficits. *Neuropsychologia*, *38*, 935-943.

Talcott, J. B., Witton, C., McLean, M. F., Hansen, P. C., Rees, A., Green, G. G. R., & Stein, J. F. (2000). Dynamic sensory sensitivity and children's word decoding skills. *Proceedings of the National Academy of Sciences*, *97*, 2952-2957.

Taylor, N. M., Jakobson, L. S., Maurer, D., & Lewis, T. L. (2009). Differential vulnerability of global motion, global form, and biological motion processing in full-term and preterm children. *Neuropsychologia*, *47*, 2766-2778. doi:10.1016/j.neuropsychologia.2009.06.001

Thompson, B., Richard, A., Churan, J., Hess, R. F., Aaen-Stockdale, C., & Pack, C. C. (2011). Impaired spatial and binocular summation for motion direction discrimination in strabismic amblyopia. *Vision Research*, *51*, 577-584. doi:10.1016/j.visres.2011.02.001

Tong, J., Lien, T. C., Cisarik, P. M., & Bedell, H. E. (2008). Motion sensitivity during fixation in straight-ahead and lateral eccentric gaze. *Experimental Brain Research*, *190*, 189-200. doi:10.1007/s00221-008-1462-1

Tootell, R. B., Mendola, J. D., Hadjikhani, N. K., Ledden, P. J., Liu, A. K., Reppas, J. B., . . . Dale, A. M. (1997). Functional analysis of V3A and related areas in human visual cortex. *Journal of Neuroscience*, *17*, 7060-7078.

Tootell, R. B., Reppas, J. B., Kwong, K. K., Malach, R., Born, R. T., Brady, T. J., . . . Belliveau, J. W. (1995). Functional analysis of human MT and related visual cortical areas using magnetic resonance imaging. *Journal of Neuroscience*, *15*, 3215-3230.

Tsermentseli, S., O'Brien, J. M., & Spencer, J. V. (2008). Comparison of form and motion coherence processing in autistic spectrum disorders and dyslexia. *Journal of Autism & Developmental Disorders, 38*, 1201-1210. doi:10.1007/s10803-007-0500-3

Vikesdal, G. H., & Langaas, T. (2016). Optically induced refractive errors reduces fixation stability but saccade latency remains stable. *Journal of Eye Movement Research*, 1-8.

von Noorden, G. K. (1990). *Binocular vision and ocular motility*. St. Louis, MO: Mosby.

Wali, N., Leguire, L. E., Rogers, G. L., & Bremer, D. L. (1991). CSF interocular interactions in childhood ambylopia. *Optometry & Vision Science*, *68*, 81-87.

Wang, J., Ho, C. S., & Giaschi, D. E. (2007). Deficient motion-defined and texture-defined figure-ground segregation in amblyopic children. *Journal of Pediatric Ophthalmology & Strabismus*, *44*, 363-371.

Wang, Y. Z., Morale, S. E., Cousins, R., & Birch, E. E. (2009). Course of development of global hyperacuity over lifespan. *Optometry & Vision Science*, *86*, 695-700. doi:10.1097/OPX.0b013e3181a7b0ff

Watson, A. B., & Pelli, D. G. (1983). QUEST: a Bayesian adaptive psychometric method. *Perception & Psychophysics, 33*, 113-120.

Weakley, D. R. (2001). The association between nonstrabismic anisometropia, amblyopia, and subnormal binocularity. *Ophthalmology*, *108*, 163-171.

Welch, B. L. (1947). The generalisation of Student's problem when several different population variances are involved. *Biometrika*, *34*, 28-35.

Welch, B. L. (1951). On the comparison of several mean values: An alternative approach. *Biometrika*, *38*, 330-336.

White, C., Brown, J., & Edwards, M. (2014). Alterations to global but not local motion processing in long-term ecstasy (MDMA) users. *Psychopharmacology*, *231*, 2611-2622. doi:10.1007/s00213-014-3431-7

White, S., Milne, E., Rosen, S., Hansen, P., Swettenham, J., Frith, U., & Ramus, F. (2006). The role of sensorimotor impairments in dyslexia: a multiple case study of dyslexic children. *Developmental Science*, *9*, 237-55; discussion 265. doi:10.1111/j.1467-7687.2006.00483.x

Wyatt, H. J., & Pola, J. (1984). A mechanism for suppression of optokinesis. *Vision Research*, *24*, 1931-1945.

Yu, T.-Y., Jacobs, R. J., Anstice, N. A., Paudel, N., Harding, J. E., & Thompson, B. (2013). Global motion perception in 2-year-old children: A method for psychophysical assessment and relationships with clinical measures of visual function. *Investigative Ophthalmology & Visual Science*, *54*, 8408-8419. doi:10.1167/ iovs.13-13051

Zanker, J., Mohn, G., Weber, U., Zeitler-Driess, K., & Fahle, M. (1992). The development of vernier acuity in human infants. *Vision Research*, *32*, 1557-1564.

Zeki, S., Watson, J. D., Lueck, C. J., Friston, K. J., Kennard, C., & Frackowiak, R. S. (1991). A direct demonstration of functional specialization in human visual cortex. *Journal of Neuroscience*, *11*, 641-649.

Zwicker, A. E., Hoag, R. A., Edwards, V. T., Boden, C., & Giaschi, D. E. (2006). The effects of optical blur on motion and texture perception. *Optometry & Vision Science*, *83*, 382-390. doi:10.1097/01.opx.0000222919.21909.1e

Appendices

Appendix A Staircase threshold estimation

The following appendix includes greater detail on the staircase running procedure and on the Weibull-fitting procedure used in this dissertation.

A.1 Inspection of staircase runs during data collection

When research assistants (RAs) or I take participants through the global motion tasks, we inspect a plot of the staircase function after each run. Figure A.1 demonstrates one such plot for a good run. Figure A.2 demonstrates a plot for an exaggerated run where incorrect responses early in the run have prevented the staircase from reaching coherence levels near a participants' threshold. In this scenario, we will re-run the staircase for this condition. If there was not enough time to re-run this staircase, data from this condition will be excluded from analysis since the data collected will not lead to a reliable threshold measurement.

Figure A.1 Example of a good staircase.

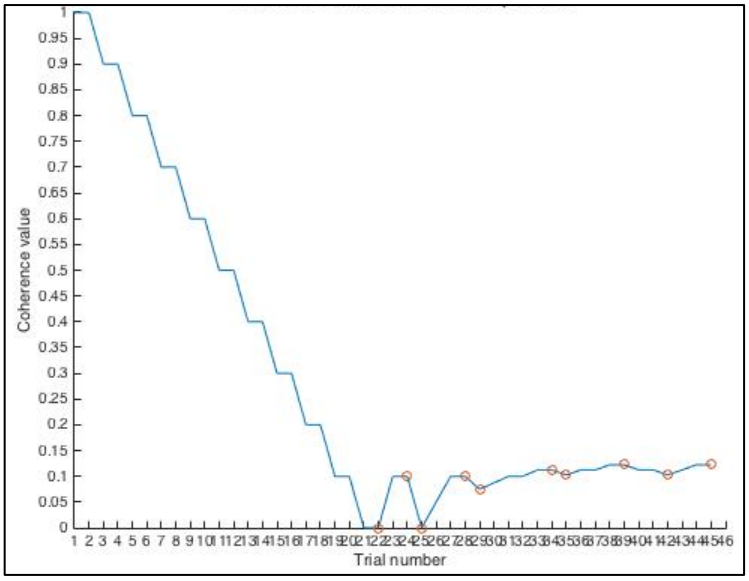

Note. Plot shows the coherence of a stimulus from the first trial to the last trial. Response reversals are circled in red.

Figure A.2 Example of a staircase that never converges.

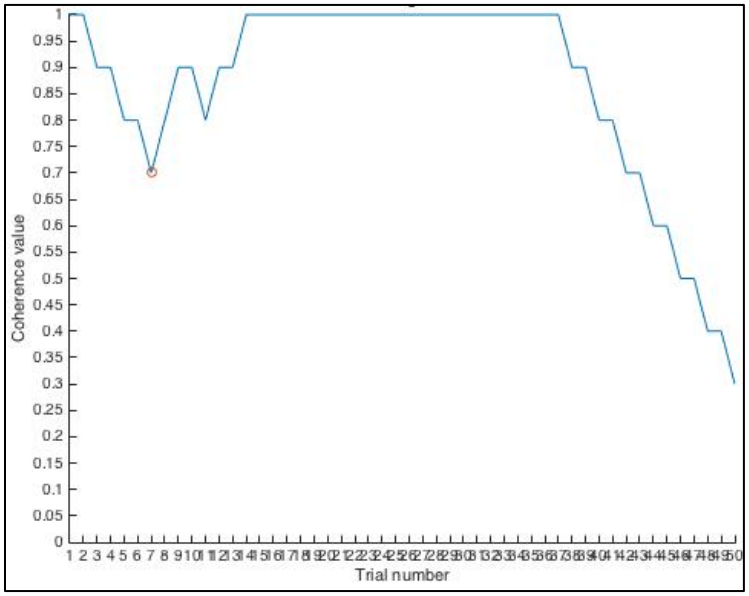

Note. Plot shows the coherence of a stimulus from the first trial to the last trial. Response reversals are circled in red. This staircase never converges on a true reversal (i.e., the coherence value continues to decline at the end of the experiment, and it has not reached a range of coherence values that the participant finds difficult). This is an indication that the participant made some early mistakes that prevented the staircase algorithm from presenting trials with coherence near a participant's threshold.

Figure A.3 demonstrates a run where a participant is responding randomly. This may be because they cannot see the stimulus, or because they do not understand the task. If this occurs, we will go over the instructions again and give more practice trials if necessary. Such performance, particularly in younger children, can also indicate that participants do not care about being correct or are not interested in playing the research game. In this case, we will end the experiment early.

Figure A.3 Example of a staircase that does not advance.

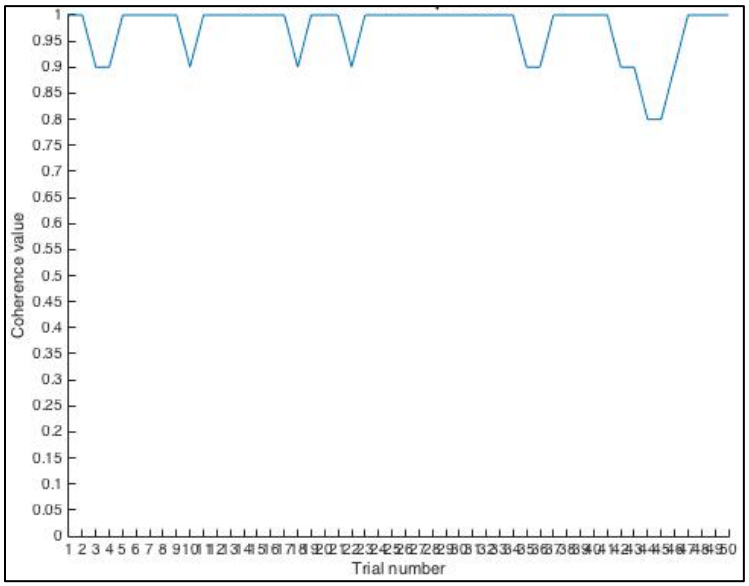

Note. Plot shows the coherence of a stimulus from the first trial to the last trial. The staircase above never advances. This is an indication that the participant is giving random responses.

A.2 Inspection of coherence thresholds during data analysis

As described in section 2.7, a Weibull function was fit to participants' coherence by accuracy data using a maximum-likelihood minimization bootstrap procedure. The coherence level at the slope of maximum inflection on the Weibull curve (α; equivalent to 82% correct for this two-alternative forced choice task) was defined as threshold. For the data in Chapter 4, I used an in-house version of Denis Pelli's *Quick3.c*, modified by a previous student to incorporate variability estimates for the bootstrapping procedure, to compute coherence thresholds. For the data in Chapters 3, 5, and 6, I used the *Palamedes Toolbox* (www.palamedestoolbox.org) created by Nicolaas Prins and Frederick Kingdom. I opted for the switch because of the greater flexibility of Palamedes, which is implemented in MATLAB and can model a variety of other psychometric functions that we use in my lab. Prior to switching programs, an analysis was conducted that computed coherence thresholds separately using the two programs and compared their values. As expected, thresholds calculated by the two programs were extremely similar (r = 0.97, 95% CI: [0.94, 0.98]) since they implemented the same methods.

A goodness-of-fit test was used to assess the psychometric function fit for each threshold. Where this goodness-of-fit test failed, trial-by-trial data were inspected and re-fit after removing early mistakes at high coherence levels and/or trials reflecting a coherence level that was presented only once. If fit did not improve, the participant's threshold for this condition would be removed from analysis. This scenario occurred rarely, as the majority of the poor fits occurred due to early mistakes that impacted fit but not the estimated threshold. Figure A.4 demonstrates the plots that are inspected after each coherence threshold is estimated.

Figure A.4 Example of a Weibull function fit.

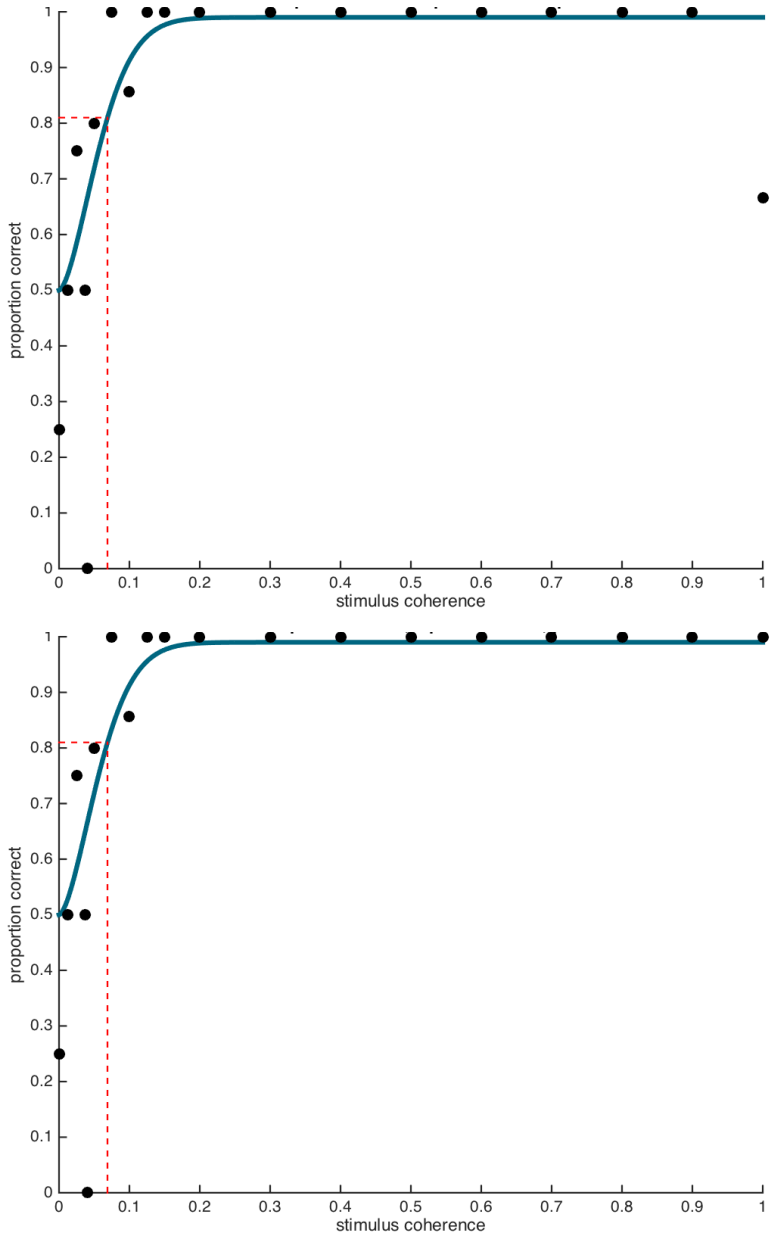

Note. Both plots show mean accuracy for each coherence level presented (black circles), along with the Weibull function fit to this data (blue line) and the coherence threshold (red dashed line). The top function shows a poor fit due to a series of mistakes made by the participant at 100% coherence. The bottom function shows the same data with the early mistakes removed. Removal of the mistakes affects the goodness-of-fit, but not the estimated coherence threshold.

A.3 Exclusion of participants and data

The number of participants excluded because we needed to end the experiment early (either because they demonstrated random responding, or because they did not want to begin the experiment after the practice trials) is described in the individual chapters. In summary: 11 participants were excluded in Chapter 3; two children with amblyopia were excluded in Chapter 4; three children were excluded in Chapter 5; and no participants were excluded in Chapter 6.

The number of participants who did not have complete datasets for all conditions tested in each experiment (either due to poor staircase runs, poor Weibull fits, or for running out of time) is described in the individual chapters. In summary: for Chapter 3, one participant had data missing from two conditions (age 16.3 years); thirteen participants had data missing from one of the six conditions (age range 7.1 to 24.2 years), and the remaining 168 participants had data for all six conditions. In Chapter 4, no participants were missing data. In Chapter 5, one child had data missing from three of the nine conditions, one child had data missing from two of the nine conditions, and three children and four adults had data missing from one of the nine conditions tested. The remaining participants (22 children and 23 adults) had data for all nine conditions. In Chapter 6, no participants were missing data.

Appendix B Eyetracking in participants with amblyopia

The following appendix includes data from adults with a history of amblyopia to complement the data presented in Chapter 6. Because collection is ongoing, the data are presented without formal statistical conclusions comparing participants with amblyopia and controls.

B.1 Participants

Nine adults (eight female; 27 – 61 years old; *M* age = 42 years, *SD* = 13) with a history of amblyopia participated in this experiment. Participants' visual acuity and stereoacuity are described in Table B.1.

Table B.1 Vision characteristics for participants with amblyopia included in data analysis.

		Visual acuity at testing (logMAR)		
ID	Age (years)	Amblyopic eye	Fellow eye	Stereoacuity (arcsec)
A1	56	*n/a* (R)	-0.05	NM
A2	29	0.30 (L)	0.04	NM
A3	29	0.74 (L)	0.01	100
A4	29	0.05 (L)	-0.08	NM
A5	27	0.26 (L)	0.03	NM
A6	42	0.26 (R)	-0.16	60
A7	47	0.40 (R)	-0.06	NM
A8	55	0.48 (R)	0.11	NM
A9	61	0.88 (R)	-0.03	NM

Note. (L) = left eye amblyopic; (R) = right eye amblyopic; n/a = participant unable to count fingers at 1.5 m distance so no measurement available; NM = stereoacuity not measurable at the largest disparity tested (800 arcsec).

B.2 Behavioural performance

Figure B.1 displays control data from Figure 6.1 along with data from the participants with amblyopia in Table B.1. One participant, A1, was unable to see the motion stimulus when viewing with the amblyopic eye, so there is no threshold available.

Figure B.1 Mean coherence thresholds, including participants with amblyopia.

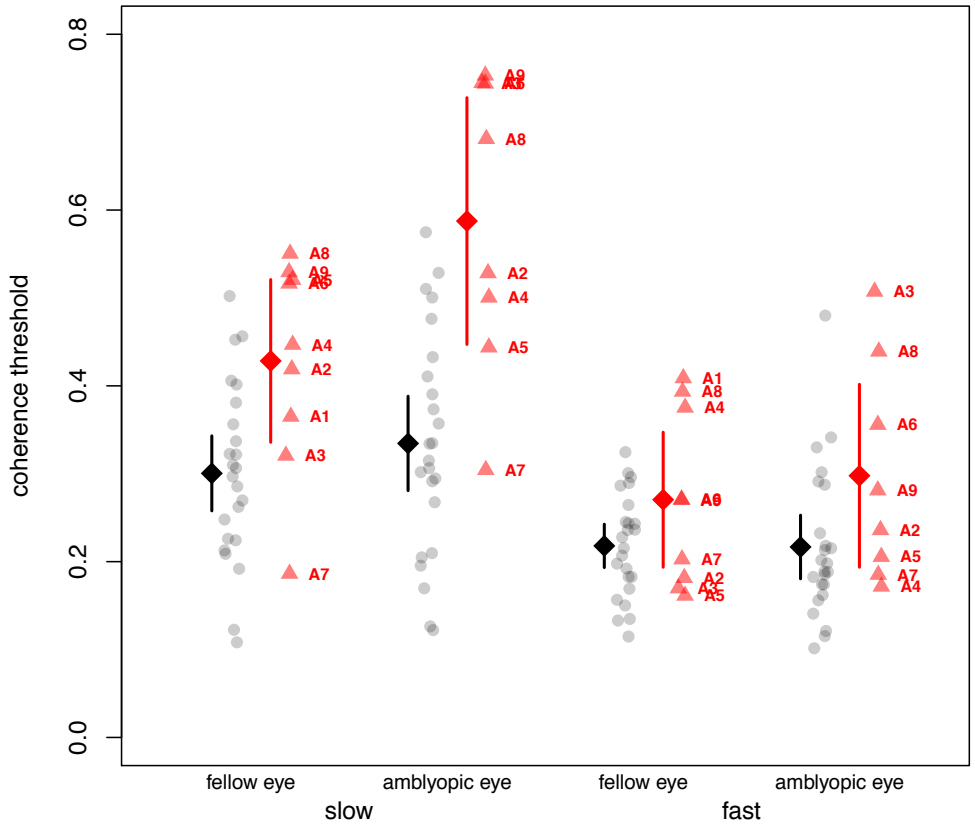

Note. Grey dots represent individual control participants. Red triangles represent participants with amblyopia, with labels corresponding to Table B.1. The means of the control group (in black) and the amblyopia group (in red) are shown with error bars representing 95% confidence intervals.

B.3 Stability measures

Stability on stationary trials, trials at high coherence, and trials near the participants' thresholds are shown in Figure B.2 along with the control data from Figure 6.2. Figure B.3 displays the relationship between acuity and stability for the amblyopic eye and the fellow eye. Figure B.4 displays scatterplots of the relationship between stability and performance for participants with amblyopia, along with the control data from Figure 6.4.

Figure B.2 Mean $\log_{10}$ BCEA for controls and participants with amblyopia for all conditions.

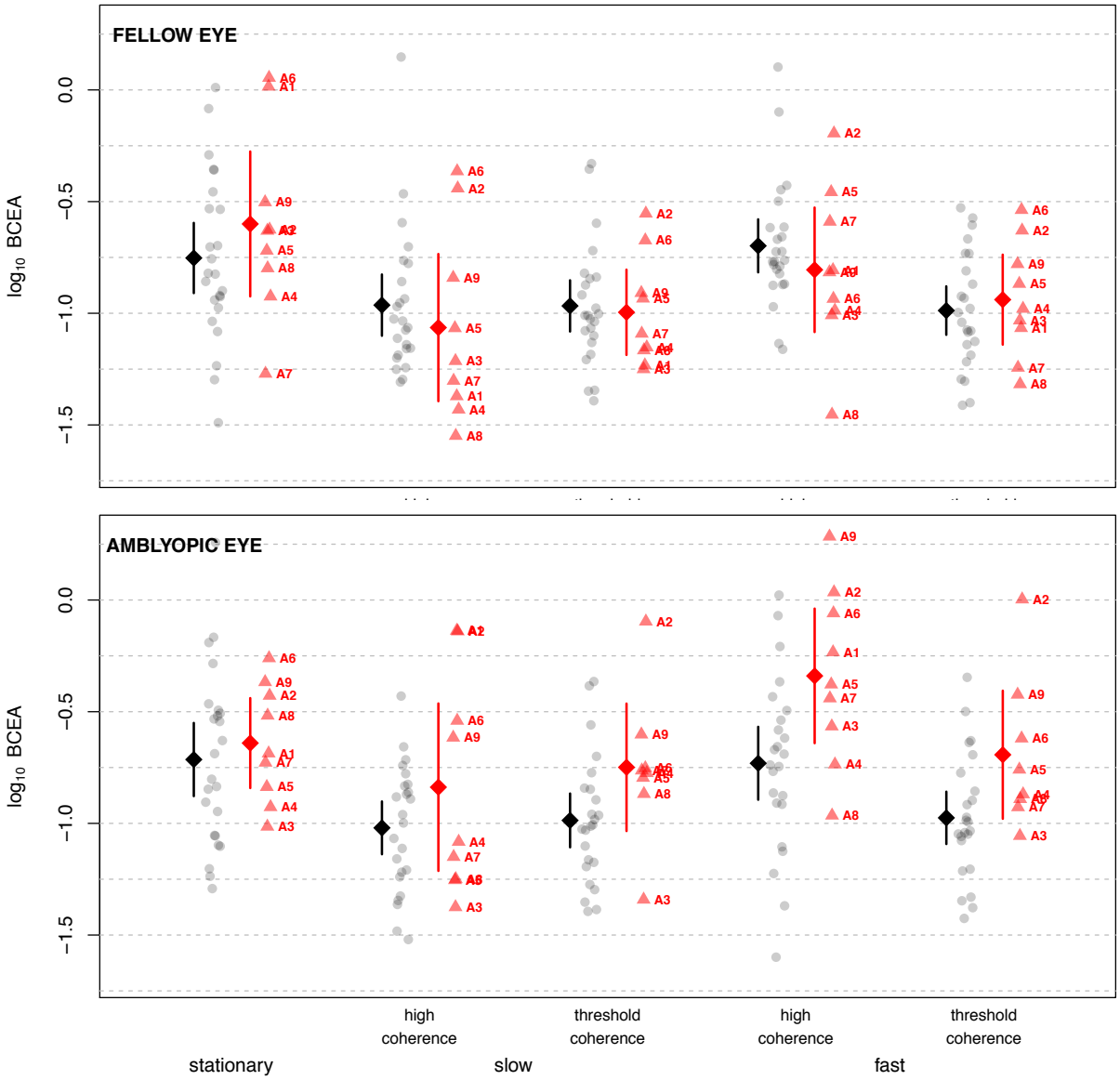

Note. Grey dots represent individual control participants. Red triangles represent participants with amblyopia, with labels corresponding to Table B.1. The means of the control group (in black) and the amblyopia group (in red) are shown with error bars representing 95% confidence intervals.

Figure B.3 Scatterplots showing visual acuity (logMAR) and stability (log_{10} BCEA) for participants with amblyopia.

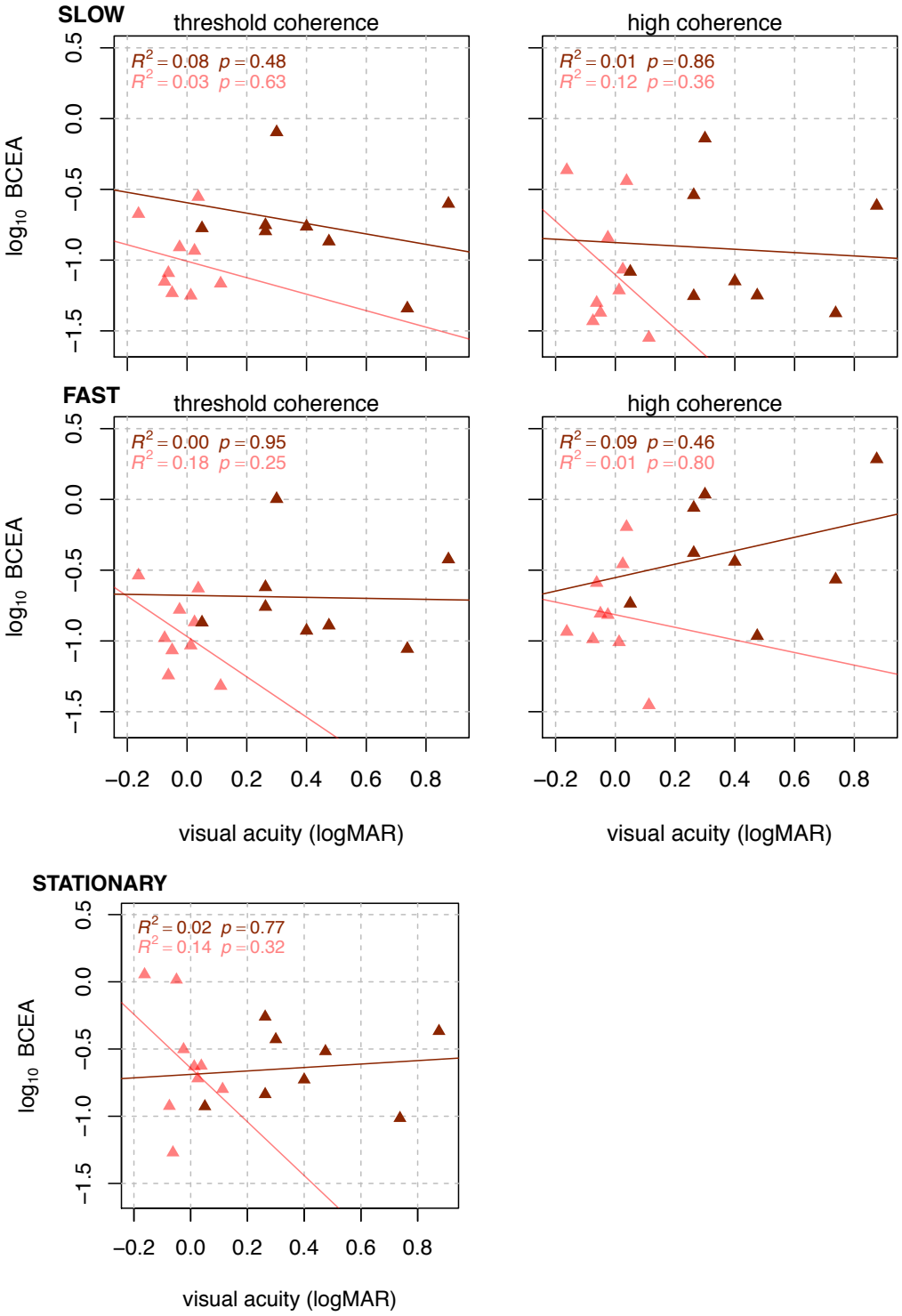

Note. Each plot displays participants' amblyopic eyes (dark red) and fellow eyes (light red). Lower values indicate better visual acuity or greater stability. Top row, data collected in the slow condition; middle row, data collected in the fast condition. Left column shows stability on trials at threshold coherence; right column shows stability on trials at high coherence. Bottom panel shows stability on stationary trials.

Figure B.4 Scatterplots showing the relationship between stability (log_{10} BCEA) and performance (coherence threshold) in participants with amblyopia.

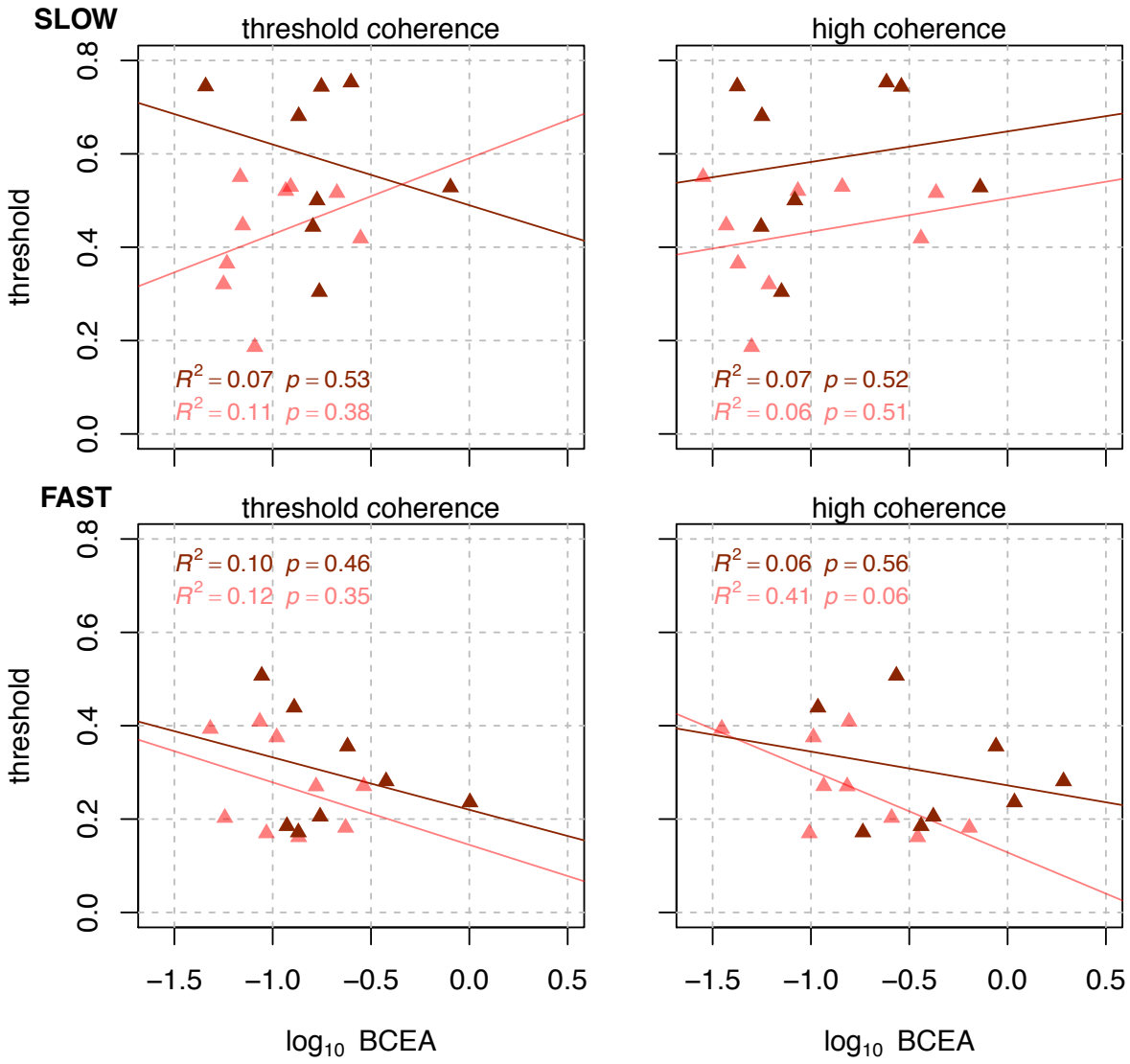

Note. Each plot displays participants' amblyopic eyes (dark red) and fellow eyes (light red). Lower values indicate more stable fixation (BCEA), and better performance (threshold). Top row, data collected in the slow condition; bottom row, data collected in the fast condition. Left column shows stability on trials at threshold coherence; right column shows stability on trials at high coherence.